Biopolymers for enhancing the engineering properties of soil

by

Antonio Soldo

A dissertation submitted to the Graduate Faculty of

Auburn University

in partial fulfillment of the

requirements for the Degree of

Doctor of Philosophy

Auburn, Alabama

May 2, 2020

Keywords: biopolymers, soil stabilization, eco-friendly

Approved by

Marta Miletić, Assistant Professor, Department of Civil Engineering

Maria L. Auad, Associate Professor, Department of Chemical Engineering

Jack Montgomery, Assistant Professor, Department of Civil Engineering

James S. Davidson, Gottlieb Professor of Structural Engineering, Department of Civil Engineering

Aleksandr Vinel, Assistant Professor, Department of Civil Engineering, Industrial and Systems Engineering

ACKNOWLEDGMENTS

This dissertation is the result of many aligned actions, moments, chances, and people that paved the road for me to reach this goal. I am thankful for all of that.

Foremost, I would like to express my utmost gratitude and respect to my advisor, Dr. Marta Miletić, whose patience, kindness, and extensive knowledge guided me towards my Ph.D. title. Her guidance and help were constant in every step of my research. I don't think I could have had a better advisor.

Also, I would like to say thank you to Dr. Maria L. Auad, Dr. Jack Montgomery, James S. Davidson, and Dr. Aleksandr Vinel for improving my work with their constructive critics.

I am thankful to Mary Beth, Katie, Debbie, and Sherry for all administrative help and for being gear wheels that run Auburn University.

I would like to thank my colleagues Victor, Dinu, Devdeep, Mehran, Michael K., Michael I., Dan, and Wu, that helped me with my work and research.

Also, I would like to thank my family and friends for all their support. Luckily, there are too many of them to count.

TABLE OF CONTENTS

LIST OF FIGURES

LIST OF TABLES

ABSTRACT

The need for constant construction rapidly expands the built environment which often spreads over areas with unfavorable site conditions. In such events, soil stabilization is an inevitable process. Increasing soil strength with chemical stabilizing agents such as cement often rises environmental concerns. Therefore, the need for eco-friendly solutions for soil stabilization is in constant demand. One of the most promising solutions for that issue is the utilization of biopolymers. This study experimentally and numerically investigated five different biopolymers and their effect on soil strength. Biopolymers that were investigated were xanthan gum, guar gum, beta 1.3/1.6 glucan, chitosan, and alginate. Their effect was observed while interacting with three types of soil: sand, clay, and silty sand. The experimental research included unconfined compression tests, splitting tensile tests, triaxial tests, direct shear tests, and water durability tests. The testing was performed under different biopolymer concentrations and different curing times. The broad experimental research showed that the strength of treated soil tends to increase with the biopolymer concentration and curring time, but that it also depends on the volume of the soil, type of the soil and type of biopolymers. The tests indicate an optimum biopolymer concentration and optimum curing time after which the soil improvement does not increase. This study focused more on the biopolymers that showed a more promising effect on the increase of soil strength. Therefore, some sections of this study focused more on xanthan gum, guar gum and beta-glucan. In the majority of cases, the biopolymer xanthan gum showed the most dominant effect on the increase of the soil strength. Xanthan gum and guar gum demonstrated promising properties to reduce soil degradation through the process of wetting and drying. Furthermore, it was observed that the regenerative properties of xanthan gum can restore some levels of lost soil strength. From the experimental studies, the three most influential polymers were investigated in the numerical part of this study. The

numerical part was focused on investigating the effect of biopolymers on the onset of strain localization. For the needs of the numerical study, an analytical-numerical model was created in order to capture the stress-strain response of biopolymers-treated soil under the state of pressure. The extensive experimental investigation provided large sets of data from which were used either for calibration or verification. Analyzing the stress-strain response of the treated and plain soil, it was noticed that the presence of biopolymers tends to postpone the onset of strain localization and by that, the failure of soil mass can be postponed.

1. INTRODUCTION

1.1 BACKGROUND AND LITERATURE REVIEW

The rapid industrialization, urbanization, and population growth often cause the need to build over soft and unfavorable soil present in adverse surroundings. This further urges the need to stabilize and improve the initially unsuitable soil. Most common approaches to mitigating unfavorable soil can be divided into four major groups:

- Mechanical stabilization
- Thermal stabilization
- Biological stabilization
- Chemical stabilization

Mechanical soil stabilization is the process of improving the soil properties by altering its gradation and densification. This process includes soil compaction and densification by application of mechanical energy using various sorts of rollers, rammers, vibration techniques, to name a few. For instance, one of the commonly used methods is dynamic compaction that represents dropping a hefty weight on the soil surface. The weight can be up to 40 tons heavy. The repeated process of weight-dropping produces shock waves that increase soil density. Vibro-compaction is another method of soil stabilization where a vibrating probe is inserted into the ground or vibrating surfaces are placed over the soil surface. The vibration sends waves into the surrounding soil and densifies it. The mentioned methods are intended for loose granular material, but they are not suitable for fine-grained soil. Fine-grained soil is usually compacted by the weight of heavy kneading machines that roll over the soil surface (Holtz et al. 1981).

Thermal stabilization is achieved either by sending a source of heat into boreholes or heating the soil surface. However, the thermal stabilization significantly affects biological,

chemical, and physical processes under the soil surface. At high temperatures, the soil melts, biological activity increases and the organic material decomposes (Hinchee and Smith 1992).

One of the biological stabilization approaches, known as microbially induced calcium carbonate precipitation (MICP), is becoming more popular in recent years as it represents an eco-friendly way for soil stabilization. It is based on cultivating bacteria in the soil. Certain types of bacteria create cementitious formations while interacting with soil particles, which further increases soil strength. Several researchers investigated that phenomena and some of the pioneering work can be found in the following references (DeJong et al. 2006; Umar et al. 2016; Ashraf et al. 2017).

Chemical soil stabilization includes introducing chemical additives to the soil to alter its properties. The traditional chemical additives are cement, lime, and fly ash. Non-traditional chemical additives are best represented by polymers. Currently, cement is the most commonly used additive for soil stabilization. The use of cement can change the physical and chemical properties of soil (Guo, 2014). Portland cement is the most commonly used cement type for the cement stabilization of soil. Standard Specification for Portland Cement (ASTM C150 - 19a) describes ten types of Portland cement:

- Type I - if the special properties specified for any other Portland cement type are not required
- Type IA - for the same uses as Portland cement Type I, where air-entrainment is desired.
- Type II - for general use, especially if moderate sulfate resistance is desired.
- Type IIA - for the same purposes as Portland cement Type II, where air-entrainment is desired.
- Type II(MH) - for general use, especially if moderate heat of hydration and moderate resistance to sulfates are desired.

- Type II(MH)A - for the same applications as Portland cement Type II(MH), if air-entrainment is desired.
- Type III - for use if high early strength is desired.
- Type IIIA - for the same use as Portland cement Type III, where air-entrainment is desired.
- Type IV - for use when a low hydration heat is desired.
- Type V - for use when high resistance to sulfates is desired.

Lime is another traditional stabilizing agent consisting of calcium and magnesium oxides. Furthermore, several processes occur during the interaction of lime and soil particles. During cation exchange and flocculation-agglomeration between lime and soil, plasticity, workability, load-deformation, and strength are increased. Pozzolanic reactions between soil and lime create calcium silicates and aluminates, which are similar to the formations that occur during the reactions between the Portland cement and soil (Guo, 2014).

Fly ash is also a traditional soil stabilizer created by the burning of coal. Standard Specification for Coal Fly Ash and Raw or Calcined Natural Pozzolan for Use in Concrete (ASTM C618 - 19) classifies three types of fly ash based on their chemical and physical properties

- Class N - includes raw or calcined natural pozzolans that comply with ASTM C618 – 19.
- Class F - includes fly ash that complies with ASTM C618 – 19. This type of fly ash has pozzolanic properties.
- Class C - includes fly ash that complies with ASTM C618 – 19. This type of fly ash has pozzolanic properties and specific cementitious properties.

Polymers are non-traditional chemical additives and represent a group of small molecules bound in chain. Broadly, polymers can be divided into two major categories. The first group represents synthetic polymers such as rubber, foam, and plastic. The second group of polymers is natural polymers, also known as biopolymers, such as starch, proteins, and carbohydrates. Biopolymers are the main focus of this research study. They are heavily utilized as mass thickeners, and particle binders, especially in the food industry (Katzbauer 1998; Thombare et al. 2016). Biopolymers are natural products extracted from plants, fungi, yeast, and animal shells. No negative effect of biopolymers on the environment has been reported. For that reason, they represent a potentially eco-friendly solution for the various industries where they can be utilized. In the civil engineering industry, they are being investigated as soil stabilizers.

As mentioned previously, cement treatment is currently the most common chemical treatment for soil stabilization. Even though cement provides a practical and cost-effective solution, the use of cement has several adverse effects on the environment. Therefore, the demand for eco-friendly ways for soil stabilization is in constant rise. The use of biopolymers is one of the options and is gaining momentum. The origins of the idea to use biopolymers as soil stabilization dates back to 1946 (Martin 1946; Geoghegan and Brian 1946). Martin (1946) investigated the interaction of soil with six types of bacteria that were known to synthesize polysaccharides. Geoghegan and Brian (1946) noticed that bacterium B. subtilis created a polysaccharide levan, which is a gum product, during wet sieving of soil. The levan concentration with 0.1 % or more nitrogen content caused soil aggregation. Chepil and Woodruff (1963) discussed the use of polysaccharides as the means for soil erosion against the wind, pointing out their drawbacks related to their degradation, which was also supported by other researchers (Martin and Aldrich 1955; Harries et al. 1966). In 1977, Cruse and Larson investigated the effect of rainfall on biopolymer-treated soil erosion and strength. They demonstrated that adding organic polymer to the soil increases its strength

parameters. Their research was one of the first that showed the quantitative correlation between soil strength and an organic polymer. Karimi (1998) investigated the permeability and strength of biopolymer-treated soil. Their research showed that biopolymers can reduce the permeability of soil for an extended period and that the triaxial strength of soil can be increased.

Over the years, certain biopolymers emerged as more efficient than others for amending the soil properties. Five types of biopolymers were selected in our studies: xanthan gum, guar gum, beta-glucan, alginate, and chitosan. Xanthan gum is a polysaccharide type of biopolymer created by the fermentation of a carbohydrate-source medium such as glucose. Xanthan gum was named after the bacterium that induces the process of fermentation, Xanthomonas campestris. Xanthan gum can be dissolved in hot and cold water. Solutions containing Xanthan gum are non-Newtownians and highly pseudoplastic. Therefore, their viscosity depends on the sharing rate—higher shearing results in lower viscosity. At a lower shearing rate, the xanthan gum chains are in the state of rest and bound by hydrogen bonds. Increasing the shear rate, the cluster of bound chains is reduced, which leads to lower viscosity. Due to its fast interaction with water, rapid agitation and mixing are needed to dissolve xanthan gum in water efficiently. The chains of xanthan gum remain stable over wide ranges of pH values. Therefore, it can be successfully implemented in cleaning products as well as acidic food additives (Katzbauer 1998). Other than that, it can be found in the cosmetic industry, agriculture, and oil drilling industry (Katzbauer 1998). In addition, the different researchers investigated it as an agent for the improvement of different soil characteristics. Chang et al. (2015a) investigated the increase of the compressive strength of soil by adding xanthan gum. They found out that adding only 1% xanthan gum can increase the soil compressive strength more than adding 10% cement (Figure 1-1). Ayeldeen et al. 2017 showed that the addition of xanthan gum to the soil could decrease the collapsible potential of soil. Furthermore, several other researchers confirmed

that xanthan gum can reduce the permeability of soil (Wiszniewski et al. 2013; Ayeldeen et al. 2017; Cabalar et al. 2017).

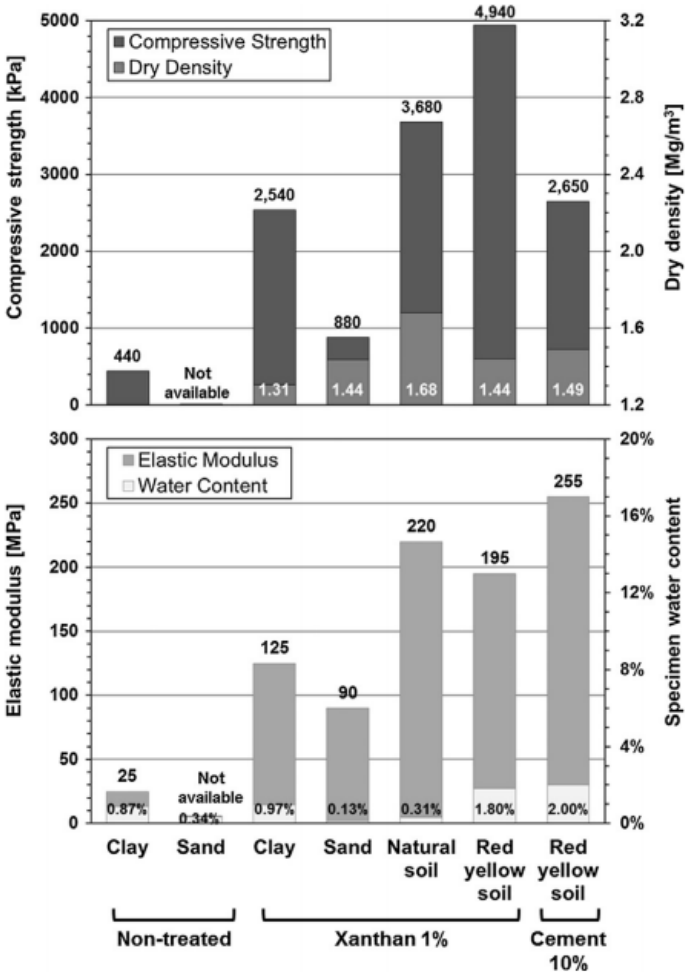

Figure 1-1: Compressive strength, elastic modulus, dry density, and water content of 1% Xanthan gum treated soil specimens 28 days after mixing. Non-treated pure clay, sand, and 10% cement treated Red Yellow soil are plotted together for comparison (Chang et al. 2015a)

Guar gum is a polysaccharide extracted from Cyamopsis tetragonoloba that is commonly known as guar beans or guar. Guar can be found in India, Pakistan, Sudan, and some regions of the USA. The guar gum accumulations are present in seeds of the guar plant. During the process of the extraction, the guar gum is separated from the rest of the plant, ground, sieved and packed in a powder form for commercial purposes. Unlike the majority

of plant-based gums, guar gum does not have any uronic acid in its molecular structure (Figure 4-2). Also, it has a relatively high molecular weight when compared with other naturally occurring water-soluble polysaccharides. It is worth mentioning that guar gum formations are stable over a broad range of pH. Therefore, water is the primary dissolving agent for guar gum, and it can be dissolved in hot and cold water. Even small concentrations of guar significantly increase the viscosity of the solution. Some of its applications can be found in the cosmetic industry, food industry, agriculture, and oil drilling (Thombare et al. 2016). The use of guar gum for civil engineering purposes was investigated in the past. Gupta et al. (2009) investigated the means to reduce the viscosity of guar gum solutions for the purpose of grouting stabilization of the desert sand. Previous research also showed that the addition of guar gum can increase the compressive strength of soil (Ayeldeen et al. 2016; Toufigh and Kianfar 2019) and decrease the permeability of soil (Ayeldeen et al. 2016; Dehghan et al. 2018). Chen et al. 2013 showed that the increase of guar gum concentration increases the liquid limit of soil and the undrained shear strength.

Beta-glucan is a polysaccharide type biopolymer that consists of glucose molecules. There is a spectrum of beta-glucan types that vary based on the source of beta-glucan. They can be extracted from the cells of yeast, fungi, some types of bacteria, and certain types of cereals. The molecular structure of beta-glucans depends on the source they were extracted from. Beta-glucans molecules can vary on the kind of linkages, branching, molecular weight, solubility, and polymer charge (Volman et al. 2008). The extraction process of beta-glucan depends on the parent source and the molecular bonds of the polymer. Therefore, an appropriate solving agent has to be selected. Molecular structures of beta-glucan that are held loosely outside the cells can be extracted with hot water. Beta-glucan molecules that are held tightly to the cell walls can be released by hot alkali. Beta-glucan in its powder form can be dissolved in water at any temperature, which results in forming a gelatinous solution (Bacic et al. 2009). Beta-glucans are heavily investigated in medicine for its potential for

health improvement (Volman et al. 2008; Bacic et al. 2009). Furthermore, their potential for amending the soil properties has been investigated. Chang and Cho (2012) showed that small quantities of beta-glucan can increase the compressive strength of soil more than higher amounts of cement. Chang and Cho (2014) showed that Beta 1.3/1.6 glucan can enhance the compatibility of residual soil, liquid limit, index of plasticity, and swelling index. On the other hand, it can decrease the coefficient of consolidation (Chang and Cho 2014).

Alginate is a polysaccharide type of biopolymer, and it is extracted from brown seaweed. Commercially, alginate is mostly derived from Laminaria hyperborea, Ascophyllum nodosum, and Macrocystis pyrifera. To a lesser extent, it can also be extracted from Laminaria japonica, Laminaria digitate, Eclonia maxima, and Lesonia negrescens (Smidsrod and Skjakbrk 1990). Alginate is characterized by low toxicity, biocompatibility, and mild gelation at the presence of divalent cations. Therefore, alginate found its application in the medical industry for wound healing, tissue engineering, and drug delivery (Lee and Mooney 2012). Those properties, together with nonimmunogenicity of alginate, have led to the discovery of alginate's potential as a protein delivery agent (Gombotz and Wee 2012). Due to the increased need for eco-friendly soil stabilization agents, alginate was investigated as one of the potential solutions. Galán-Marín et al. 2010 showed that the strength of clay can increase by more than 1500 kPa by adding alginate. Fatehi et al. 2019 investigated the increase of the unconfined compressive strength of the dune sand by adding sodium alginate. It was found out that the unconfined compressive strength of the sand increased with the increase of alginate concentration.

Chitosan is a carbohydrate type of polymer, and it is derived from chitin. After cellulose, chitin is the most present biopolymer in nature. It can be found in shells of animals, insects, fungi, and yeast. Chitosan is not dissolvable in water, but it can be dissolved in acidic solutions with pH value bellow 6. The difference between chitin and chitosan is that chitosan has a free amino group in a molecular structure (Figure 1-2).

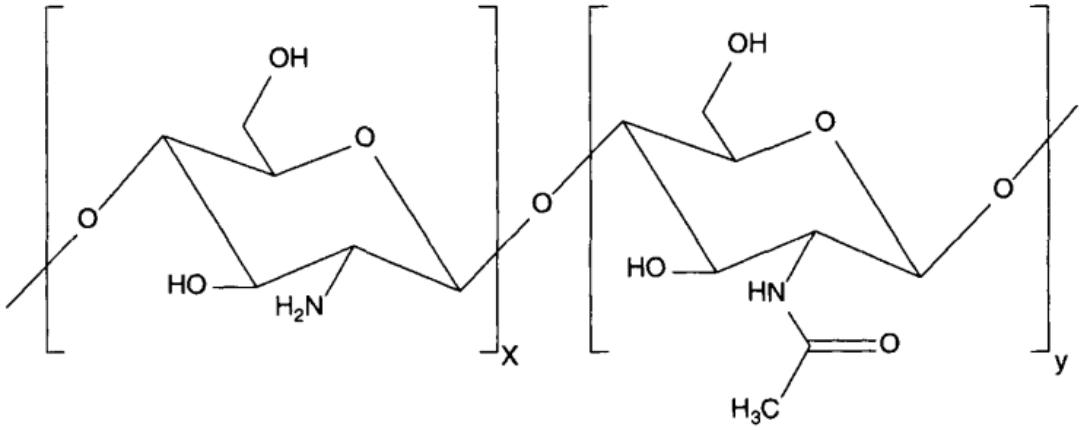

Figure 1-2: Chemical structure of chitin (X<Y) and chitosan (X>Y) (Kalia and Avérous 2011)

Chitosan has positive ionic charges that can cause chemical bonds with fats, proteins, metal ions, and other negatively charged atoms or molecules while chitin cannot. Due to its biodegradable and non-toxic properties, chitosan is heavily used in the field of medicine for wound treatment, anti-tumor influence, and bone regeneration (Kalia and Avérous 2011). In the field of civil engineering, it was shown that chitosan can be used to reduce the permeability of sand (Khachatoorian et al. 2003), and increase the strength of soil (Hataf et al. 2018). Even though chitosan can increase the strength of soil, Hataf et al. 2018 reported that the loss of water content causes the chitosan links to shrink, which ultimately reduces the strength of treated soil. Since the loss of water content is inevitable due to the drying of soil with time, chitosan might not be suitable for the long service in dry climate or areas with large fluctuations in temperature. In this research, chitosan was investigated without the use of the acidic solution in order to avoid the increase of pH value in soil.

Biopolymer-treated soil is expected to be exposed to atmospheric influence such as heat, wind, and moisture. Several researchers showed that biopolymer treatment of sand can be effective against wind erosion (Kavazanjian Jr et al. 2009; Alsanad 2011; Chen et al. 2015). Qureshi et al. (2017) investigated biopolymer-treated soil and cement-treated soil under the

slaking test. The finding was that concentrations of 2, 3, and 5% of the tested biopolymer showed better resistance to slaking than specimens with 10% cement (Figure 1-3).

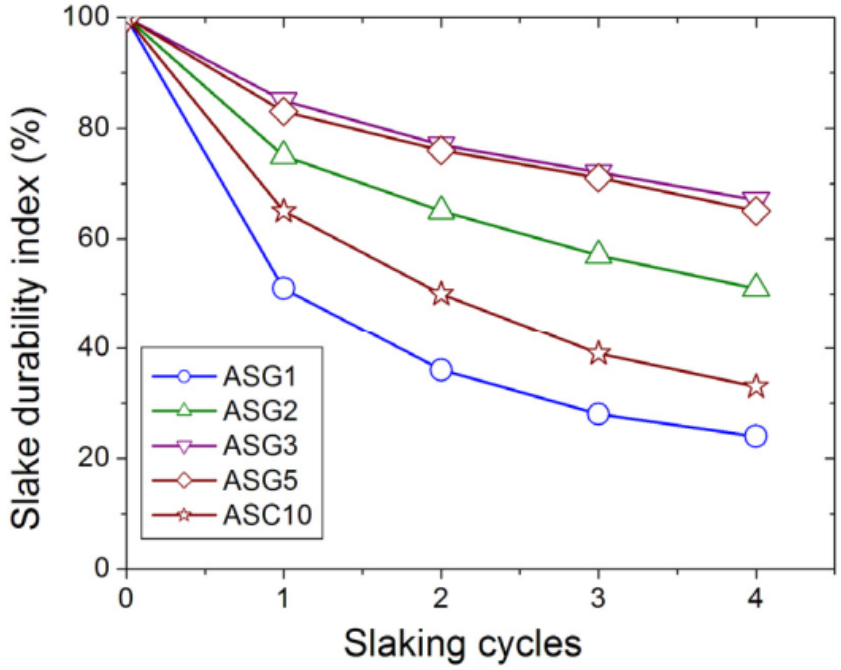

Figure 1-3: Slake durability test results (ASC10 - soil treated with 10% cement; ASC - soil treated with xanthan gum) (Qureshi et al. 2016)

Biopolymers are soluble in water, and therefore, biopolymer-treated soils being exposed to cyclic wetting and drying in the field can significantly affect the mass of biopolymer-treated soil and its engineering properties. The interaction of biopolymers with water increases the water content of the soil mass, which is directly related to the strength of the soil. That phenomenon will be further discussed in Chapter 4. Experimental observation related to wetting and drying of biopolymer-treated soil has been previously performed (Chen et al. 2015b). Chang et al. 2017 showed that the compressive strength and Young's modulus of gellan gum treated sand decreases due to cyclic wetting and drying. However, the comprehensive investigation of the durability against cyclic wetting and drying of the different types of biopolymer-treated soil composites has not been investigated.

Even though certain researchers contributed to the numerical analysis of biopolymer-treated soil, this area of study is still severely underinvestigated. Khachatoorian et al. 2003 investigated the gelation of a biopolymer-treated porous medium and its correlation to permeability. Chen et al. (2016) made a comparison between numerical and experimental analysis of the strength of biopolymer-treated composites for mine tailings. The strength of the composites was experimentally investigated by penetration tests. The material properties obtained from the penetration tests were used for the numerical analysis. Their discrete element method confirmed the findings of the experimental research. Ayeldeen et al. (2017) created a numerical model that showed the interaction between a linear-elastic footing and the underlying soil. The soil, before and after the biopolymer treatment, was characterized by Mohr-Coulomb's failure criterion and it was analyzed under the finite element method. The numerical analysis showed the increase in bearing capacity in the soil after the biopolymer treatment. The numerical responses of the soil before the biopolymer treatment were also in agreement with in situ testing. The numerical analyses of biopolymer-treated soil are the key factors that have to be deeply researched in order to implement biopolymers as additives for soil stabilization in the engineering practice.

Additional background and literature review will be presented in each of the following chapters.

1.2 RESEARCH OBJECTIVES

The main objectives of this research are listed below in the order in which they are addressed in the dissertation:

- Obtain comprehensive knowledge on the theories and current research on the properties and behavior of biopolymer-treated soil

- Examine the influence of different biopolymers, biopolymer concentration, and time on the gain in strength of biopolymer-treated soil.
- Investigate the change in mechanical properties of different types of soil after being treated with xanthan gum, which is one of the most promising biopolymers for soil stabilization.
- Analyze the influence of water on the degradation of the mass of soil after being treated with xanthan gum and guar gum
- Evaluate the loss of strength of soil enhanced with xanthan gum and guar gum due to cyclic wetting and drying
- Develop and implement a combined analytical-numerical algorithm to capture the stress-strain response of biopolymer-treated soil and perform diagnostic strain localization
- Conduct the quantitative assessment on the influence of the biopolymers on the inception of strain localization and the orientation of the deformation bands
- Validate the inception of strain localization through the digital image correlation analysis.

1.3 MOTIVATION AND CONTRIBUTION

The primary motivation for this study is the search for eco-friendly solutions for soil stabilization. We live in a fast-developing world where environment destruction poses constantly growing treat. Therefore, the need for eco-friendly solutions in every type of industry in high demand. Over the course of the years, biopolymers showed great potential for eco-friendly soil stabilization. However, they have not found their way into civil engineering practice because of the lack of understanding of biopolymer-soil-water interaction.

In particular, this study continues on the previous research that revealed the potential of biopolymers on soil strength improvement. Five different biopolymers and their effect on compressive and tensile strength of soil were researched. Previous foundings were affirmed and expanded for xanthan gum, guar gum, beta-glucan, chitosan, and alginate. Additionally, soil strength properties under the influence of xanthan gum, as one of the most effective biopolymers for soil remediation, were observed in the interaction of xanthan gum with different categories of soil together.

Previous research revealed xanthan gum and guar gum as some of the most dominant biopolymers for the improvement of soil strength. What previous findings did not take into account is the susceptibility of xanthan gum and guar gum to water. Even though often was accentuated that biopolymers are soluble in water, only limited research on this topic was performed with biopolymer gellan gum (Chang et al. 2017). There has been no research that investigated the influence of wetter durability on the behavior of soil treated with xanthan gum or guar gum. This research investigates the loss of strength of two types of soil treated with xanthan gum and guar gum due to the influence of wetting and drying. Furthermore, the degradation process of the treated soil due to wetting and drying was investigated. Considering the fact that soil is likely to be exposed to cyclic wetting and drying, this aspect of biopolymer-treated soil has to be covered to implement biopolymers in civil engineering practice.

Another important reason why biopolymers have not found their way into the civil engineering practice is the lack of numerical analyses that can capture the macro-level stress-strain responses of biopolymer-treated soil. Previous numerical analyses were useful initiators of numerical analyses of biopolymer-treated soil, but there is still no significant progress in understanding and modeling the behavior of the treated soil. This study numerically investigates the stress-stress responses of the soil treated with xanthan gum, guar gum, and beta-glucan. In addition, an additional goal of the numerical analysis is to

detect the inception of the strain localization and assess the biopolymer effect on it. The strain localization is likely to be followed by the failure of the material. Therefore, understanding the link between the biopolymers and the failure of the treated soil might help to their application in civil engineering.

1.4 DISSERTATION ORGANIZATION

The dissertation is divided into six chapters as follows:

- *Chapter 1 – Introduction*: This chapter gives a general background on biopolymers and their application. In addition, it points out the objectives, motivation, and dissertation structure.
- *Chapter 2 - Biopolymers as an eco-friendly solution for the enhancement of soil mechanical properties:* This chapter talks about the strength of soil improved with five different types of biopolymers. In the second chapter, the type of soil is a constant variable while the biopolymer type, biopolymer concentration, and time are the changing variables.
- *Chapter 3 - Study on shear strength of xanthan gum-treated soil:* This chapter talks about the influence of xanthan gum on the mechanical properties of three different types of soil. In this chapter, the biopolymer type, biopolymer concentration, and time are constant factors, while the type of soil is the changing variable.
- *Chapter 4 - Durability against wetting-drying cycles of biopolymer-treated soil:* This chapter describes the durability of biopolymer-treated soil under wetting and drying cycles. In this chapter, soil type, biopolymer type, and biopolymer concentration are the changing values.
- *Chapter 5 - Effect of biopolymers on the strain localization of treated soil*: This chapter describes an analytical-numerical analysis of the biopolymer-treated soil to find their influence on the inception of the strain localization in soil.

- *Chapter 6 – Summary, conclusions, and future research*: This chapter presents the concluding remarks that summarize the research findings and their application in practice. Also, this chapter presents recommendations for future research opportunities.

2. BIOPOLYMERS AS AN ECO-FRIENDLY SOLUTION FOR THE ENHANCEMENT OF SOIL MECHANICAL PROPERTIES

This chapter was published in:

Soldo, A., Miletić, M. and Auad, M.L., 2020. Biopolymers as a sustainable solution for the enhancement of soil mechanical properties. Scientific Reports, 10(1), pp.1-13. (Impact Factor: 4.011, 5-Year Impact Factor: 4.525).

This chapter was altered from the published version for the purposes of this dissertation. My primary contributions to the paper included: (i) understanding effect of different biopolymers on the strength of soil, (ii) gathering and reviewing literature, (iii) development and design of methodology, (iv) collecting, processing, analyzing, and interpretation of the experimental data, (v) most of the writing.

2.1 ABSTRACT

Improving soil engineering properties is an inevitable process before construction on soft soil. Increasing soil strength with chemical stabilizing agents, such as cement, raises environmental concerns. Therefore, eco-friendly solutions are in high demand. One of the promising solutions is the usage of biopolymers. Five biopolymer types were investigated in this study: Xanthan Gum, Beta 1,3/1,6 Glucan, Guar Gum, Chitosan, and Alginate. Their effect on the soil strength improvement was experimentally investigated by performing unconfined compression, splitting tensile, triaxial, and direct shear tests. All tests were performed with different biopolymer concentrations and curing periods. Additionally, in order to have an insight on the susceptibility to natural elements, plain soil, and biopolymer-treated specimens were exposed to real atmospheric conditions. The extensive experimental results showed that the soil strength tends to increase with the increase of biopolymer

concentration and with the curing time. However, it was shown that the soil strength does not considerably change after a certain biopolymer concentration level and curing time. Furthermore, it has been observed that the biopolymer-treated specimens showed better resistance to the influence of the environmental conditions. In general, Xanthan Gum, Guar Gum, and Beta 1,3/1,6 Glucan showed the most dominant effect and potential for the future of eco-friendly engineering.

2.2 INTRODUCTION

Rapid population growth and urbanization often cause the need to build over soft and unfavorable soil present in adverse surroundings. This further urges the need to improve the originally non-favorable soil. Soil improvement technologies can be divided into three major groups: mechanical, biological and chemical soil improvement technologies. The most common chemical stabilizing agents that are used for chemical soil stabilization are cement and lime. However, their use raises many environmental concerns such as CO_2 emissions due to cement production (Andrew 2018), prevention of vegetation growth, groundwater contamination, and heat island creation, to name a few. In fact, in 2002, the production of cement contributed about six percent to the world's CO_2 emission (Metz et al. 2005), and Andrew (2018) had pointed out the possible increase of that number in more recent years. Therefore, the demand for eco-friendly solutions for ground improvement is in high increase.

Biological approaches are emerging in the field of geotechnical engineering and techniques like microbial induced carbonate precipitation (MICP) have shown to be an effective means of effectively improving soil strength and the load-bearing capacity (DeJong et al. 2010; Chang et al. 2016; Choi et al. 2016; Umar et al. 2016; Li et al. 2018). However, these biological approaches require the presence of a large microbial community which may result in the generation of effluent ammonia. Furthermore, the MICP method is limited to the

coarse-grained soils due to microbe infiltration problems. This is because the pores of the fine-grained soils are too small to provide an appropriate bacteria growth environment (Ashraf et al. 2017). Therefore, it is desirable to seek a non-microbe, but still bio-inspired and eco-friendly ground improvement solution.

An attractive alternative to MICP is the soil improvement with biopolymers because it does not require microorganism's cultivation in the soil (Ashraf et al. 2017). Biopolymers are organic polymers that are produced by different biological organisms (Chang et al. 2016). In nature, biopolymers can be found in large amounts. They are biodegradable with no reported negative effects on the environment. Therefore, they might be favorable soil-improvement material (Chang et al. 2016). Also, unlike MICP, biopolymer treatment can be used for the improvement of fine-grained soil (Chang et al. 2015c; Aguilar et al. 2016).

According to the previous research, biopolymers, such as Guar Gum (GG), Xanthan Gum (XG), Chitosan (CHI), and Beta 1,3/1,6 Glucan (BG), can significantly improve engineering properties of soils (Chen et al. 2013, 2019; Latifi et al. 2017; Wiszniewski et al. 2017; Hataf et al. 2018; Toufigh and Kianfar 2019). The effect of XG on soil properties was investigated by various researchers and it was found that XG can considerably increase the compressive and shear strength of soils, especially of soils that contain a significant amount of fine-grained aggregates (Chen et al. 2013; Das et al. 2015; Chang et al. 2015a). In was also shown that XG can decrease the settlement of collapsible soils (Ayeldeen et al. 2017). GG, aside from soil strength improvement, can also be used for sand stabilization, liquid shoring (Day 1999; Gupta et al. 2009), and the reduction of soil compressibility (Ayeldeen et al. 2017). Chang & Cho (2012, 2014) showed that BG can increase the compressibility of soil, as well as the plasticity index and the compressive strength. CHI can improve soil strength, but its effect decreases with the reduction of water (Hataf et al. 2018). Therefore, the additional strength that could be achieved with the addition of CHI to the soil fades as the soil becomes

dry. Alginate (ALG) is a biopolymer that was extensively used in biomedical industries (Lee and Mooney 2012), but its potential for soil improvement has not been well investigated yet.

Nevertheless, even though biopolymers show substantial environmental and technological contributions to the improvement of soil engineering properties, biopolymers are still underutilized in geotechnical engineering practice. Some of the main reasons are the lack of adequate characterization of their engineering behavior and the lack of analysis methods that engineers could use to incorporate biopolymers into their designs. Therefore, the main objectives of this research are to develop an eco-friendly, biopolymer-based soil improvement and to investigate the effect of biopolymers on soil strength. In the presented study, five types of biopolymers (XG, BG, GG, CHI, and ALG) with different biopolymer concentrations were investigated (1%, 2%, and 4%). Furthermore, since curing time and water content are some of the key factors that influence the strength of soil, the relation between them and the strength of the biopolymer-treated soil was observed.

2.3 MATERIALS AND METHODOLOGIES

2.3.1 BASE SOIL

The selected base soil for this study was Piedmont soil. It was classified following the American Society for Testing and Materials (ASTM), ASTM D6913-17 and ASTM D4318-17. Figure 2-1 depicts the grain size distribution curve for the soil used in this study and inticates it was mostly sand. The soil had 39% fine particles with the liquid limit, plastic limit and the index of plasticity being 49, 29, and 20, respectively. Therefore, according to the Unified Soil Classification System, fine particles are classified as silt with low plasticity, and the overall classification of the soil that was used in this study was SM (silty sand).

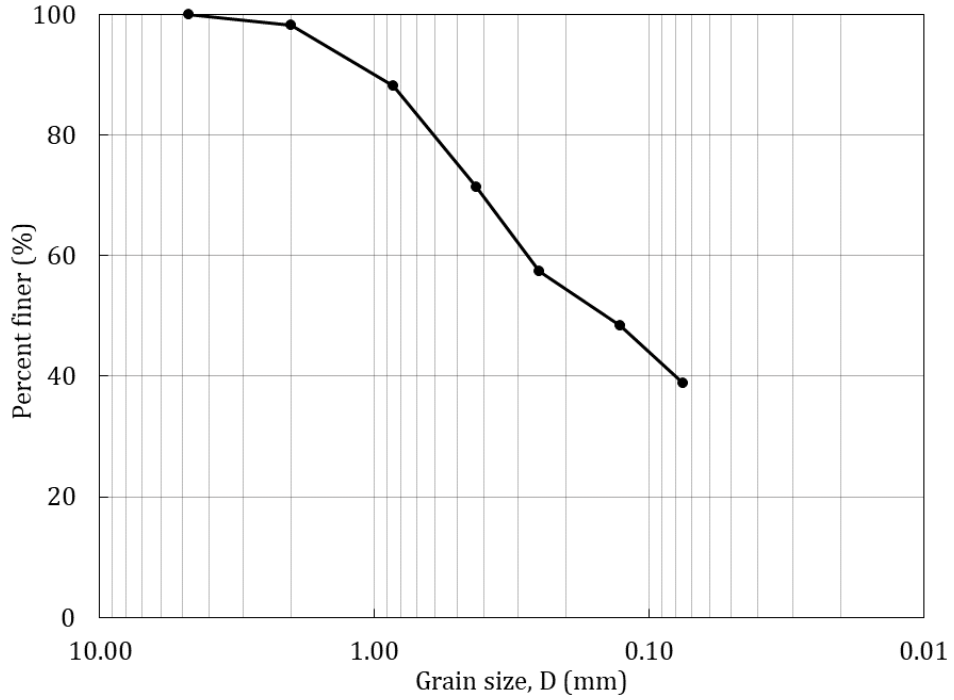

Figure 2-1: Grain size distribution of the base soil

2.3.2 BIOPOLYMERS

Five different biopolymers were used in this study and their properties are described in the text below.

2.3.2.1 Xanthan gum

XG is a polysaccharide made by the fermentation of a carbohydrate-source medium e.g. glucose. Xanthomonas campestris bacterium is the bacteria which induces the fermentation process that creates XG (Katzbauer 1998). XG can be dissolved in hot and cold water and it also increases the viscosity of the medium it is mixed in. Solutions containing XG are non-Newtonian with high pseudoplasticity, which means that their viscosity decreases with an increase in shear stress (Katzbauer 1998). Nowadays, it can be found in the cosmetic industry, food industry, agriculture (Katzbauer 1998), oil drilling industry (Rosalam and England 2006), and civil engineering (Chang et al. 2015a).

2.3.2.2 Guar gum

GG is a polysaccharide extracted from guar beans or guar, officially known as Cyamopsis Tetragonolba. Like XG, it can dissolve in hot and cold water. Because solutions with GG act as gels or binders, it is found in various industries e.g. cosmetic industry, food industry (Bourriot et al. 1999), oil and gas drilling industry (Thombare et al. 2016), and in civil engineering (Chang et al. 2015a).

2.3.2.3 Beta 1,3/1,6 glucan

BG is a carbohydrate made of glucose molecules that are bound by glucopyranose (Volman et al. 2008). Yeast, fungi, cellulose, cereals and some bacteria contain BG (Bacic et al. 2009) . Like XG and GG, BG dissolves in water at any temperature and creates gelatinous solutions (Bacic et al. 2009). This type of biopolymer is being extensively investigated for its potential for providing health improvement benefits (Volman et al. 2008; Baldassano et al. 2017). Furthermore, it has been used in civil engineering (Chang and Cho 2012; Chang and Cho 2014).

2.3.2.4 Chitosan

Amino polysaccharide chitosan can be obtained by deacetylation of chitin. Chitin is a biopolymer abundant in nature and it is contained in shells. CHI is characterized by hydrophilicity, biocompatibility, biodegradability, and non-toxicity (Ahlafi et al. 2013). Currently, CHI is present in the cosmetic industry, pharmaceutical industry, agriculture (Shahidi and Synowiecki 1991), food industry, and in civil engineering (Hataf et al. 2018).

2.3.2.4 Alginate

ALG is an anionic biopolymer and is usually obtained from brown seaweed e.g. Laminaria japonica, Macrocystis pyrifera, Ascophyllum nodosum, Laminaria hyperborean, etc. (Smidsrod and Skjakbrk 1990). It is characterized by low toxicity, relatively low cost,

biocompatibility, and mild gelation when mixed with divalent cations. Therefore, it is being investigated for more different applications while mostly being used for biomedical purposes (Lee and Mooney 2012; Gombotz and Wee 2012).

2.3.3 SPECIMEN PREPARATION

All mixing quantities were batched using an electronic balance and mixed with the stainless-steel stirrer. Due to the different nature of the biopolymers, several mixing techniques were considered.

- Method A; dry soil and dry biopolymers were uniformly mixed and water was additionally sprayed and mixed with the soil
- Method B; dry soil and dry biopolymers were uniformly mixed and water was gradually poured in and mixed with the soil
- Method C; the soil was mixed with water and biopolymers were mixed into the wet soil
- Method D; biopolymers were dissolved in water and mixed into the dry soil
- Method E: biopolymers were dissolved in water and mixed into that was previously wetted

Two out of five methods showed the best workability of the soil-biopolymer-water blend and were selected for this study. Method A was used for the majority of biopolymer treatments.

While using Method A, all dry components (base soil, and biopolymer) were first slowly mixed together for a few minutes. Four types of biopolymers (XG, GG, CHI, and BG) were mixed into the soil with three different concentrations (1%, 2%, and 4 %) with the respect to the mass of the base soil. After mixing a biopolymer with soil, water was sprayed in the soil-biopolymer mixture up to 16.5 % of the mass of the base soil. Water was the most important factor in the preparation of the specimens. The water content of 16.5 % corresponded to the optimum water content of the soil and it was selected as relatively best

for the specimen preparation. Lower water contents produced non-uniform soil samples, whereas higher water contents increased the softness of specimens which hindered the specimen preparation. While adding water, the soil-biopolymer mixture was continuously mixed to ensure homogeneous water distribution.

ALG was the only biopolymer that was prepared with Method D. The reason for that was the fact that ALG required a binding agent, such as calcium chloride, which has the ability to hold the ALG chain-molecules together. Therefore, alginate was first dissolved in water (13.5 % of the mass of the base soil). Separately, calcium chloride was also dissolved in water (3 % of the water of the mass of the base soil). In this case, water was not sprayed into the soil, but the dissolved alginate was mixed with the base soil. After that, the dissolved calcium chloride was added into the mixture. In addition, it was noticed that the dissolving process was not the same for all ALG concentrations. The lower concentrations of ALG in the ALG-water solutions were more uniform than higher concentrations. Therefore, the higher ALG concentration (4%) was omitted from the research due to the bad workability of the 4% ALG-water solution.

Finally, once the dry components were fully mixed with the liquid part, the blends of soil, biopolymer, and water were placed in cylindrical molds and evenly compacted. The mold for the specimens which were tested for unconfined compression had a diameter of 3.3 cm and a height of 7.1 cm. Specimens were compacted in five layers with a standardized hammer. Each layer was compacted by applying pressure twenty-five times on the surface of the soil that was in the cylinder. The mold that was used to make the specimens for the splitting tensile strength test had a diameter and height of 3.5 and 1.8 cm, respectively. The mold was filled with soil and compacted in three layers with twenty-five hits for each layer. Specimens for the triaxial test were compacted in five layers in a mold with a diameter of 7 cm and a height of 14 cm. The mold used for the direct shear test had a diameter of 6.3 cm and a height of 2.5 cm. The soil was compacted in three layers where each layer was

compressed approximately twenty-five times. After compaction, specimens were extruded from the molds (Figure 2-2) and left to cure for a specific amount of time. Specimens for the unconfined compression and splitting tensile test were tested after one hour, five days, and 30 days of the preparation. Additionally, specimens with 1% XG, GG, and BG were tested under uniaxial compression conditions every 24 hours during the first five days after the preparation. Triaxial tests and direct shear tests were performed after five and 30 days of curing.

Molds for the unconfined compression and splitting tensile strength tests were also used to make specimens that were investigated under the influence of the environment. After preparation, those specimens were first left to dry in the laboratory conditions for 10 days after which they were placed in the open air to go through cycles of wetting and drying for 30 days. For this type of experiment, specimens were made of plain soil and soil with 2% XG.

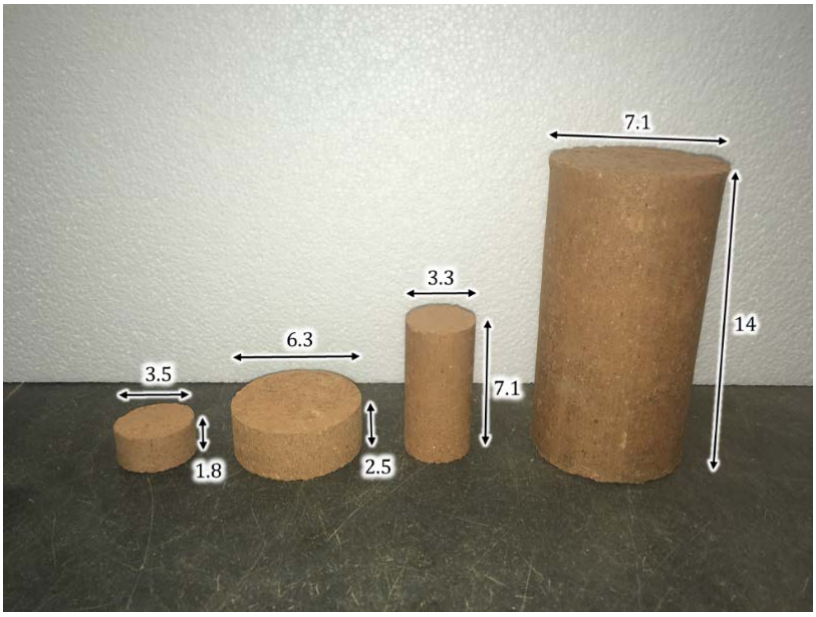

Figure 2-2: Photo of the splitting tensile test (left), direct shear test (middle-left), the unconfined compressive test (middle-right), and the triaxial test (right) specimens with their dimensions (all dimensions are in centimeters)

2.3.4 MECHANICAL TESTING

Unconfined compression (UC), splitting tensile (ST), unconsolidated undrained triaxial (UU), and direct shear (DS) tests were carried out to determine and analyze the mechanical properties of specimens made of plain and biopolymer-treated soil. After compaction and extraction from the molds, one portion of specimens was tested within an hour of preparation (wet specimens) and other specimens were tested after designated curing time.

2.3.4.1 Unconfined compression test

The uniaxial or unconfined compression test also known as a cylinder compression test is the appropriate test for determination of the compressive strength of a cohesive soil regardless of the amount of biopolymers that it may contain. For determination of compressive strength, the axial load was applied with a strain rate of 1.5% /min, as per American Society for Testing and Materials Standard (ASTM) ASTM D2166. The compressive strength of the specimen was computed by dividing the maximum load attained during the test by the cross-sectional area of the specimen. Furthermore, in order to obtain Young's modulus, E, of a sample from an UC test, the applied load, and a longitudinal deformation were recorded. Young's modulus was extracted from the slope of the straight line passing through the origin.

2.3.4.2 Splitting tensile strength test

A direct tension test is the most direct way of collecting the information needed for the determination of material tensile properties experimentally. However, direct testing of the tensile strength of soil comes with a lot of issues regarding boundary conditions and the fragility of the material. Therefore, a quicker and simpler alternative to the direct tension test is an indirect ST test. Its advantages over the direct tension test are that it is fairly easy to conduct, it has already been standardized, which makes it a cheap and highly applicable

test in practice. ST tests were performed following general procedures described in the ASTM D3967-16 but with a modified apparatus to accommodate small specimen sizes and relatively low loads. The load was applied at the constant strain rate of 1.5 %/min. It must be noted that an ST test does not give direct soil tensile properties under tensile loading. Thus, the tensile strength was back-calculated from the maximum compressive load and the dimension of the specimens using the following formula (Akin and Likos 2017):

$$\sigma = \frac{2P}{\pi LD} \tag{2.1}$$

where σ_T is tensile strength; P is a compressive force at failure; D is the diameter of the specimen; L is specimen thickness.

2.3.4.3 Undrained unconsolidated triaxial test

One of the advantages of triaxial tests is that they can be performed under a broad range of confining pressures. That means that triaxial tests can be used, to some extent, to replicate the stress conditions in soil that are present in the field. UU test is the fastest triaxial test which can be used to find the maximum deviatoric stress and undrained shear strength at different confining pressures. In this study, UU was performed in accordance with ASTM D2850-15. The specimens were placed in a plexiglass chamber under the confining pressure of 100 kPa. During the shearing stage of the test, the axial strain was applied under the rate of 0.7 %/min. UU tests were carried out after five and 30 days of curing. From the preliminary data collected by the authors, it was evident that XG, GG, and BG showed the most promising results for the improvement of soil strength. Therefore, only those three types of biopolymers were investigated under the UU test.

2.3.4.2 Direct shear test

The DS test is commonly used to determine the cohesion and internal friction angle of soil. Those shear strength parameters cannot be obtained from UC, ST, and UU tests. Consolidated

drained triaxial test, and consolidated undrained triaxial test can provide cohesion and friction angle, but they are not suitable for biopolymer-treated soil specimens. The reason behind that is that biopolymers tend to dissolve in water (Endres and Siebert-Raths 2011). Therefore, adding water to biopolymer-treated soil would hinder the strength of the soil. The DS test was performed in accordance with ASTM D3080-11. The shearing was conducted under normal loads in the range between 100 kPa and 760 kPa. The rate of shearing displacement was set as 0.06 cm/min. Since it was concluded from the preliminary UC and ST test results that XG, GG, and BG had the most dominant effect on the soil strength, the DS tests were conducted only on the soil specimens improved with these three biopolymer types. From the preliminary results of the UC test, the selected concentrations were 2% XG, 1% GG, and 4% BG. The tests were conducted after five and 30 days of curing.

2.3.5 SCANNING ELECTRON MICROSCOPE IMAGING

Soil-biopolymer interaction varies depending on the engaged types of soil and biopolymer. For instance, fine-grained particles and biopolymers have electrically charged surfaces which creates an electrostatic bond between them (Chang et al. 2015a). The electrical surface charge in coarse-grained soils is practically non-existent; thus, the bond that is created between coarse-grained material and biopolymer can be presented as a thin film wrapped around coarse particles (Chang et al. 2015c). In this study, a Scanning Electron Microscope (SEM) Zeiss EVO 50 was used to closely observe the interaction between the silty sand and different types of biopolymers. Small fractions of biopolymer-treated soil, with a size of 0.2-0.3 cm^3, were glued to a carbon tape on the top of aluminum stubs. The specimens were then coated with a thin layer of gold to prevent charging of the analyzed surface, to promote the emission of secondary electrons so that the specimen conducts evenly, and to provide a homogeneous specimen surface for analysis and imaging.

2.4 RESULTS AND DISCUSSION

Several samples that were prepared in the same manner were tested in each test, and the average values of the results are presented in this chapter.

One of the issues that this study did not consider was separating the effect of particle bonding and the effect of soil suction due to the presence of biopolymers. Therefore, all presented material properties are related to the parameters of total stress. However, it is considered that the main effect on the soil strength was the result of biopolymer bonding. The effect of water and water surface tension on the soil strength will be more discussed in Chapter 4.

2.4.1 UNCONFINED COMPRESSION TEST

Soil with different admixtures showed different strengths when tested in the UC test. Figure 2-3 shows the influence of different types and different concentrations of biopolymers on the compressive strength of the wet specimens which were tested within an hour of the preparation. It can be seen that for the biopolymer-treated specimens, an increase in the biopolymer concentration resulted in the increase of its compressive strength. The only series of specimens that did not follow this trend was with 2% XG and 2% CHI. ALG-treated specimens stand out with the lowest achieved compressive strengths as a result of their specific way of preparation. Even though Figure 2-3 shows a variety of achieved compressive strengths, further research showed that the change of strength that happens within one hour is not as substantial as the change that happens over a longer period of time. This indicates that within one hour of the preparation, the strength of wet specimens depended more on the base soil strength and less on the soil-biopolymer bond. This is because the biopolymers within one hour were still in a gelatinous form with low strength. Similar behavior was reported by Swain et al. (2018) where a dispersive soil was treated with various concentrations of XG and GG.

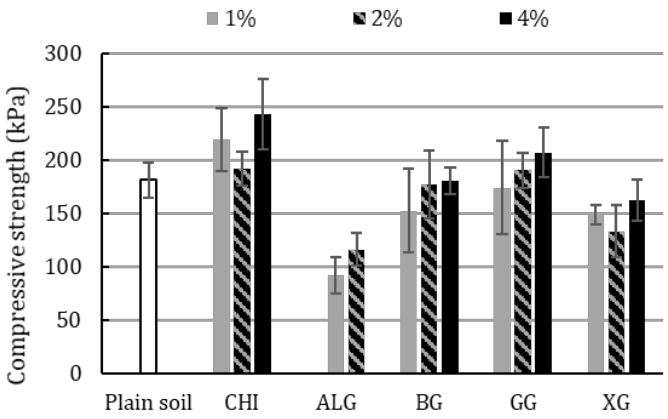

Figure 2-3: Influence of different type biopolymers and biopolymer concentration on the compressive strength of the specimens tested after one hour of curing (with standard deviation)

Figure 2-4 depicts the impact of different biopolymer types, biopolymer concentrations, and curing time periods (one hour, five days, and 30 days) on the compressive strength. The standard deviation of the results after five and 30 days can be found in Table 8-1 in the Appendix section. It is evident from the plot that the soil compressive strength considerably improved with time and biopolymer concentration. These findings coincide with other research studies that showed as well that the compressive strength of soil increases with the increase of biopolymer concentration and curing time of biopolymer-treated soil (Khatami and O'Kelly 2013; Chang et al. 2015a; Latifi et al. 2017). Biopolymers in soil harden with drying which further improves soil strength. XG had the highest impact on the increase of compressive strength. After five days of curing, CHI did not lead to any further increase in the compressive strength even though the specimens with CHI had the highest compressive strength right after the mixing. Therefore, CHI was excluded from further research of this type. The reason for the CHI's low effect on compressive strength was the fact that it requires acidic water to reach the maximum effect. The usage of the acidic water was avoided in this study because of its possible negative effect

on the environment. Furthermore, ALG solution showed a promising effect on strength improvement. However, the difference in the compressive strengths between ALG samples with different concentration levels was not high. Even though the higher concentration of ALG might have a larger impact on the improvement of the compressive strength, the workability at the higher concentrations of ALG can restrict the amount of ALG which can be applied to the soil. Specimens modified with BG, GG, and XG biopolymers showed the most dominant effect on the compressive strength with the XG being the most promising.

In addition, after comparing the achieved compressive strengths after five and 30 days of curing for all biopolymer-treated soil mixtures, it can be concluded that the strength did not go under major changes in the period between five and 30 days. Thus, it can be stated that the majority of the compressive strength developed within the first five days after the preparation. Similar behavior was reported by Cabalar et al. (2017) where XG-treated soil after three days achieved more than 70% of the compressive strength that was recorded after 28 days.

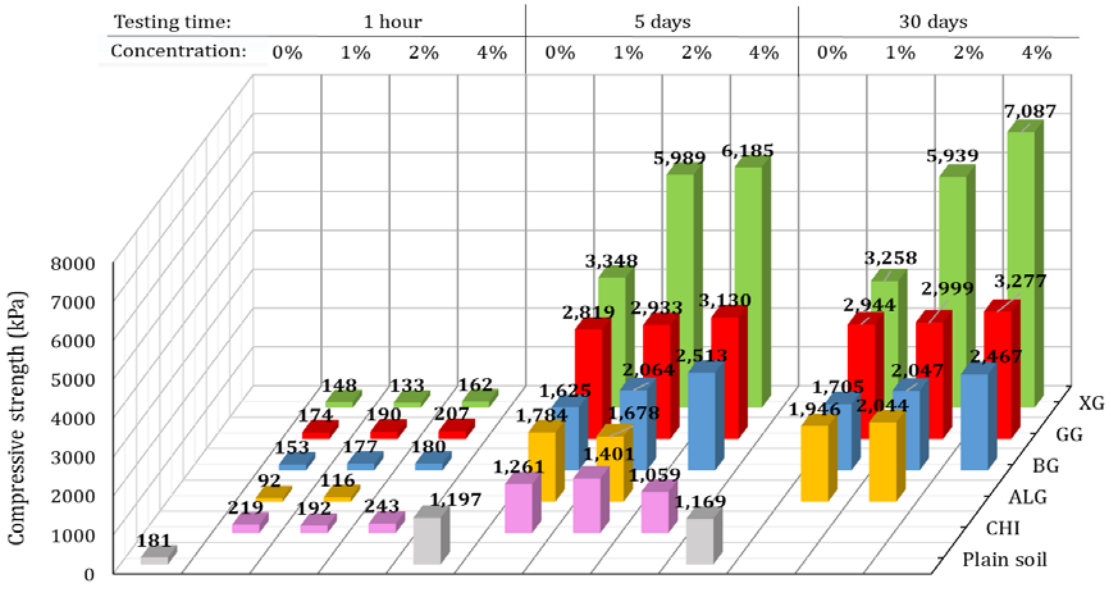

Figure 2-4: Change in compressive strength under the influence of time, biopolymer-type, and biopolymer concentrations

The presence of biopolymers increases Young's modulus (modulus of elasticity, E) of soil in a nonlinear manner.

Figure 2-5 depicts the change of E with the different concentrations of XG, GG, and BG after five days of curing. It can be seen that there is an optimum concentration at which E reaches its peak value. The optimum biopolymer concentration changes depending on the biopolymer type. From the experimental data, the optimum biopolymer concentration for GG, and XG is approximately around 1%, and 2%, respectively. Unlike for XG and GG, the optimum biopolymer concentration of BG cannot be well predicted from the obtained results and it might be past 4%. These results support the hypothesis of the existing optimum concertation of biopolymers which varies with the type of biopolymers and should be considered when utilizing biopolymers for soil stabilization. Also, Ayeldeen et al. (2017) investigated the effect of GG and XG on Young's modulus of silt. The concentration levels of biopolymers ranged between 0.25% and 2%. The results indicated that the optimum concentration for GG was between 1% and 2%, while in the case of XG, their results suggested that the optimum concentration was not under 2%.

Additional testing was performed in order to closely determine the time needed for the specimens to achieve their compressive strength. The specimens with 1% XG, GG and BG were mixed in the previously described manner and tested for UC (Figure 2-5b). Tests were performed an hour after the preparation and every 24 hours during a period of five days. As stated previously, moisture content has a major effect on soil strength. Thus, after each test, specimens were placed in the oven (110° C) for the purpose of measuring the moisture content. Figure 2-5b shows that the decrease in water content corresponds to the increase in the strength of the soil. Furthermore, it can be noted that most of the strength developed after three to four days of curing. After that time period, water content and compressive strength became constant. The inverse proportionality of water content and compressive strength is a typical relationship that was reported in other research as well (Chang and Cho

2012; Chang et al. 2015a).

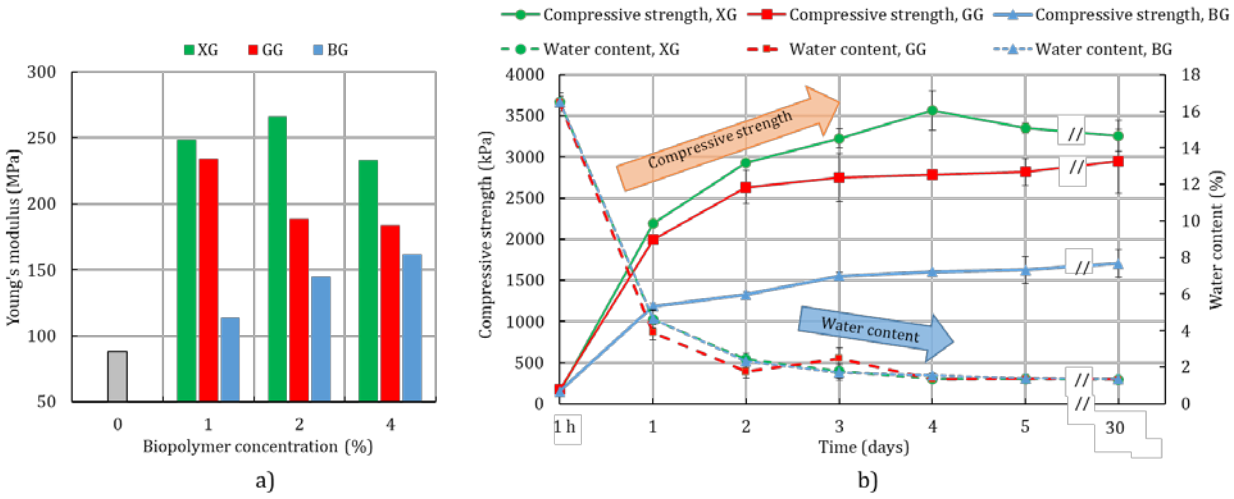

Figure 2-5: a) Influence of biopolymer type and concentration on Young's modulus (after five days of curing); b) Change in the average compressive strength and water content during 30 days of curing (with standard deviation)

2.4.2 SPLITTING TENSILE STRENGTH TEST

The increase of soil tensile strength with the addition of XG and GG was proven by direct tensile tests performed by Muguda et al. (2017). They have found that the tensile strength of soil increases with biopolymer concentration and time. Furthermore, Ma and Ma (2019) also showed an increase in the tensile strength of soil with the increase of sodium carboxymethyl cellulose concentration. In this study, during the first hour after the preparation, all tensile strengths were in the range of 20-60 kPa, and biopolymer-treated soil tensile strengths did not show a major deviation from the tensile strength of the plain soil (Figure 2-6). Errorbars in Figure 2-6 represent the standard deviation from the averaged results. Specimens made with ALG stood out with the lowest tensile strength. This is most likely due to the different preparation methods of ALG-improved specimens, which accentuates the importance of the

preparation method. Similar to the UC test results, one hour curing time was not long enough to develop a strong soil-biopolymer bond.

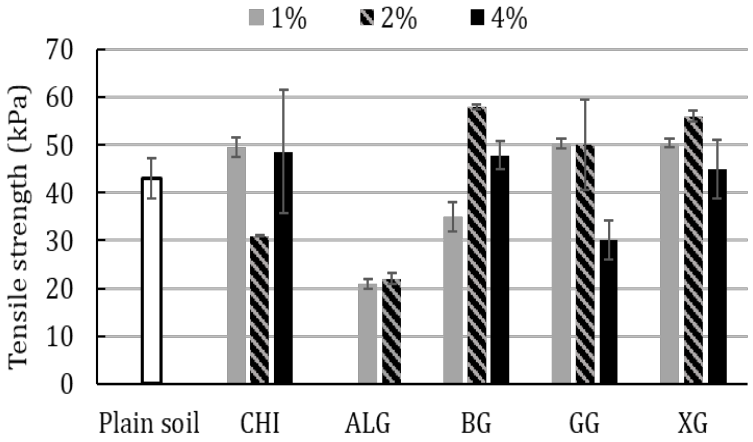

Figure 2-6: Influence of biopolymers on the tensile strength of the fresh specimens (with standard deviation)

Figure 2-7 shows the effect of different types of biopolymers, biopolymer concentration, and curing time on the soil tensile strength. The deviation from the averaged results in represented in Table 8-2 in the Appendix section. It is evident that the strength is considerably higher after five and 30 days than the strength which was achieved within one hour after preparation. Thus, once again, it can be concluded that biopolymers need curing time to achieve their potential. CHI showed the most negative influence on the tensile strength of soil, which happened mostly due to the loss of water. The concentration of 4% CHI had an especially negative effect on the tensile strength. Therefore, CHI was excluded from further research on tensile strength. ALG, BG, GG, and XG showed a positive effect on the tensile strength after five and 30 days but XG had the most dominant effect. As in the case of the UC, most of the strength was achieved during the first five days.

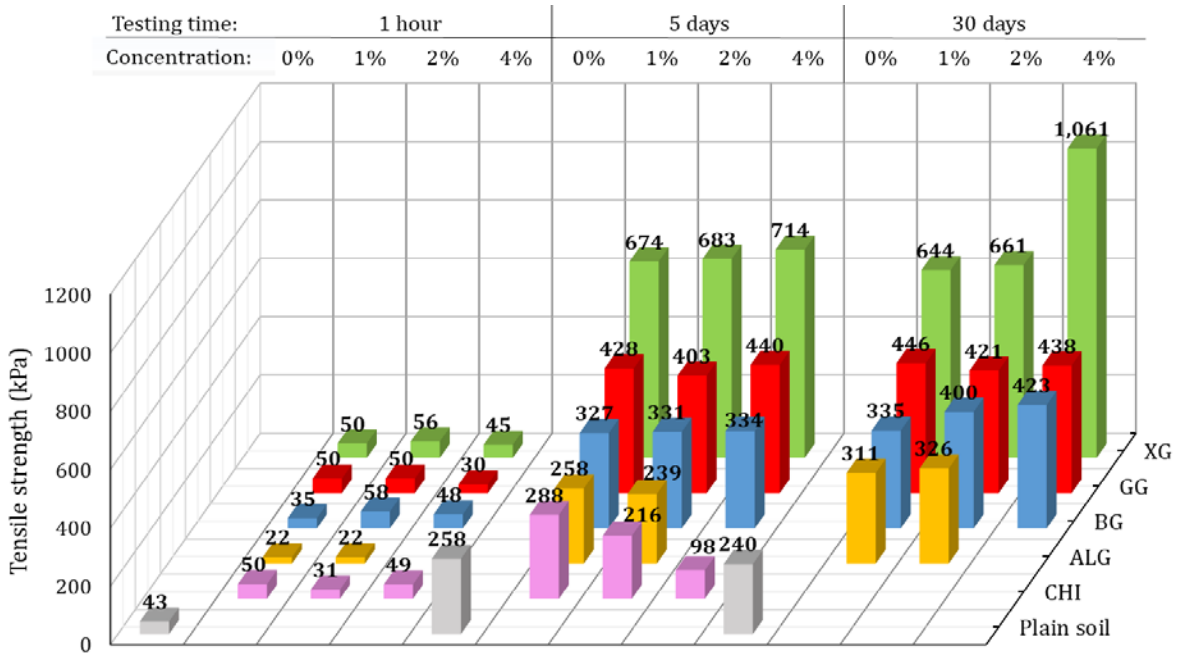

Figure 2-7: Change in tensile strength under the influence of time, biopolymer-type, and biopolymer concentration

2.4.3 UNCONSOLIDATED UNDRAINED TRIAXIAL TEST

Figure 2-8 shows the experimental stress-strain responses obtained from the UU triaxial tests on plain and biopolymer-treated specimens. Only those polymers that have achieved the most promising results in the prior testing were used in the UU testing program, namely, BG, GG, and XG. All specimens were tested five and 30 days after preparation. Unlike UC and ST test results, the difference in the maximum deviatoric stress of specimens tested after five and 30 days of preparation was notable. The reason for that is the fact that larger specimens need more time for water content to decrease while drying, and the soil strength increases with the loss of water content. Specimens for UC test and ST test had a volume of 60.7 cm^3 and 17.31 cm^3 respectively, but the specimens for UU test had a volume of 538.51 cm^3. Furthermore, this difference in the maximum deviatoric stress was more noteworthy for biopolymer-treated soil than it was for the plain soil. It was found that the improvement in

strength during the period between five and 30 days for the plain specimens was 10%.

For the soil specimens treated with XG, the concentration of 1% caused the increase in the maximum deviatoric stress by 66% between five and 30 days, whereas concentrations of 2 and 4% caused an increase of 64 and 22% for the same period, respectively (Figure 2-8a). It is important to notice that after 30 days the maximum deviatoric stress of the specimens made with 2% and 4% XG was higher than the testing machine capacity. Therefore, the highest measured values were taken as the maximum achieved values.

The addition of 1% GG resulted in the improvement of the maximum deviatoric stress by 51%, and for the specimens with 2% GG the improvement was 68% (Figure 2-8b). In addition, after five days of curing, specimens with 4% GG had lower peak deviatoric stress than the specimens with 1 and 2% GG. This might be related to optimum biopolymer concentration. A similar effect of the optimum biopolymer concentration was presented in Figure 5-2a where Young's modulus of soil started decreasing for the concentrations higher than 1% GG. After 30 days, the maximum deviatoric stress of soil treated with 4% GG increased by 120% in comparison to the maximum stress that was achieved after five days.

Similar as in the cases with XG and GG, BG also increased the maximum deviatoric stress of the specimens that were tested in the UU test. In the period between five and 30 days, specimens with 1, 2 and 4% BG had improved for 22, 20 and 34%, respectively (Figure 2-8c).

These findings are consistent with previous research studies of biopolymer-treated soil under triaxial loading conditions showing that biopolymers can increase the peak deviatoric stress (Cabalar et al. 2017; Muguda et al. 2017; Dehghan et al. 2018; Swain et al. 2018; Ma and Ma 2019). On the other hand, Karimi (1999) showed that the maximum deviatoric stress of 1% XG-treated silt can decrease in the period between five and 30 days. Even though consolidated triaxial tests were frequently used to demonstrate the strength of soil, the authors recommend using unconsolidated undrained tests for testing of biopolymer

treated soil. The reason behind that, as stated previously, is that biopolymers tend to dissolve in water (Endres and Siebert-Raths 2011). Adding water to biopolymer-treated soil would hinder the strength of the soil.

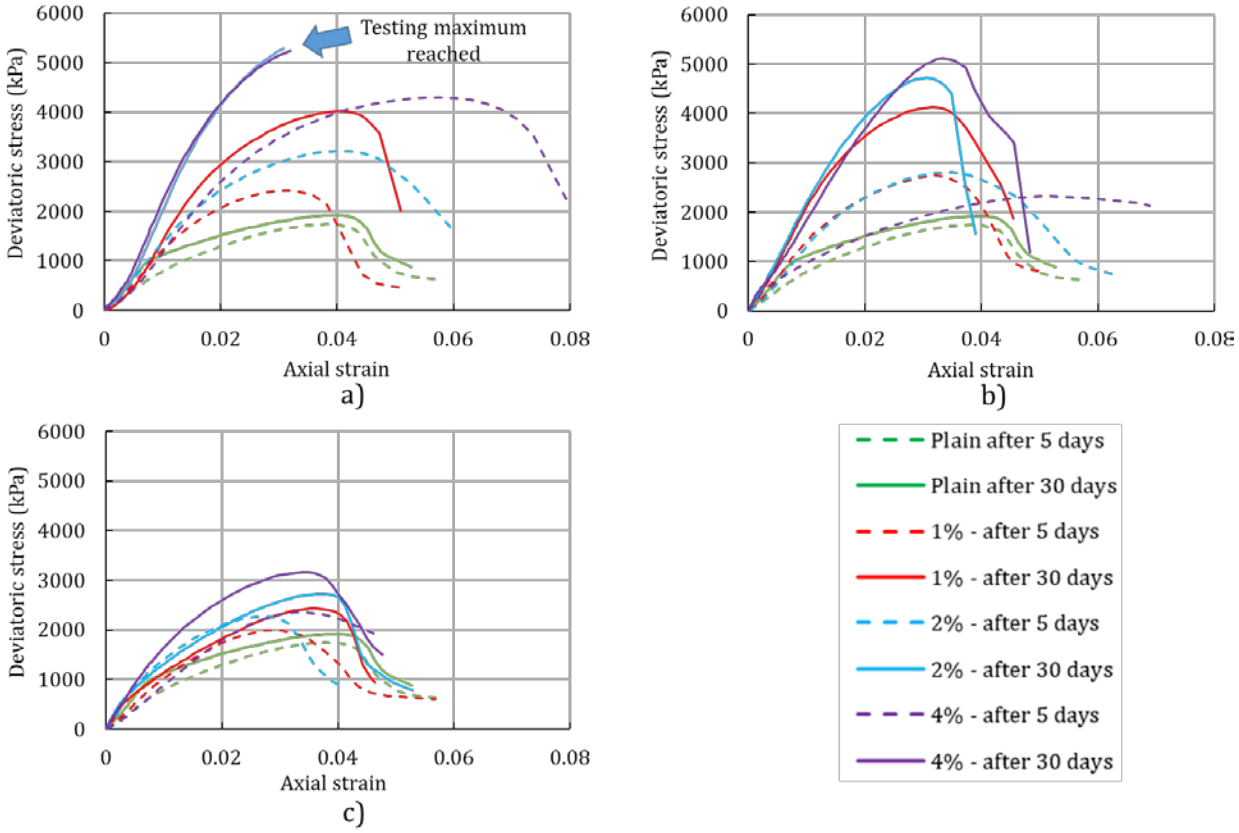

Figure 2-8: Experimental deviatoric stress versus axial strain. UU testing plots for different curing periods, biopolymer concentrations, and type of biopolymer: a) XG, b) GG, c) BG.

2.4.4 DIRECT SHEAR TEST

Previous research showed that the change in cohesion and the friction angle is depended on biopolymer and soil types. Cho and Chang (2018) used the direct shear test to investigate the effect of different concentrations of gellan gum on the cohesion and friction of sandy and clayey soil. Their results indicated that the cohesion increased with the increase of gellan gum concentration. The friction angle increased with the increase of gellan gum for the pure

clay and for the sand that had between 20% and 50% of clay. However, the change in the friction angle of pure sand was found negligible. Khatami and O'Kelly (2013) showed that agar and starch increase the cohesion of sand but reduce the friction angle. Ayeldeen et al. (2017) demonstrated with the direct shear test that XG and GG increase the cohesion of a soil that had a significant presence of fine particles, but the biopolymers slightly decreased the friction angle that soil.

In the present study, the main objective was to quantify the change in cohesion and the friction angle due to the influence of XG, GG, and BG for two different curing times. The strength envelopes from DS test results are depicted in Figure 2-9. The test results of the direct shear tests are presented in Figure 8-1 in the Appendix. The slopes of the plotted lines relate to the friction angles, and the intercepts with the vertical, shear stress axis represent the cohesion. The DS results are summarized in Table 2-1.

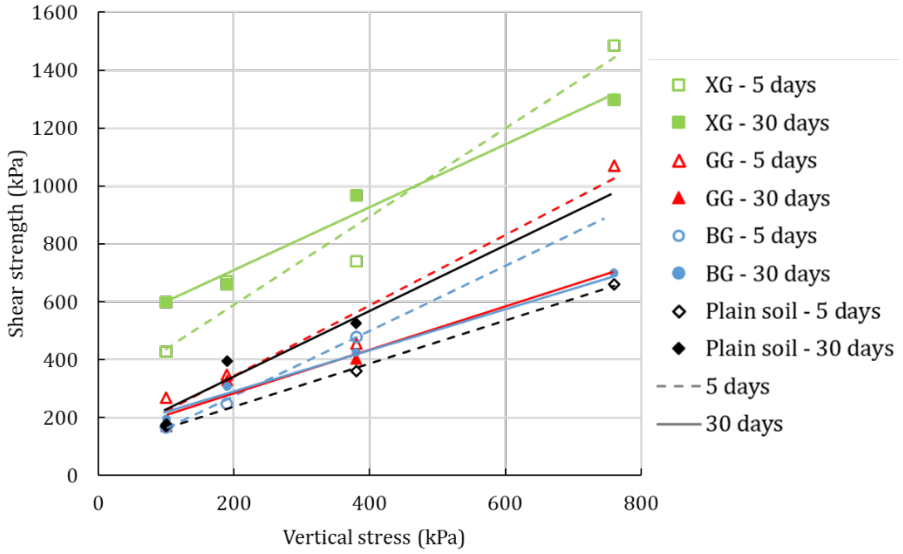

Figure 2-9: : Strength envelopes from DS test results

The plain soil had a cohesion of 89 kPa and the angle of friction of 36˚ after five days of curing. The cohesion increased by about 20 kPa in the period between five and 30 days. The soil reached a high friction angle through a period of 30 days because of its highly

compacted state.

The addition of the XG tripled the cohesion of the plain soil five days after the preparation. After 30 days, XG-treated soil had the cohesion of almost 500 kPa. The friction angle of XG-treated soil was 57˚ after five days of curing, but it dropped by 10˚ in the period between five and 30 days and it was close to the friction angle of the plain soil.

After five and 30 days of curing, the cohesion of GG-treated soil was 9 and 24 kPa higher than the cohesion of the plain soil, respectively. However, for the period between five and 30 days of curing, the friction angle dropped from 51˚ to 37˚ which was lower than the friction angle of the plain soil.

The cohesion of BG-treated soil, after five days, was half of the cohesion of the plain soil, but the cohesion increased by 100 kPa between five and 30 days after curing. In the same period, the friction angle reduced from 48˚ to 36˚ which was lower in value than the final friction angle of the plain soil.

This research concludes that XG, GG, and BG have the tendency to increase the cohesion of silty sand, but ultimately reduce the friction angle of the silty sand. The increase of cohesion is the result of the binding properties of biopolymers that glue the soil particles together. However, biopolymer formations tend to smoothen the surface of coarse particles which results in reducing the friction between soil particles and the overall friction angle of the soil (Ayeldeen et al. 2016).

Table 2-1: Influence of biopolymers and time on the cohesion and friction angle of soil.

Curing time	Plain soil		XG		GG		BG	
	Cohesion (kPa)	Friction angle (˚)	Cohesion (kPa)	Friction angle (˚)	Cohesion (kPa)	Friction angle (˚)	Cohesion (kPa)	Friction angle (˚)
5 days	89	36	285	57	98	51	44	48
30 days	107	49	493	47	131	37	144	36

2.4.5 SPECIMENS EXPOSED TO ATMOSPHERIC CONDITIONS

Nine samples were fully exposed to the influence of the environment. They were left uncovered in the open air. Daily temperature and relative humidity were measured in the field are they are summarized in Figure 2-10a. Also, days with rain presence were noted. Specimens were intended to be tested in the UC and ST test after 30 days. It can be noted from Figure 2-10b that the XG-improved specimens showed higher wetting-drying durability under the atmospheric influence. Plain specimens were severely damaged after 30 days and could not be tested in the UC nor ST tests. Specimens with 2% XG kept their shape for the entire 30 days. Thus, specimens with 2% XG were tested for UC and ST tests. Figure 2-10c shows the comparison in the strength of the biopolymer-treated specimens (with 2% XG) exposed to atmospheric conditions and the strength of plain specimens tested after 30 days of curing in the laboratory. It is evident that the treated specimens had higher strength even after being exposed to the influence of the environment.

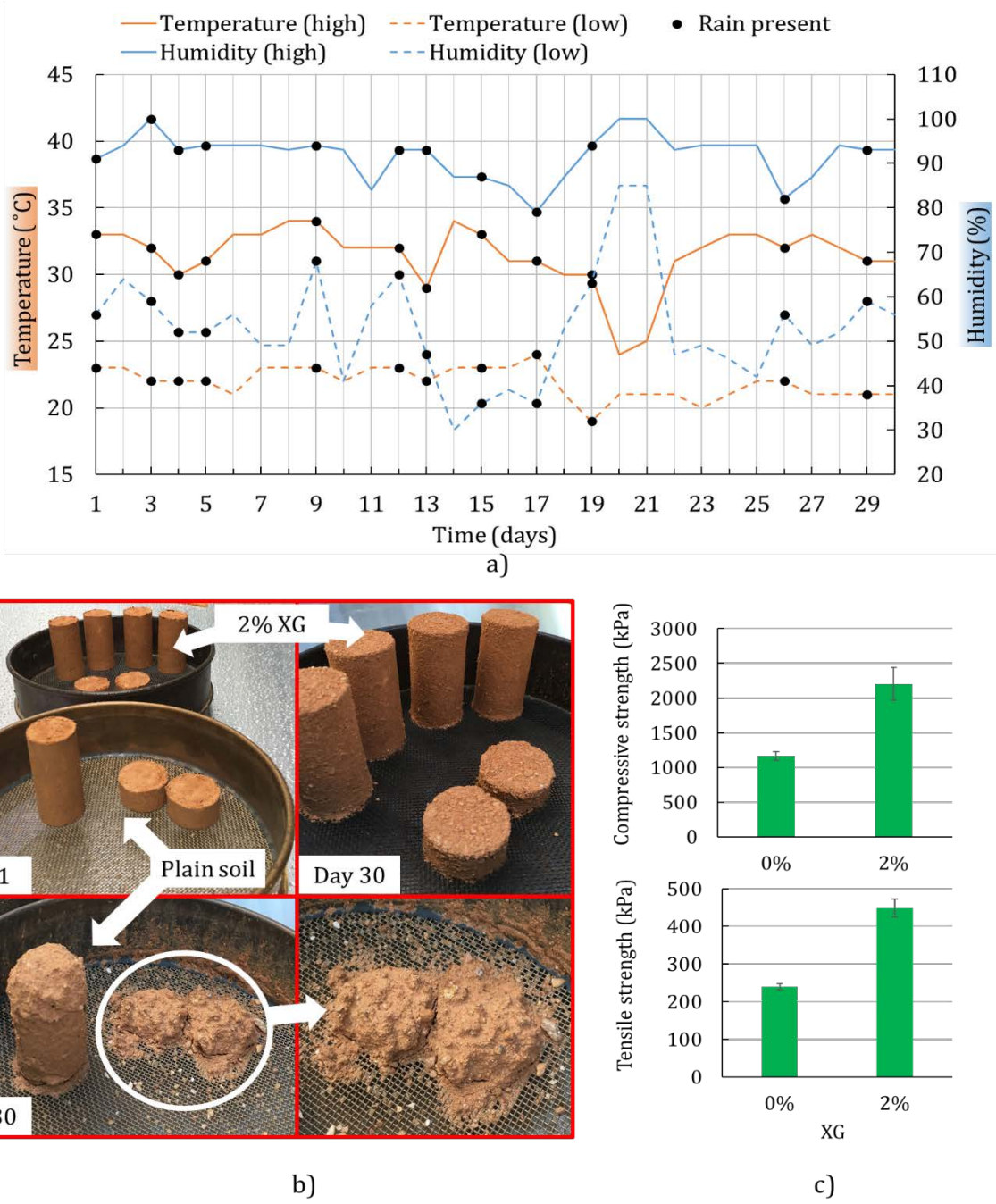

Figure 2-10: a) Daily temperature and relative humidity measured in the field, b) Specimens exposed to atmospheric conditions, c) Strength of the specimens with 2% XG (after being exposed to atmospheric conditions) compared with the strength of plain soil specimens which were kept in the laboratory for 30 days (with standard deviation)

2.4.6 SEM ANALYSIS

For comparison purposes, Figure 2-11a shows the interaction of an XG biopolymer and pure sand. The formation of XG can clearly be seen as a coating agent surrounding coarse-grained particles and bridging the particles that are not in direct contact. Figure 2-11b depicts the SEM image of the GG-treated silty sand from this study. Due to the presence of the fine-grained particles in the soil, the clear biopolymer coating formation cannot be seen. GG and fine particles formed a dense structure that is attached to the larger sand particles. This tendency of biopolymers to create conglomerates together with the fine particles is presented in Figure 2-11c as well, where lumps of fine particles were formed due to the presence of XG. To observe biopolymer-fine grained particle interaction, the magnification had to be more than 30 times higher than for the pure sand with XG. The high presence of fine-grained soil makes the biopolymer linkages more difficult to see on SEM images. Figure 2-11d shows a thin formation of BG that is visible due to the detachment of two soil masses of the silty sand. The thin foil that is spreading in the crack in Figure 2-11d is BG linking.

Observation of the biopolymer-soil interaction leads to two main conclusions. Biopolymers act as a coating agent on coarse-grained soil and can be easily observed under SEM. On the other hand, in sand-silt mixtures biopolymers create, through the electrostatic bond, conglomerates of fine particles that attach to the larger coarse-grained particles. To better understand the interaction between biopolymers and different soil particles, further research on the microscopic scale is required.

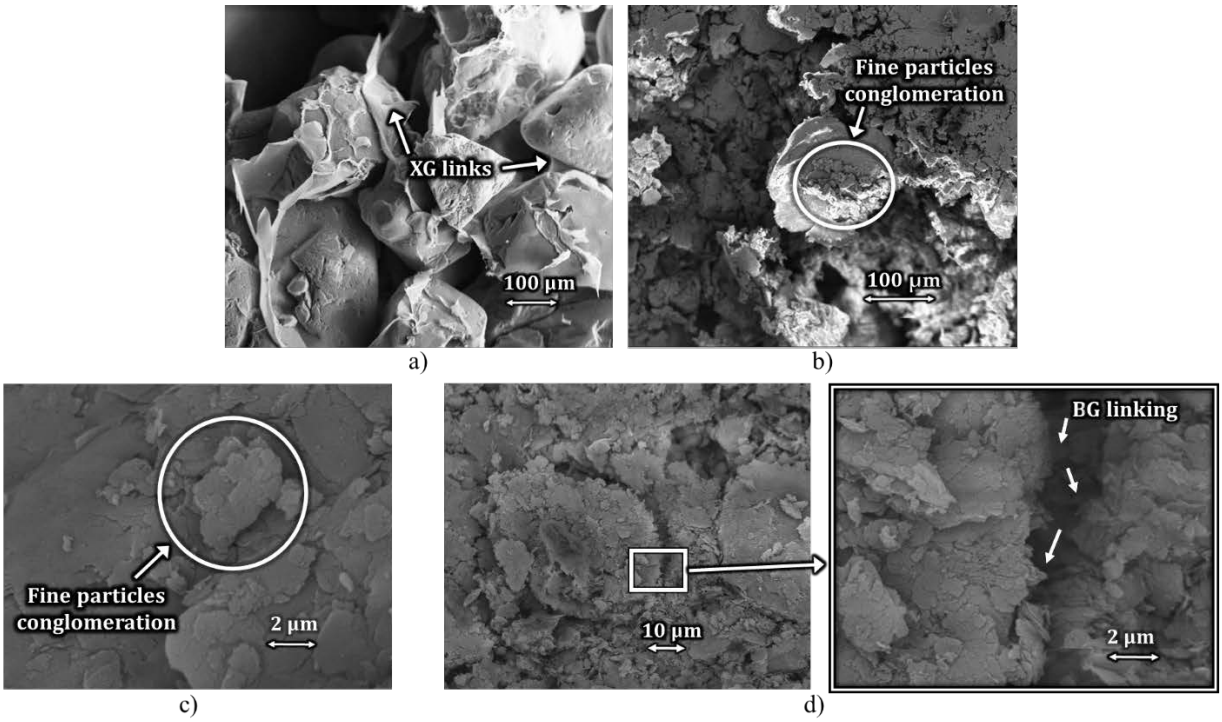

Figure 2-11: a) XG with coarse-grained soil; b) GG with silty sand; c) XG with silty sand; d) BG with silty sand

2.5 CONCLUSION

The main objective of this research was to experimentally investigate the biopolymer effect on soil mechanical properties. In order to achieve these objectives, five different biopolymer types (XG, BG, GG, CHI, and ALG), three different biopolymer concentrations (1%, 2%, and 4%), and several different curing times were investigated. Four mechanical strength tests were performed: UC, ST, DS, and UU tests.

Since curing time and water content are some of the key factors that influence the biopolymer-soil strength, the relation between them and the strength of the biopolymer-treated soil was observed. It has been concluded that the curing time increased the strength values measured in the UU test, ST test, and UU test. For the UC and ST tests, the most notable improvement in mechanical properties occurred within the first five days of curing, with

only slight changes in the period between five and 30 days. For the UU test, changes recorded in the mechanical properties between five and 30 days were considerable. Since the specimens for the UU test were larger than the specimens for the UC and the ST test, it can be concluded that the size of the specimens has an important role in achieving the maximum strength. In other words, larger specimens need more time to dry and to achieve maximum strength.

It was found that the increase in biopolymer concentration enhances the strength of the soil. However, the direct shear test showed that XG, GG, and BG tend to increase the cohesion of the silty sand, but that the friction angle of the treated soil decreases with time. Furthermore, it should be noted that the relation between mechanical properties and biopolymer concentration is not necessarily linear. In other words, each biopolymer-treated soil has an optimum biopolymer concentration. Thus, a high concentration of biopolymers does not guarantee high soil strength. The optimum biopolymer concentration may vary with the biopolymer type, soil type, and water content.

Furthermore, biopolymers proved to be an effective solution to increase the strength of soil in laboratory conditions, but it is still unclear how long they can endure in the natural environment. Comparing the wetting-drying durability to the atmospheric conditions, XG-treated specimens showed higher durability than the specimens made of plain soil, which shows more potential in biopolymers (foremost XG) which should be further researched. The SEM analysis showed the difference in the biopolymer-soil interaction depending on the soil type. It can be concluded that biopolymer links are more exposed in pure sand and that interaction of biopolymers with water will happen faster in that type of soil than in soil with a high concentration of fine particles. This study only scraped the surface regarding the durability of biopolymers in the environment. Therefore, further research should be conducted to investigate in greater detail the durability of biopolymers in relation to environmental influence.

In summary, out of the five different biopolymers which were used for this research, XG, GG, and BG showed the most dominant effect on the improvement of soil strength. For the soil that was used in this research, the optimum biopolymer concentration of XG was close to 2%, whereas the optimum GG concentration was close to 1%. Investigation at higher concentrations of BG is needed to provide an estimate for the optimum BG concentration. However, XG, GG, and BG showed promising results for soil stabilization and provided enormous potential for future eco-friendly engineering.

3. STUDY ON SHEAR STRENGTH OF XANTHAN GUM-TREATED SOIL

This chapter was published in:

Soldo, A. and Miletić, M., 2019. Study on Shear Strength of Xanthan Gum-Amended Soil. Sustainability, 11(21), p.6142. (Impact Factor: 2.592, 5-Year Impact Factor: 2.801).

This chapter was altered from the published version for the purposes of this dissertation. My primary contributions to the paper included: (i) understanding the effect of xanthan gum on shear strength of different types of soil, (ii) gathering and reviewing literature, (iii) development and design of methodology, (iv) collecting, processing, analyzing, and interpretation of the experimental data, (v) most of the writing.

3.1 ABSTRACT

When construction work is planned on soil with inadequate shear strength, its engineering properties need to be improved. Chemical stabilization is one of the solutions for soil strength improvement. Currently, the most common additive that is used for chemical soil improvement is cement. Cement is an effective solution, but it has several negative effects on the environment. Therefore, the urges for environment-friendly solutions that can replace cement and show good potential for eco-friendly engineering are rising. One of the promising environment-friendly solutions is the use of biopolymers. Therefore, the main aim of the present study was to investigate the effect of the biopolymer xanthan gum on the strength of different types of soil. Xanthan gum was mixed with three different types of soil: sand, clay, and silty sand. The strength of treated and non-treated soil was experimentally investigated by performing unconfined compression, direct shear, and triaxial tests. From the results, it was observed that xanthan gum significantly increased the strength of each soil, which shows its major potential for the future of eco-friendly engineering.

3.2 INTRODUCTION

Soil improvement is a process often needed for the construction on an unfavorable soil. There are several ways in which soil strength can be improved. There is physical, biological, and chemical soil improvement. Physical soil improvement can include dynamic compaction, static compaction, and mixing aggregates method, to name a few. The biological approach represents using bacteria that can create calcium carbonate precipitation. That approach is known as MICP (Microbiologically Induced Calcium Carbonate Precipitation). Bacteria, such as Bacillus pasteurii reacts with the calcium in the soil and creates cementitious soil clogs. DeJong et al. (2006) introduced Bacillus pasteurii to Ottawa 50–70 sand and reported the cementation of sand which was created by the bacteria.

The chemical improvement of soil represents mixing certain chemicals with the soil that can improve the strength and durability of the soil. Currently, the most popular additive for chemical soil improvement is cement, but the use of cement raises certain environmental concerns. The use of cement can increase the urban water runoff, prevent the growth of plants, and create the heat islands (Chang et al. 2016) which represent metropolitan areas with significantly high temperatures. Certainly, the most concerning fact related to the use of cement is the contribution to the worldwide CO_2 emissions. In 2002 CO_2 emissions caused by the production of cement were 6% of the total CO_2 emissions in the world (Metz et al. 2005).

Therefore, the search for alternative and eco-friendly solutions that can improve soil properties is in high demand.

MICP represents a biological approach to this problem and several authors reported the effectiveness of MICP (DeJong et al. 2010; Umar et al. 2016). Another approach is the use of biopolymers. In general terms, polymers represent chains of small chemical units. They can be artificial (synthetic polymers) and biopolymers (natural polymers). Biopolymers are extracted from natural materials such as plants, wood, and animal shells. To the best of the

authors' knowledge, no negative effect of biopolymers on the environment has been reported. They are present in the food industry, agriculture, cosmetic industry, and oil drilling industry (Shahidi and Synowiecki 1991; Katzbauer 1998; Bourriot et al. 1999; Rosalam and England 2006; Volman et al. 2008). Furthermore, their potential for the improvement of soil mechanical properties was investigated (Chen et al. 2013; Latifi et al. 2017; Wiszniewski et al. 2017; Hataf et al. 2018). Some biopolymers proved effective in reducing the erosion of soil (Orts et al. 2000; Kavazanjian Jr et al. 2009; Chang et al. 2015b) and the collapsibility of soil (Ayeldeen et al. 2017). Even though both MICP and biopolymers proved to be effective in improving the mechanical properties of soil, biopolymers have certain advantages over MICP. In particular, the MICP procedure can only be used in coarse-grained soils such as sand. Large pores in the sand are suitable for the habitation of bacteria, but fine soils like clay have narrow pores where bacteria cannot survive (Chang et al. 2016). Biopolymers are not a living organism; therefore, they can be used in coarse-grained and fine-grained soils because the narrowness of the pores does not have a negative influence on them. Furthermore, MICP treatment might require a special environment and nutrition for the bacteria in order to keep them alive (Ashraf et al. 2017). On the other hand, biopolymers do not require that treatment.

To demonstrate the potency of biopolymers as a soil improvement additive, the present study focuses on the investigation of the effect of the biopolymer xanthan gum on the improvement of the strength of different types of soil: pure sand, silty sand, and high-plasticity clay. Xanthan gum-treated soil was tested by using the unconfined compression, triaxial, and the direct shear tests.

3.3 MATERIALS AND METHODS

3.3.1 SOIL TESTED

Three types of soil were used for the present study: silty sand, pure sand, and a high-plasticity clay. These soils were selected in order to represent different granulometric groups of soil. They were classified following ASTM D6913-17 and ASTM D4318-17.

3.3.1.1 Silty sand

The silty sand had 39% fine particles (≤0.075 mm) with liquid limit and plastic limit of 49 and 29 respectively, which classifies them as silt with low plasticity according to USCS (Unified Soil Classification System). The sieve analysis provided the grain size distribution curve (Figure 3-1) which classified the coarse particles as sand. Therefore, a general classification of this soil, according to USCS, is SM (silty sand).

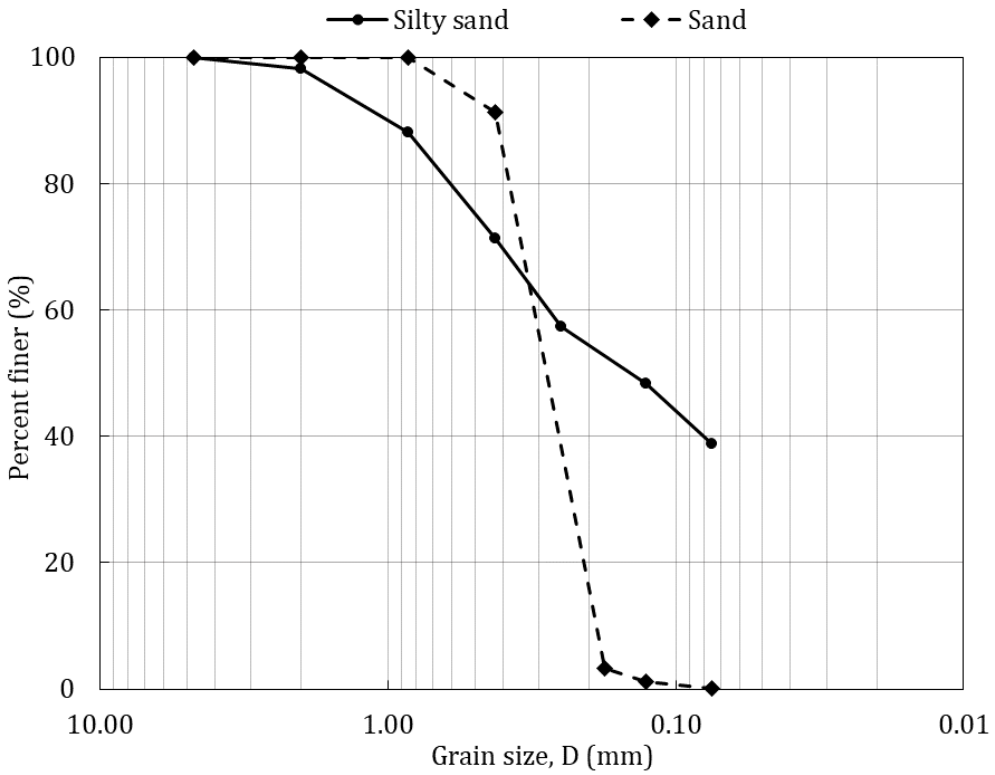

Figure 3-1: Grain size distribution of the sand and silty sand.

3.3.1.2 Pure sand

Sand used in the present study was obtained from a site close to Destin, Okaloosa County, Florida, USA. It was mostly made of quartz and was highly uniform. Fine particle content was almost non-existent. The grain distribution curve obtained from the sieve analysis is presented in Figure 3-1 as well. The coefficient of uniformity and the coefficient of curvature that were calculated from the grain distribution curve were 1.46 and 0.93, respectively. Since the presence of gravel and fine particles was practically non-existent, USCS classifies this sand as SP (poorly graded sand).

3.3.1.3 High-plasticity clay

Fine-grained soil that was used for the present study was high-plasticity clay (bentonite). The liquid limit of the clay was 505, and the plasticity index was 456, classifying this soil as CH (high-plasticity clay) according to USCS. The grain size distribution was not performed on this type of soil because all particles were smaller than 0.075 mm.

3.3.2 BIPOLYMER XANTHAN GUM

Xanthan gum (XG) is a biopolymer from a group of polysaccharides and is created by the fermentation of a medium containing carbohydrates such as glucose. The fermentation process is induced by the Xanthomonas campestris bacterium (Katzbauer 1998). XG increases the viscosity of the solution that it is dissolved in, and it can be dissolved in hot and cold water.

Furthermore, XG-solutions are high-plasticity non-Newtonian solutions, and the increase of shear stress decreases their viscosity (Katzbauer 1998). Additionally, the molecular structure of XG can be affected by salt, temperature, and microorganisms (Katzbauer 1998; Hou et al. 1986)

3.3.3 SPECIMEN PREPARATION AND MECHANICAL TESTING

Silty sand sieved through the sieve N_o 4 with the opening of 4.76 mm. To start the procedure a certain amount of the silty sand was placed into a mixing bowl. XG was hand-mixed slowly into the bowl with the soil in the amount of 1% with respect to the mass of the soil. Once uniformly mixed, water was sprayed into the bowl until the water amount was approximately 16.5% with respect to the mass of the silty sand. The concentration of 1% XG was based on Chapter 1. Higher concentrations had the tendency to increase the strength of certain specimens beyond the testing limits.

Choosing the right water content was crucial for this type of preparation of specimens because too high water content creates specimens that are too soft, while on the other hand, too low water content causes non-uniform specimens. The water content of 16.5% was the optimum water content for this type of soil and it was selected as the most appropriate for the preparation of specimens of silty sand. The optimum water content was determined by performing Proctor (compaction) tests. The soil was compacted under different water contents into a cylindrical mold with a height of 11.6 cm and a diameter of 10.2 cm. The water content that the soil had at the maximum dry density was selected as the optimum water content. During the preparation, a small amount of the material was weighed and placed in the oven to ensure that the water content requirements were met (as per ASTM D2216).

Specimens made of sand were prepared in a similar manner. One percent XG with respect to the mass of soil was mixed into the sand. After that, water was sprayed into the soil-XG mix with constant hand-mixing. The targeted water content for the sand was 12%. That water content was based on the best workability of the sand-water mixture to compact and extrude specimens out of molds.

The same procedure was followed while preparing the clay specimens, but the targeted water content for the clay was 16% because that water content gave the clay

relatively good workability. Specimens made with higher water contents were heavily deformed when extruded from the molds. Therefore, higher water contents were omitted for the clay specimens.

When the mixture of soil, XG, and water was uniformly mixed it was evenly compacted in cylindrical molds. Three types of molds, for three types of tests, were used. The three types of tests were: unconfined compression (UC), unconsolidated undrained triaxial (UU), and direct shear tests (DS). After the compaction, the specimens were extruded from the molds, left in the laboratory at 21 °C and were tested five days later. The five-day period was selected on the observation of the development of the compressive strength of XG-treated silty sand through five days (

Figure 3-2).

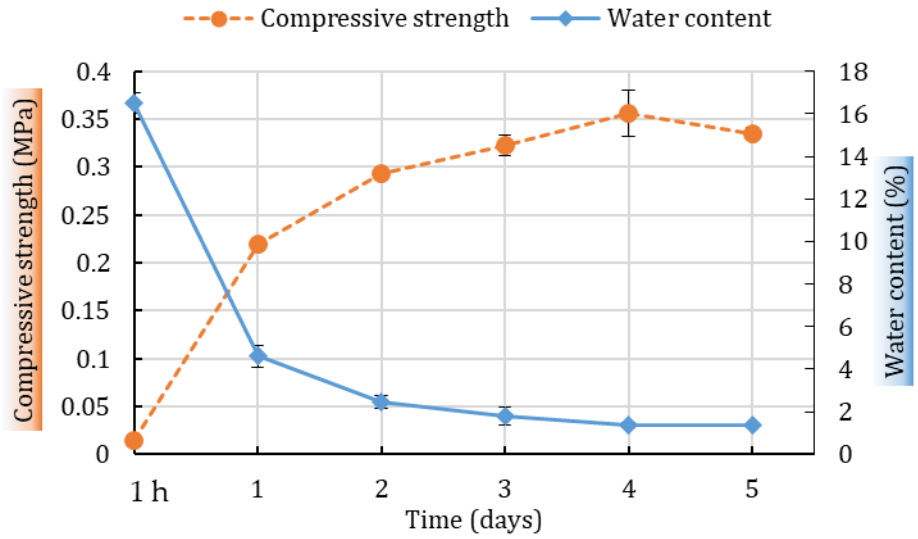

Figure 3-2: Change in the compressive strength of silty sand with 1% XG through five days (with standard deviation)

Specimens for the UC test were compacted in five layers in the cylinders with a diameter of 3.3 cm and a height of 7.1 cm (Figure 3-3b). The UC test was performed in

accordance with ASTM D2166. Strain rate was set up to 1.5%/min, whereas the maximum allowed strain was set up as 20%. The UC test was successfully performed on the specimens that were made of treated and plain silty sand and treated and plain clay. Also, the UC test was also performed on specimens that were made of treated sand, however, the sand in a natural state could not be formed into cylindrical specimens needed for this test, and therefore the UC test had to be omitted in that case.

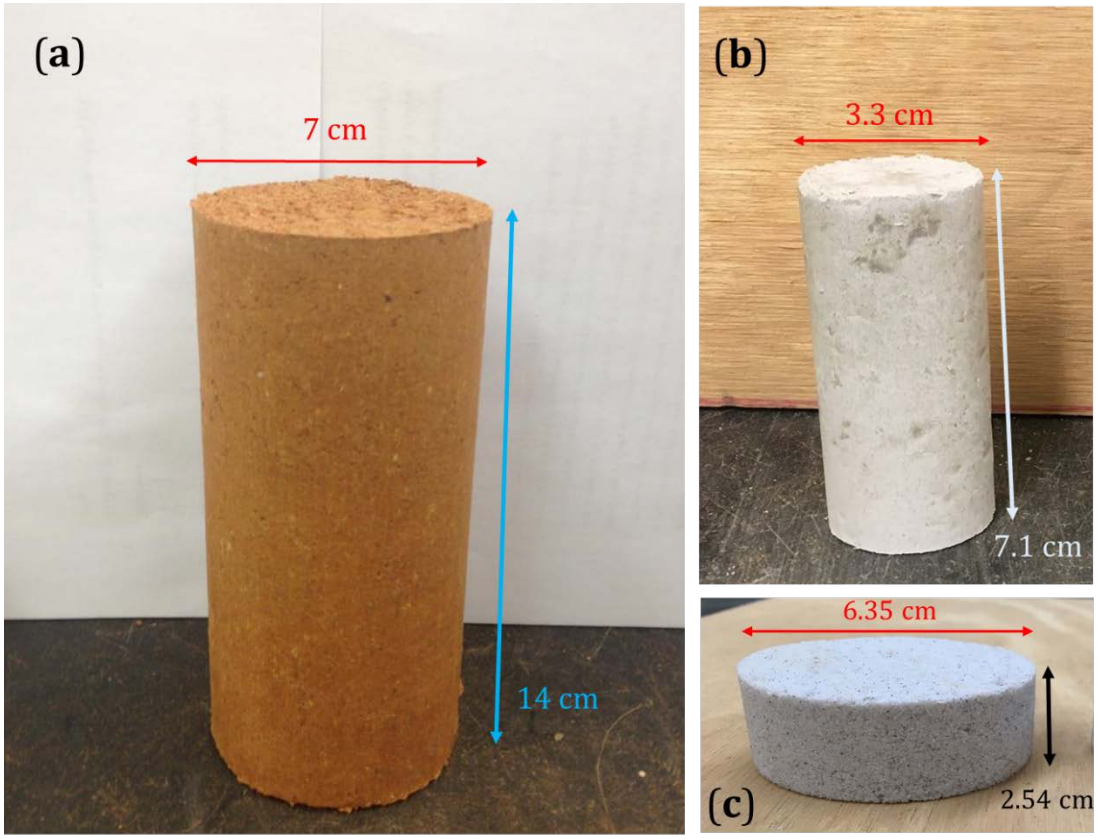

Figure 3-3: Examples of the specimens that were used for testing: a) XG-treated silty sand specimen used for UU test; b) XG-treated clay specimen used for UC test; c) XG-treated sand specimen used for DS test

Specimens for the UU test were compacted in five layers into molds with a diameter of 7 cm and a height of 15 cm (Figure 3-3a). Silty sand and clay were compacted in five layers

with a standardized hammer with a mass of 2.5 kg. The hammer was released 25 times from the height of 30.5 cm to fall free on each soil layer. Each impact sent approximately 7.5 J of energy into the soil. However, the sand was not compacted in the same manner, but it was tapped into the molds because the compacting of the sand-water-biopolymer mixture could not be well executed with a metal hammer. After compaction and extraction, the specimens for the UU test had to be trimmed with a knife to ensure a flat surface at the top and bottom and appropriate cylindrical shape. The UU test was performed according to ASTM D2850. Axial stress was applied under the strain rate of 0.7%/min and under confinement pressure of 103 kPa. This level of the confinement pressure was in the ranges of confinement of similar research which allowed us to compare the results. The same test could be performed with higher or lower confinement pressures since the level of the confining pressure would not affect the maximum value of the deviatoric stress in the UU test.

Specimens for the DS test were compacted in molds with a diameter of 6.35 cm and a height of 2.54 cm (Figure 3-3c). Similar to the specimens for the UU test, plain and treated sand were tapped into the molds, while silty sand and clay were compacted in four layers where each layer was compressed 25–30 times with a force of 100 N. This test was performed with the guidance of ASTM D3080. The strain rate for the DS test was 0.06 cm/min and was conducted under different normal pressures (0.1, 0.38 and 0.77 MPa).

All specimens after extraction out of the molds had the dimensions that corresponded to the inner diameters of the molds except the specimens for the triaxial tests that had a height of 14 cm instead of 15 cm because of the required trimming. Examples of specimens used for the testing can be seen in Figure 3-3. A series of plain specimens were made in the same manner as the treated specimens.

3.3.4 SEM IMAGING

The interaction between biopolymer and different types of soil is not the same. Fine particles and XG are electrically charged which creates an electrostatic bond between XG and fine particles (Chang et al. 2015a). The electrical charge in coarse-grained soils is practically non-existent; therefore, the bond that is created between coarse-grained material and XG can be presented as a thin film wrapped around coarse particles (Chang et al. 2015c). A Scanning Electron Microscope (SEM) Zeiss EVO 50 was used to observe the XG-treated soil. Small pieces of XG-treated soil were cut to about 0.2–0.3 cm^3 and glued to metal pin stubs with carbon tape. The stubs were coated with a thin layer of gold to prevent charging of the analyzed surface, to promote the emission of secondary electrons so that the specimen conducts evenly, and to provide a homogeneous specimen surface for analysis and imaging.

3.4 RESULTS

As stated in Chapter 2, this study did not separate the effect of particle bonding and the effect of soil suction due to the presence of biopolymers. All presented material properties are related to the parameters of total stress. It is assumed that the main effect on the soil strength was the result of biopolymer bonding. The effect of water and water surface tension on the soil strength will be more discussed in Chapter 4.

3.4.1 UNCONFINED COMPRESSION TEST

The UC test is commonly used in civil engineering practice to obtain the compressive strength (UCS) of materials like soil and concrete. While loading the specimens under constant axial strain rate, the specimens should fail on their weakest plain after their compressive strength was reached. Figure 3-4 depicts the effect of XG on the compressive strengths of the studied soils five days after curing. Tests were performed on four specimens

of each type and the mean values are presented with the standard deviations. Striped columns represent the compressive strength of soil specimens without biopolymers, whereas the specimens with 1% XG are represented with solid columns. There are no results for the plain sand because it is cohesionless, and therefore it could not be formed into specimens for the test. Introducing XG to sand cohesion was achieved, allowing sand to be shaped into desired specimens and to retain the shape for five days. Comparing the compressive strength of silty sand with and without XG, it is evident that the strength of the treated silty sand is significantly higher. The compressive strength increased from 1.2 to 3.35 MPa, which represents an increase of about 180%. The compressive strength of sand treated with XG was 2.02 MPa. That amount of achieved strength is significant considering the fact that the plain sand could not be tested for the unconfined compression. The XG-treated clay showed an increase of about 0.3 MPa with respect to the plain clay. The strength of the clay could have been improved more with the addition of more water during the preparation, but the workability of the used clay with water content above 16% was not appropriate for the unconfined compression test. Therefore, relatively weaker specimens were prepared. The findings are in agreement with previous research (Chang et al. 2015a; Ayeldeen et al. 2016; Wiszniewski et al. 2017; Cabalar et al. 2017). Chang et al. (2015a)investigated the effect of XG on the UCS of sand, silty sand and high plasticity clay. In their study, XG increased UCS for all of the mentioned types of soil, and the highest increase was also for the silty sand.

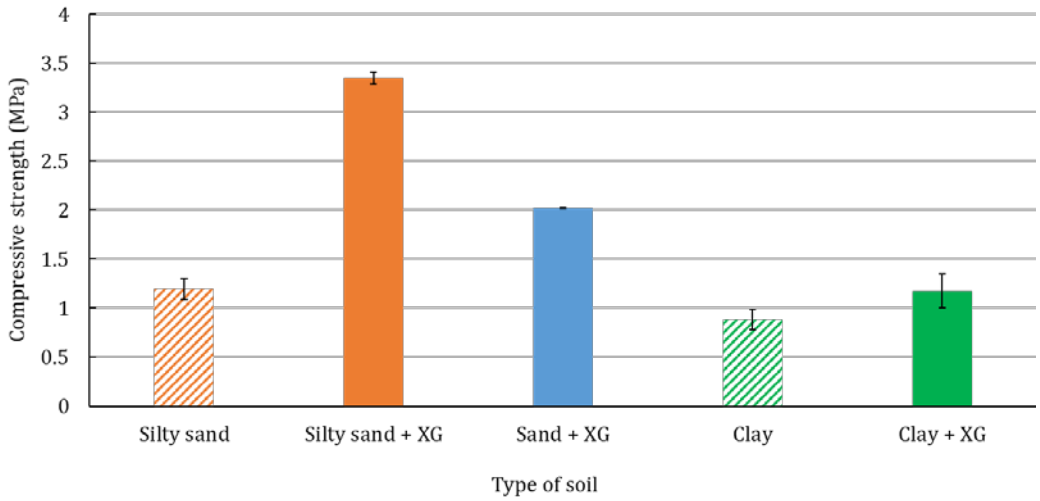

Figure 3-4: Influence of 1% of XG on different types of soil after five days of curing (with standard deviation)

From the results of the unconfined compression test, it is evident that XG increased the compressive strength of the base soils presented in this study. The highest compressive strength was achieved for silty sand when mixed with XG. Therefore, this test indicates that sands with a certain amount of fine particles respond best to XG.

3.4.2 UNCONSOLIDATED UNDRAINED TRIAXIAL TEST

The UU test was performed according to ASTM D2850. Axial stress was applied under the strain rate of 0.7%/min and under confinement pressure of 103 kPa. This level of the confinement pressure was in the ranges of confinement of similar research which allowed us to compare the results. Figure 3-5 shows the stress-strain curves for the studied soil tested in a triaxial apparatus after five days of curing. Dashed lines represent the stress-strain curves for the soil specimens with no treatment whereas the solid lines represent the soil-specimens with 1% of XG. Figure 3-5a shows the results for silty sand with and without

the biopolymer. The plain silty sand had the maximum deviatoric stress of 1.7 MPa which increased by 42% after the soil was mixed with XG. The UU test on sand showed that sand can achieve the maximum deviatoric stress of 1.47 MPa five days after it was mixed with XG (Figure 3-5 b). The maximum deviatoric stress of the plain sand showed extremely low values which is related to the incohesive state of the plain sand. The strength of the clay was 1.63 MPa before it was mixed with XG, but after the mixing, the strength increased by 42% which is the same percentage as that of the silty sand (Figure 3-5c).

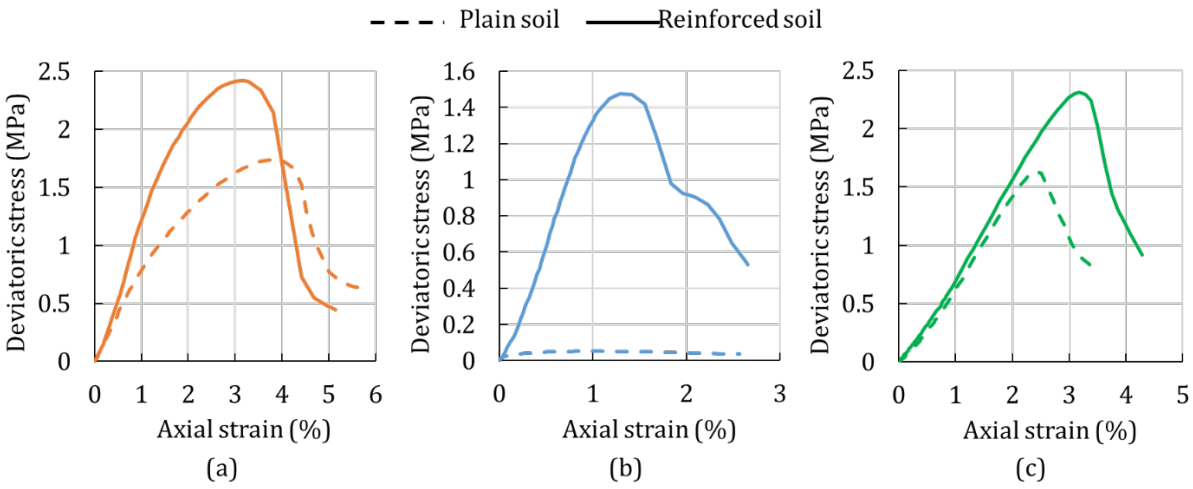

Figure 3-5: UU test results under confining pressure of 103 kPa: Influence of 1% XG on different types of soil: a) Silty sand; b) Sand; c) Clay (please note that the axes are differently scaled)

Results from the UU test showed that the maximum deviatoric strain was achieved for the silty sand mixed with XG, while the maximum deviatoric strain of the clay-XG mixture was only slightly lower. Unlike in the unconfined compression test, the achieved strengths of treated silty sand and clay were not significantly different in the UU test. This indicates that the size of the tested specimens can play an important role in achieving the strength of

the soil. On the other hand, the highest increase in strength was achieved in the sand, which is not surprising when considering that the plain sand had a virtually negligible strength compared to other soils that had a significant amount of fine particles. The peak of the deviatoric stress of the plain sand was close to the results of other researches that performed triaxial tests on the plain poorly graded sand under similar confining pressures (Ayeldeen et al. 2016; Wiszniewski et al. 2017). Furthermore, the same research showed that the addition of XG increases the peak deviatoric stress during the triaxial stress state.

3.4.3 DIRECT SHEAR TEST

The DS test is suitable to obtain the shear strength parameters of soil, i.e., cohesion and friction angle. It is especially favorable for sands and other cohesionless materials that cannot be tested in the unconfined compression test. The DS test was performed on the plain and XG-treated soils. Figure 3-6 presents the achieved shear strength-displacement behavior of the tested soils. Each line corresponds to one normal stress that was applied during the process of shearing.

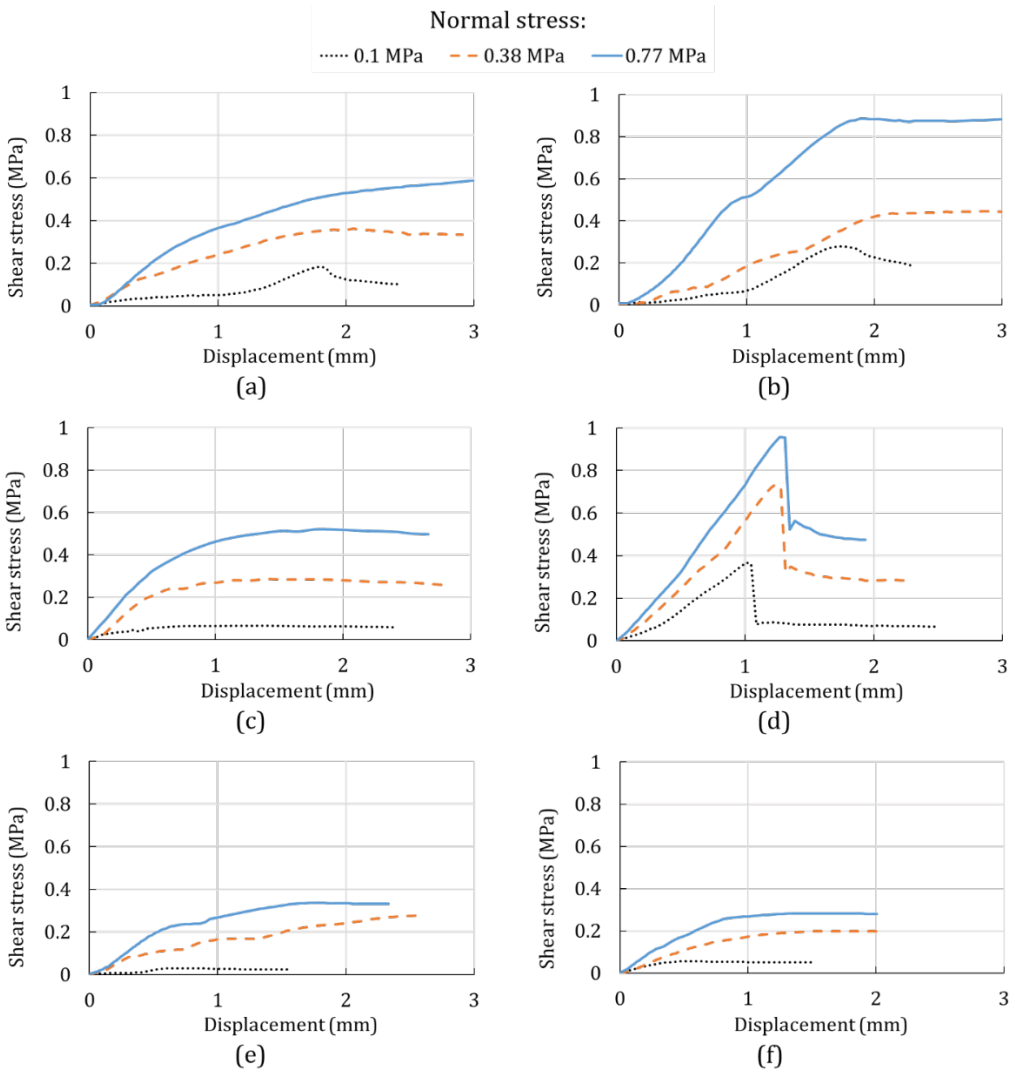

Figure 3-6: DS test shear stress-displacement results: a) Plain silty sand; b) Silty sand with 1% XG; c) Plain sand; d) Sand with 1% XG; e) Plain clay; f) Clay with 1% XG.

For the plain silty sand (Figure 3-6a) the maximum shear stresses were 0.18, 0.36, and 0.60 MPa for the applied normal stresses of 0.1, 0.38 and 0.77 MPa, respectively. Figure 3-6b shows the results of the achieved shear stresses of XG-treated silty sand. The maximum shear stresses did increase to 0.27, 0.43, and 0.88 MPa for the same applied normal stresses of 0.1, 0.38 and 0.77 MPa, respectively. It is evident that the presence of XG increased the shear strength of the silty sand. The shear stress-displacement behavior of the silty sand was similar before and after it was mixed with XG (Figure 3-6a and Figure 3-6b). The most curves

for the plain and XG-treated silty sand reach a peak value for a certain amount of the shear stress and after that the stress intensity stayed constant or decreased, representing a softening behavior. The only exception was noticed for the plain silty sand that was sheared under 0.77 MPa. In that case, the maximum value of the shear stress was never achieved, but it slowly increased until the end of the test. For the shearing of the XG-treated soil under the same amount of load, the shear stress-displacement curve reached the maximum value after which it remained nearly constant. That means that the plain soil under the load of 0.77 MPa had less brittle behavior. Figure 3-6a and Figure 3-6b present the dilatant behavior of the tested samples under the normal pressure of 0.1 MPa. Higher normal pressures created contractency by reducing the freedom of particles to override each other. However, the most significant change for silty sand was the increase in strength of the XG- treated specimens.

Figure 3-6c shows the results of the direct shear that was performed on the plain sand whereas Figure 3-6d shows the results of the XG- treated sand. The maximum shear stresses of the plain sand were 0.06, 0.29, and 0.52 MPa for the applied normal stresses of 0.1, 0.38 and 0.77 MPa, respectively. For the applied normal loads of 0.1, 0.38 and 0.77 MPa, the XG-treated sand specimens reached the maximum shear stresses of 0.36, 0.69, and 0.95 MPa, respectively. The change in the behavior is prominent for the sand even though the plain and XG- treated sand showed the contractant behavior. All curves that represent the shearing of the plain sand have a similar trendline where softening continues after the peak value of stress. The behavior of the XG-treated sand is significantly different. Under each normal loading, shear stresses dropped abruptly for a significant amount after the highest shear stress was achieved. After the abrupt failure, the residual shear strength corresponded to the strength of the untreated sand. The reason for that is the loss in cohesion along the failure surface. Note that the plain sand did not have any cohesion and that cohesion entirely depended on the presence of biopolymers. That change in behavior shows the property of XG to influence the strength and behavior of sand. Unlike the increase in strength, the

increased brittleness of the sand is not a desirable behavior in civil engineering practice. The brittle behavior can result in an unpredictable failure of materials. Therefore, for engineering purposes, the actual peak shear strength can not be considered as the allowable strength. It would be recommended to adopt safety factors that will decrease the allowable strength of the sand.

Figure 3-6e,f present the results of the test performed on the plain clay and XG-treated clay. Both figures show fairly similar results for the tests under different normal stresses and a contractant behavior of the clay. The shear stresses at failure for the treated clay were close in value with the shear stresses at failure for the plain clay. In fact, the shear stress at failure under the normal pressure of 0.77 MPa was slightly higher for the plain clay. The changes in the shear stress-displacement curves were marginal for the clay before and after XG-treatment, indicating no significant change in the behavior during shearing of clay material. Table 2.1 summarises the changes in the friction angle and cohesion of the silty sand, sand, and clay. The peak stress value was selected for determining the friction angle and cohesion as it represents the maximum shear strength which can be translated into allowable strength for the engineering projects.

Table 3-1: Influence of 1% XG on friction angle and cohesion.

	Silty sand		Sand		Clay	
	Cohesion (MPa)	Friction Angle (°)	Cohesion (MPa)	Friction Angle (°)	Cohesion (MPa)	Friction Angle (°)
Plain soil	0.09	36	0	37	0.04	21
1% XG	0.14	43	0.32	40	0.041	18

The results from the direct shear test indicated that XG can change the friction angle in soils that have some level of cohesion such as silty sand and clay, but that it might not significantly change the cohesion for the same soil type. On the other hand, for the cohesionless soils such as sand, XG can significantly increase cohesion but it might not significantly affect the friction angle. Cho and Chang (2018) performed a study where gellan gum was used as the biopolymer for soil improvement on sand, clay, and clayey sand. The study showed that gellan gum increased the cohesion of sand, but it did not have a significant influence on the friction angle. The study also showed that gellan gum increased the cohesion of all three types of soil and the friction angle of clay and clayey sand. The present study, which was conducted with XG, showed a small influence of XG on the friction angle of sand and a higher influence on the friction angle of the silty sand. The increase in cohesion was more prominent for the sand which initially had no cohesive properties. This experimental studies on clay showed that XG did not increase the friction angle, but decreased it slightly. Similar results were reported by Ayeldeen et al. (2017) who performed the direct shear test on a soil with a high concentration of fine particles. Also, this study showed only a slight influence of XG on the cohesion of clay.

3.4.4 SEM ANALYSIS

Figure 3-7 depicts the SEM images of the XG- treated soils used in the present study. The bond created by the biopolymer XG with sand particles is best presented in Figure 3-7a. The tin film that coated the sand particles was XG formation. Additionally, XG created an interaction between particles that were not in direct contact. Creating a stronger bond between sand particles, XG increased cohesion and stiffness of the sand. Figure 3-7a also shows a debonding of sand particles. The formation marked in Figure 3-7a clearly represents a void created by a sand particle that detached from the XG film. This suggests that some of the higher concentrations of XG would create a wider spread of XG, stronger XG mass, and a

stronger bond between XG and soil particles which would lead to the greater strength of the treated soil. Chapter 2 showed that the optimum concentration for the strength improvement of XG-treated silty sand is 2%. Chapter 2 also indicated that the strength increase of the silty sand is not significant for XG concentrations above 2%. Figure 3-7b shows a schematic interaction between coarse sand particles and XG.

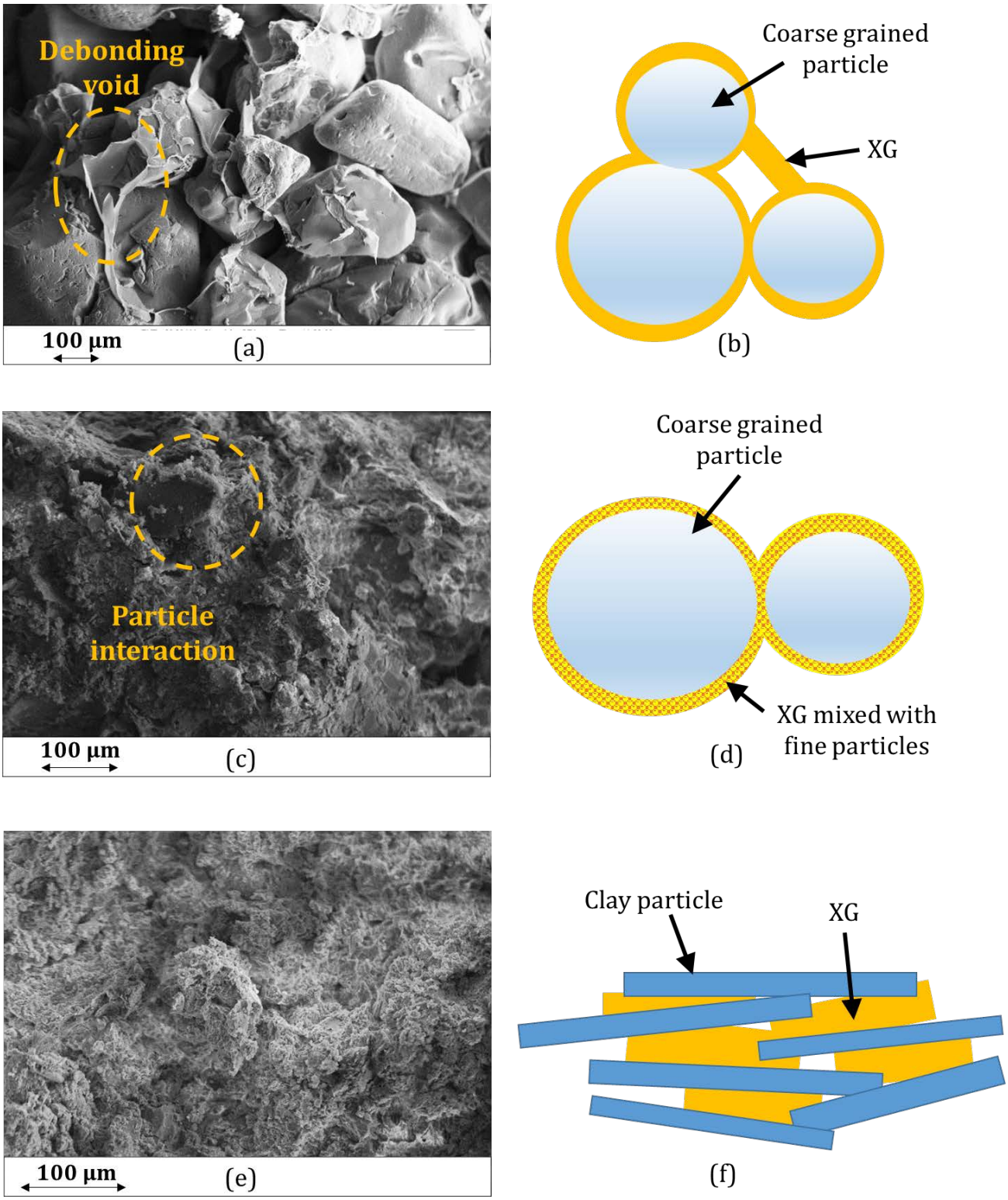

Figure 3-7: SEM images of XG with: a) Clay; c) Silty sand; e) Sand; Schematic representation of the interaction of XG with: b) Clay; d) Silty sand; f) Sand.

In Figure 3-7c a different interaction between silty sand and XG can be observed. Observing Figure 3-7c closely we can see an interaction between a sand particle, XG, and fine particles. The mass surrounding the sand particle was created by the interaction of XG and fine particles. Because of the range of particle sizes, a clear transition between soil and XG could not be identified. The scheme of the interaction of XG, fine particles, and coarse particles is presented in Figure 3-7d.

Figure 3-7e shows the SEM image of clay mixed with XG. Due to the small size of clay particles and their electrostatic bond with XG, the clay-XG mixture is a highly homogeneous mass for which it is hard to determine where clay particles stop and where XG links begin. A schematic representation of the clay-XG bond is presented in Figure 3-7e.

From Figure 3-7e it can be concluded that the interaction of XG with soil strongly depends on the size of soil particles. Coarse-grained soil experiences a coating with XG mass and bridging of distant coarse-grained particles, while fine particles create a stronger bond with XG through the electrostatic linkage which is more difficult to observe.

Even though the XG-fine particle bonds are stronger than XG-coarse particle bonds, the effect of XG is more prominent in well-graded soil that has a significant amount of fine particles. That happens because of the processes that occur in the XG-treated well-graded sand with fine particles. Those include the creation of the XG-fine particle matrix and the enhancement of interparticle characteristics due to the XG cementation. The combination of the mentioned processes results in high strength of the soil (Chang et al. 2015a).

3.5 CONCLUSION

The main objective of the present study was to investigate the effect of XG on the engineering properties of soils with different granulometry (sand, silty sand, and clay). The strength of soil was investigated by using three mechanical tests: unconfined compression test, unconsolidated undrained triaxial test, and direct shear test. Two types of specimens were

prepared for each test, specimens made of plain soil and specimens made of soil with 1% XG. In order to allow specimens to fully cure, tests were conducted five days after the specimens were prepared. Most of the tests reported the improvement in strength for all types of soils that were used.

The unconfined compression test showed that the highest compressive strength was achieved for silty sand. The strength of plain silty sand increased almost three times after XG was added to it. The strength of plain sand could not be determined in the unconfined compression test because without cohesion, sand particles would fall apart without some lateral confinement. However, XG-treated sand showed a compressive strength of 2 MPa.

During the unconsolidated-undrained triaxial test; XG-treated silty sand and XG-treated clay showed a similar magnitude of the maximum deviatoric stress. The highest increase in the maximum deviatoric stress was achieved for the sand because the sand in the natural state had a significantly lower strength.

The direct shear test showed that the presence of XG can increase the shear strength of the sand and silty sand, but the effect on clay was marginal. Furthermore, the direct shear test revealed that XG significantly increases the cohesion in cohesionless soils such as sand, but that it does not have a significant effect on the friction angle of that type of soil. Additionally, the direct shear test showed that the XG affects cohesion in the soils that initially have some level of cohesion (such as silty sand), and that it more affects the friction angle.

The SEM images showed that the interaction of XG with soil depends on the size of soil particles. XG coats coarse-grained particles and creates bonds between distant particles. Fine particles in soil have an electrostatic bond with XG which does not occur in coarse-grained soil. Therefore the bond between XG and fine particles is stronger. Even though the interaction between the biopolymer and fine particles is stronger, the higher impact of biopolymers can be seen in the soil that is mostly coarse-grained.

In summary, the present study revealed the effectiveness of XG on the improvement of three different types of soil and also shows the potential of XG for the application in civil engineering practice. The authors would suggest two possible ways to utilize XG for soil stabilization. For the stabilization at the ground surface, the suggestion would be to mix the XG mechanically in small quantities with soil and then apply water to the soil-XG composite. For the deeper ground improvement, it would be more appropriate to dissolve XG in water and then mechanically mix the solution with soil.

In-situ investigation of XG-treated soil is required to bolster the idea of XG as a medium for eco-friendly soil stabilization. Therefore, the extensive in-situ research of XG-treated soil should be supported.

4. DURABILITY AGAINST WETTING-DRYING CYCLES OF BIOPOLYMER-TREATED SOIL

This chapter is revised based on a paper submitted by Antonio Soldo and Marta Miletić:

Soldo, A., Miletić, M. (2020). Durability against wetting-drying cycles of biopolymer-treated soil. Journal of Cleaner Production (Elsevier) (Impact Factor: 6.395, 5-Year Impact Factor: 7.051). Paper under review.

My primary contributions to the paper included: (i) understanding the durability against wetting-drying cycles of different biopolymer-treated soil types, (ii) gathering and reviewing literature, (iii) development and design of methodology, (iv) collecting, processing, analyzing, and interpretation of the experimental data, (v) most of the writing.

4.1 ABSTRACT

The world today is more and more oriented towards sustainable engineering and environmental-friendly solutions in every field of science and engineering. Therefore, new eco-friendly approaches for soil improvement also emerged. One of the effective, promising, and environmental-friendly solutions is the utilization of biopolymers. Several researchers demonstrated the effectiveness of biopolymers on the improvement of mechanical properties of soil (e.g., compressive strength, collapsibility resistance, and erosion resistance). Even though the biopolymers proved to be effective, it is still unknown how fast they degrade in nature due to the influence of the environment. The effectiveness of the biopolymer-solution can be decreased by fluctuating temperatures, moisture contents, plants, microorganisms, to name a few. Therefore, it is essential to understand their resistivity on the factors that they could be exposed to in the field. This study investigates the durability of biopolymer-treated soil on the cyclic processes of wetting and drying. Two

types of biopolymers were investigated in this study: Xanthan Gum and Guar Gum. Furthermore, the effect of soil type on the mass loss and compressive strength changes of the biopolymer-treated with wetting-drying cycles soil was observed. The results indicated that the erosion and the loss of soil mass were slower for the specimens treated with biopolymers. The analyses of the compressive strength changes with the wetting-drying cycles indicated that the presence of biopolymers significantly slows down the loss of the compressive strength. Furthermore, this study showed that certain soil-biopolymer bonding could be restored with proper treatment. Repeating the process of wetting and drying can reactivate the bonding properties of biopolymers, which amends the broken bonds in soil. The property of biopolymers that they change their properties in water is an important feature that can not be neglected. It gives a clearer picture of their utilization and makes them a good option for rapid temporary construction or long-standing construction in the areas of the arid climate.

4.2 INTRODUCTION

Expansion of cities often causes the need to construct in an unfavorable environment and on soils with undesirable mechanical characteristics. As a solution to that problem, soil-mechanical characteristics can be improved by adding a medium that can increase the strength of the soil. Cement is one of the additives, and currently, it is the most commonly used one. However, the use of cement raises a series of environmental problems from which the contribution to CO_2 concentration on the planet is the most concerning. In 2002, the production of cement contributed to 6% of the world's CO_2 concentration (Metz et al. 2005) with a possible increase in recent years. Furthermore, the use of cement can irreversibly affect the urban environment. Increased urban water runoff, vegetation growth prevention, and heat islands are, also, some of the side effects of using cement as soil stabilizer (Chang et

al. 2016). Therefore, the need for an eco-friendly and effective solution for enhancing soil characteristics is continuously increasing.

New bio-inspired solutions for the improvement of mechanical characteristics of soil, such as microbiologically induced calcium carbonate precipitation (MICP) and biopolymer-treated soil mixtures, are proved to be very effective (DeJong et al. 2010; Chang et al. 2016; Umar et al. 2016; Ayeldeen et al. 2017; Cho and Chang 2018). DeJong et al. (2006) performed calcium carbonate precipitation by introducing bacterium Bacillus pasteurii to Ottawa 50-70 sand. In their experiment, the formation of sand-grain clusters was noticed. Further testing showed that the sand clusters were formed due to the presence of calcite.

On the other hand, biopolymers are a chain of smaller molecular units extracted from nature-made materials, such as wood, vegetable, algae, and animal shells. To the best of the authors' knowledge, no negative effect of biopolymers on the environment was reported. Through recent history, biopolymers were used in the food industry, cosmetic industry, medicine, agriculture (Hou et al. 1986; Shahidi and Synowiecki 1991; Katzbauer 1998; Bourriot et al. 1999; Volman et al. 2008). In previous research, it was found that biopolymers such as xanthan gum, guar gum, beta-glucan, and chitosan can improve the strength of soil (Chen et al. 2013; Latifi et al. 2017; Wiszniewski et al. 2017; Hataf et al. 2018; Soldo et al. 2020). Furthermore, some biopolymers proved effective in reducing the collapsibility of soil (Ayeldeen et al. 2017) and erosion (Orts et al. 2000; Kavazanjian Jr et al. 2009; Chang et al. 2015b). Biopolymers interact directly with clay particles and create a conglomeration effect which increases the friction angle in clay. Clays and biopolymers are electrically charged which results in forming an electrostatic bond between them (Chang et al. 2015a). In soils that have no electrical charge, such as sands, biopolymers do not interact directly with soil particles. In sand-biopolymer composites, sand particles are surrounded by biopolymer links and the created bond can be described as a thin film wrapped around sand particles

(Chang et al. 2015c). In sand, biopolymers surround sand particles and give the sand a cohesive effect, but they do not increase the friction angle (Cho and Chang 2018).

Improving soil with biopolymers has some advantages over MICP soil improvement. MICP can only be used in coarse-grained soil because fine-grained soils tend to have small pores that are not suitable for the survival of bacteria (Ashraf et al. 2017). On the other hand, biopolymers are not a living organism, and therefore, they can be effective in coarse- and fine-grained soils. Furthermore, since bacteria are living organisms, they need a controlled environment and nutrition to survive. The presence of bacteria needed for the MICP process creates the concentration of ammonia (Ashraf et al. 2017), which is an additional hindrance of MICP when compared with biopolymer-solution.

However, the raising question is how long the described solutions can sustain while being exposed to environmental influence such as wind, moisture, and temperature fluctuations. That mentioned area of research has not been well investigated yet.

Kavazanjian and Iglesias (2009) investigated the effect of wind on erosion properties of the biopolymer-treated soil. In their research, biopolymer emulsion was sprayed on the surface of the soil, and wind flow was blown over the soil surface. The conclusion was that biopolymers could reduce wind-induced detachment of soil particles, but that ultraviolet radiation and heat can diminish the effect of biopolymers.

To best of the author's knowledge, Chang et al. (2017) were the only ones that have investigated the durability of biopolymer-treated sand against cyclic wetting-drying up to date. They performed a series of unconfined compression tests on gellan gum-improved sand specimens after each wetting and drying cycle. Their research study has found that the strength of biopolymer-treated sand gradually decreases after each wetting-drying cycle. The major limitation of their study is that they only performed one type of durability testing, on one type of biopolymer. The lack of research in this area results in the lack of understanding of the behavior and the limitations of the treated soil. Therefore, the main aim

of this study is to gain a comprehensive knowledge of the change of behavior of soil after biopolymer treatment.

In this study, in order to better understand the behavior of biopolymer-treated soil, two types of soil were treated with xanthan gum and guar gum. The soil was treated under different concentrations of biopolymers and tested under two types of water-durability tests. Gellan gum-treated soil is the only biopolymer-soil composite tested for the durability against wetting and drying. Considering that xanthan gum and guar gum emerged as biopolymers with high potential for soil stabilization, the investigation of their durability will have a significant impact on their utilization in civil engineering practice.

4.3 MATERIALS AND METHODOLOGY

4.3.1 BASE SOIL

To investigate the effect of the soil type on the biopolymer-treated soil durability, two types of soil were investigated in this study: silty sand and sand. The soils were classified following ASTM D6913-17 and ASTM D4318-17.

4.3.1.1 Silty sand

The grain size distribution curve (Figure 4-1) indicates that the soil had 61% sand and 39% fines particles. The liquid limit of fine particles was 49, and the index of plasticity was calculated as 20. According to the Unified Soil Classification System (USCS), the soil was classified as SM (silty sand).

4.3.1.2 Sand

The sand was obtained from Okaloosa County in Florida. The sand was characterized by a high percentage of quartz and high uniformity. The coefficient of uniformity and coefficient of curvature were calculated as 1.46, and 0.93, respectively (Figure 4-1). The percentage of

fine particles was below five percent. Therefore, the soil was classified as poorly graded sand (SP), according to USCS.

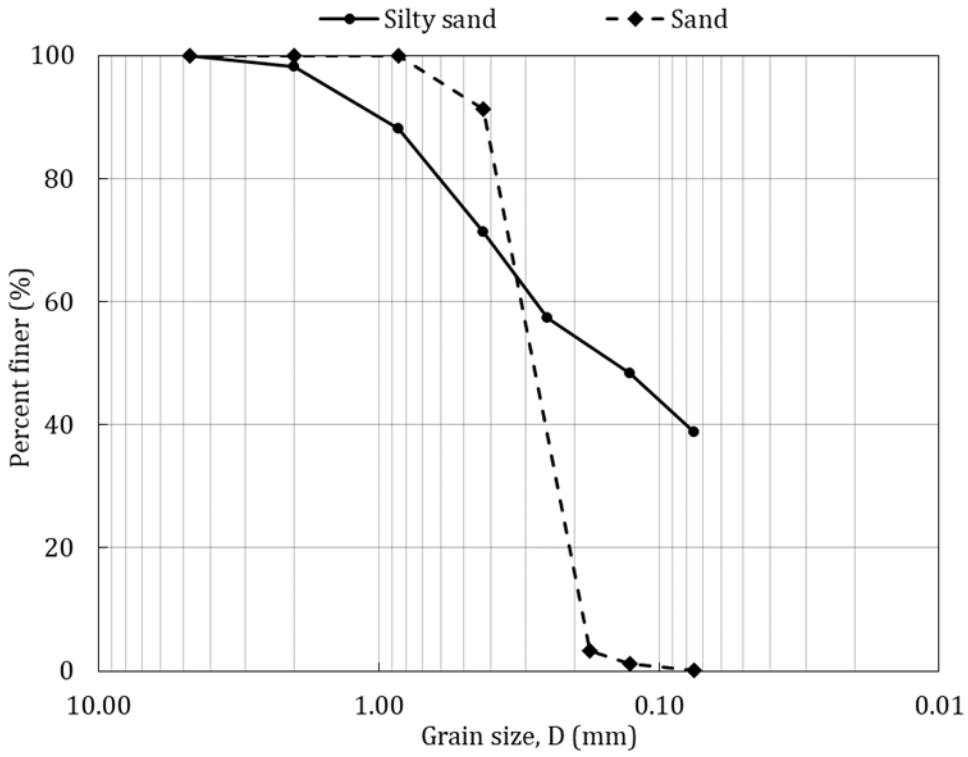

Figure 4-1: Grain size distribution of the sand and silty sand

4.3.2 BIOPOLYMERS

To study the influence of the biopolymer type on the biopolymer-treated soil durability, two types of biopolymers were used in this study: xantham gum and guar gum.

4.3.2.1 Xanthan gum

Xanthomonas campestris bacterium creates the biopolymer polysaccharide xanthan gum (XG) by inducing the fermentation of a medium containing carbohydrate, such as glucose. In other words, XG is a long-chain polysaccharide having d-glucose, d-mannose, and d-glucuronic acid as building blocks in a molecular ratio of 3:3:2 with a high number of

trisaccharide side chains (Jindal and Singh Khattar 2018). The primary chemical structure of the XG can be found in Figure 4-2a. Dissolving XG in hot or warm water creates non-Newtonian solutions with high pseudoplasticity. XG has a variety of utilities and can be found in the cosmetic and food industry, agriculture, oil drilling industry (Katzbauer 1998), and it has been researched for civil engineering purposes (Wiszniewski et al. 2013; Chang et al. 2015; Ayeldeen et al. 2017).

4.3.2.2 Guar gum

Guar gum (GG) is a galactomannan polysaccharide extracted from Cyamopsis Tetragonolba, known as guar beans or guar. Chemically, a GG biopolymer mainly consists of a high-molecular-weight polysaccharide galactomannan, which is based on a mannan backbone with galactose side groups, as depicted in Figure 4-2a. The ratio of the two building blocks in a molecular ratio seems to vary slightly depending on the origin of the seed, but the gum is generally considered to contain approximately one galactose building block for every two mannose building blocks (Rayment and Ellis 2003). In addition, GG shears certain similarities with XG. For instance, it can be dissolved in hot and cold water, and in the industry is used for similar purposes as XG. It can be found in cosmetic products, food products, oil, and gas drilling industries (Thombare et al. 2016) and it has been researched in civil engineering (Ayeldeen et al. 2016; Dehghan et al. 2018; Toufigh and Kianfar 2019)

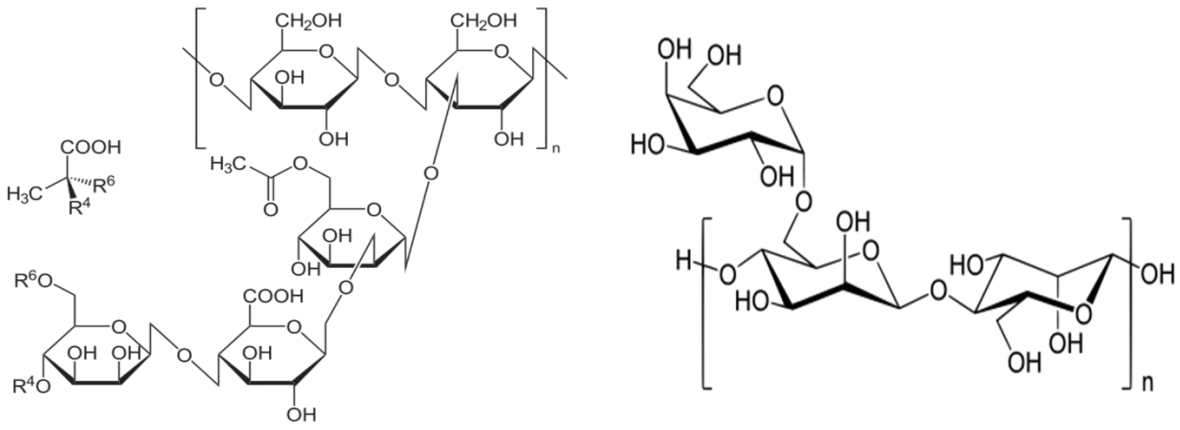

Figure 4-2: Chemical structure of a) Xantham gum, and b) Guar gum (Kalia and Avérous 2011)

4.3.3 SPECIMEN PREPARATION

Silty sand and sand were stored in the laboratory at the temperature of 21˚C. Silty sand was sieved through the sieve with a 4.76 mm opening (N_o. 4). The base soils were placed in a metal dish and hand-mixed with biopolymer powders until uniformly mixed. The biopolymer concentration that was used in this study was 1 and 2 % with respect to the mass of the plain soil. After carefully mixing the dry components (soil and biopolymers), water was added to the mix by spraying and constant stirring. The targeted water content was 16.5% for the silt with sand and 12% for the sand.

After achieving a uniform mixture, the soil-water-biopolymer mass was placed into molds. Two types of molds were used for two different parts of this study. The first mold was cylindrical and had a diameter of 10.2 cm and a height of 11.6 cm. Specimens prepared in this form and with these dimensions were used for the durability testing during cyclic wetting and drying. The second mold type was cubical, with the inner dimensions of five cm. Cubical specimens were used for the testing of the compressive strength changes with the wetting-drying cycles. Silty sand was compacted into molds in three layers. The sand was

gently tapped into the molds without excessive force in order to keep the density and structure of the treated sand close to the natural density and structure. The specimens were air-dried in the laboratory on the temperature of 21˚C for five days (cubical specimens- Figure 4-3a) and seven days (cylindrical specimens Figure 4-3b) to increase the strength of the biopolymer-treated soil and cure the specimens.

In addition, specimens made of plain silty sand were prepared in the same manner as the specimens with biopolymer additives. The plain specimens were used for comparison with the biopolymer-treated specimens. The samples of the plain sand could not be made because the plain sand used in this research had no cohesion; therefore, it could not be shaped to the desired dimensions

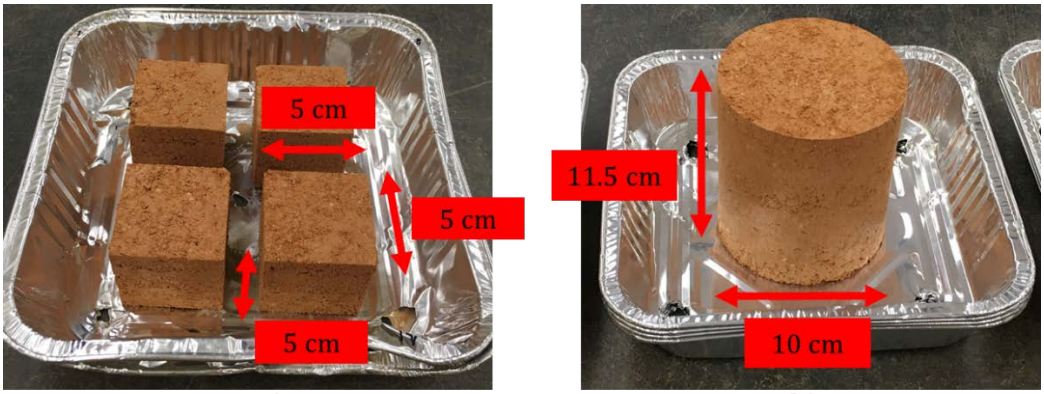

Figure 4-3: Testing specimens for a) unconfined compression test, b) durability test

4.3.4 TESTING

Two types of testing were conducted in this research. The first test was the durability testing during cyclic wetting and drying, and the second test was the unconfined compression test during cyclic wetting and drying.

4.3.4.1 Durability

The durability testing during cyclic wetting and drying was performed by the guidance of the ASTM D559. Since ASTM D559 was originally designated for cemented soil, this study introduced certain modifications to the procedure described in ASTM D559. After the cylindrical specimens have been air-dried for seven days, their mass was measured. The samples were then submerged in water for one hour. The time of one hour was selected as the most efficient for the research purposes based on several trials. The specimens' mass was measured again after one hour, and specimens were placed in the oven, on the temperature of 70˚C for 24 hours. After 24 hours, samples were taken out of the oven, gently stroked by a brush to remove all loose material, and weighed again before submerging them into the water. The same process was repeated ten times, where one hour in water and 24 hours in the oven represents one wetting-drying cycle. After ten cycles, the soil was dried on 110˚C until a constant mass was observed. This procedure was performed on XG-treated sand and silty sand, and GG-treated silty sand. The cylindrical sand specimens with GG degraded after one hour in the water; therefore, they could not be used for the continuation of the experiment. A similar degradation process happened with the cylindrical specimen of the plain silty sand. They degraded after one hour in the water; thus, the durability testing of plain silty sand could not be continued.

4.3.4.2 Unconfined compression

The unconfined compression (UC) test is a widely used test to determine the compressive strength of cohesive materials. The test was performed on the plain and biopolymer-treated silty sand. Also, it was performed on the XG-improved sand, whereas plain sand did not have any cohesion, which was required for this type of test. In addition, sand specimens with GG were not testable for this type of experiment due to their low resistance to water. The UC test was performed on cubical specimens five days after the preparation and air-drying.

Three samples were compressed with an axial strain rate of 1.5%/min, which is in agreement with the ASTM D2166 - Standard Test Method for Unconfined Compressive Strength of Cohesive Soil (ASTM D2166). The remaining specimens were submerged in water at room temperature for 20 min. This time was selected over 60 min, as it was shown more appropriate for the smaller scale specimens. They were subsequently dried in the oven at 70˚C for 24 hours. This process is referred to as one wetting-drying cycle. Cubical samples of plain silty sand were not tested in the UC test after wetting and drying due to their degradation in water. After each wetting-drying period, three specimens were tested in the UC test, while the remaining samples were placed back in the water for 20 min. For the specimens with XG, seven cycles of wetting and drying were carried out through seven days. The UC test was performed after each cycle except for fourth and sixth. Most of the cubical specimens with GG were heavily damaged after the first 20 min in water. Therefore, the remaining specimens with GG went through two or two cycles of wetting and drying.

Furthermore, the healing potential of the XG biopolymer was also investigated by wetting and re-testing previously loaded specimens after their first UC test. XG-sand cubes were placed in the water for 20 min after they were broken in the UC test for the first time. They were subsequently placed back in the oven and re-tested for the unconfined compression. The repeated cycle of wetting and drying was conducted to spread the XG chains and investigate their regenerative properties on the treated sand.

4.4 RESULTS AND DISCUSSION

4.4.1 DURABILITY

The durability of the soil was observed through the change of mass through the cyclic wetting and drying. The change of mass of the biopolymer-treated soil was calculated for each cycle by the following equation:

$$\%loss = \left(\frac{A}{B}\right) \times 100 \tag{4.1}$$

where A is the mass of the soil after each cycle; B is the mass of the dry soil after seven days of curing in the air.

Figure 4-4 shows the results of the mass percentages of biopolymer-treated soil remained after each cycle. Plain soil samples degraded when submerged under the water for one hour and could not be tested in the designed experiment. The results from Figure 4-4 indicate that the presence of biopolymers slowed the degradation process for both types of soil. It is interesting to notice that the silty sand with a concentration of 2% XG lost more soil mass than the same soil with a concentration of 1% XG (Figure 4-4a). The reason behind this is the absorptive properties of the silty sand and XG. The XG attracts and binds water molecules, which further increases the absorbing potential of already swelling silty sand. In other words, the higher presence of XG caused more trapped water. Therefore, to achieve the same water content after each drying for the specimens with 1 and 2% XG, specimens with 2% XG would require higher drying temperature or longer drying time. The constant higher presence of water can cause the reduction of negative pore pressures that can lower the apparent cohesion and cause the degradation of the soil mass. That resulted in faster degradation of specimens with 2% XG. However, the loss of the mass under all biopolymer concentrations was significantly reduced when compared with the loss in mass of the plain soil.

In the case of the silty sand treated with GG (Figure 4-4b), the specimens with higher concentrations have kept slightly more of their soil mass during ten cycles of wetting and drying. It is noticeable that the specimens with 1% GG lost more of their mass at the beginning, while for the specimens with 2% GG, the mass loss was more prominent in further stages. When compared with higher concentrations, the samples treated with only 0.5% GG had significantly higher losses of mass between each cycle.

For the sand specimens treated with XG (Figure 4-4c), the loss of mass is relatively low throughout the testing for higher concentrations when compared with silty sand. The reason for that is the fact that the sand has a higher porosity and lower water absorption capacity than silty sand. In other words, water absorption happens only due to the presence of XG. Higher porosity makes the water evaporation relatively faster in the sand than in silty sand. Cementitious effect of hardened XG gave the sand relatively good resistivity to water. However, sand with only 0.5% XG went successfully through only six cycles of wetting and drying before it became wholly degraded.

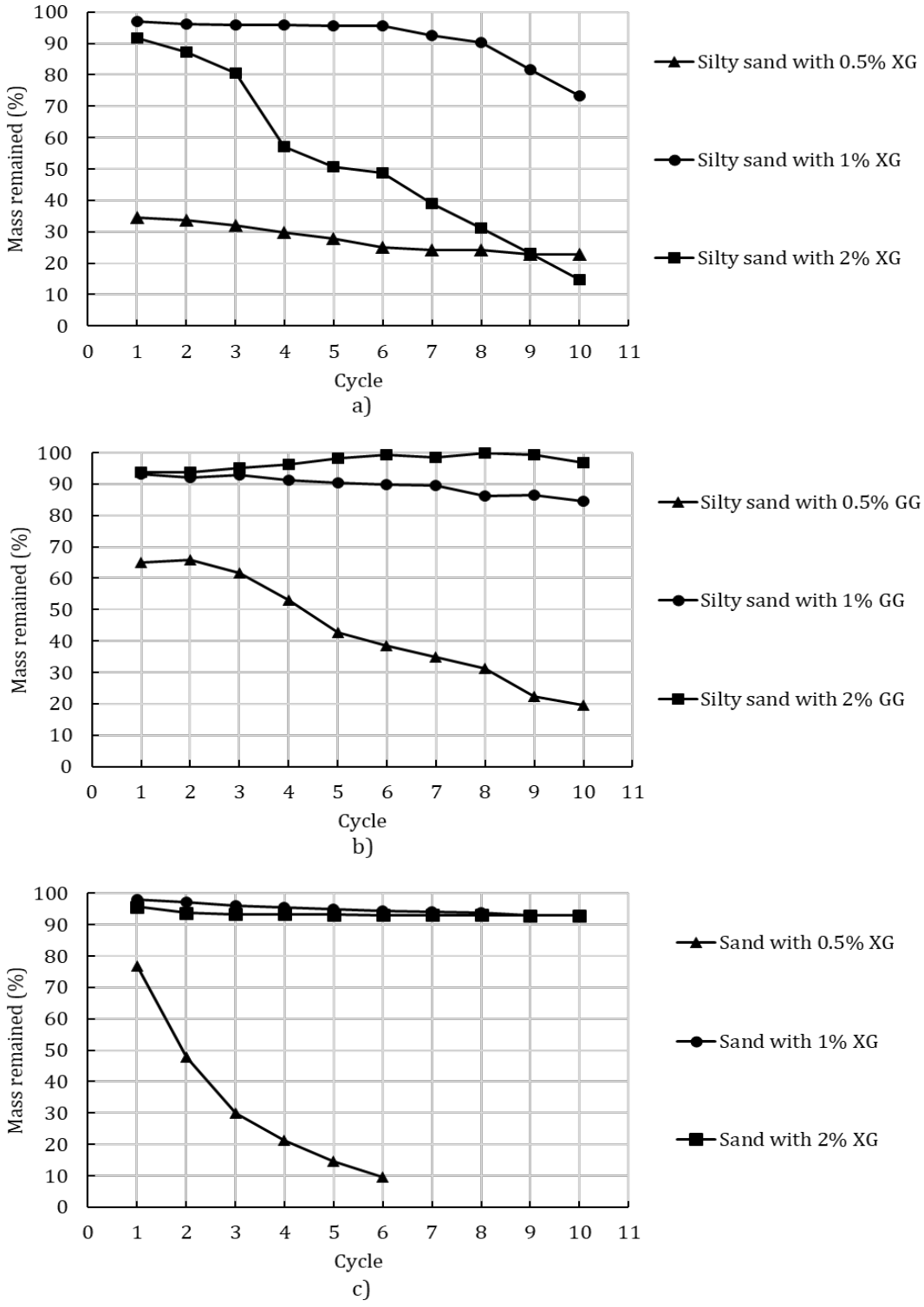

Figure 4-4: Change in mass for a) Silty sand with XG; b) Silty sand with GG, c) Sand with XG

4.4.2 UNCONFINED COMPRESSION TEST

Figure 4-5 shows the relationship between the compressive strength and the number of wetting and drying cycles for silty sand (Figure 4-5a and Figure 4-5b), and sand (Figure 4-5c). The error bars represent the standard deviation from the averaged results. In all figures, the first point, at cycle zero, represents the compressive strength of specimens tested after five days of air-drying in the laboratory at room temperature. The plain silty sand samples degraded after 20 min in water and could not be tested through cyclic wetting and drying (Figure 4-5a and Figure 4-5b). Plain sand samples were not testable because of non-existing cohesion that was needed to fabricate the specimens for this type of testing (Figure 4-5c) Both types of soil showed fast degradation in water for 0.5% of additives. Therefore, soils treated with 0.5% of biopolymers could not be used for a detailed comparison with soil treated with higher biopolymer concentrations. The exception was the sand treated with 0.5% XG that showed a slightly higher level of water resistance (Figure 4-5c).

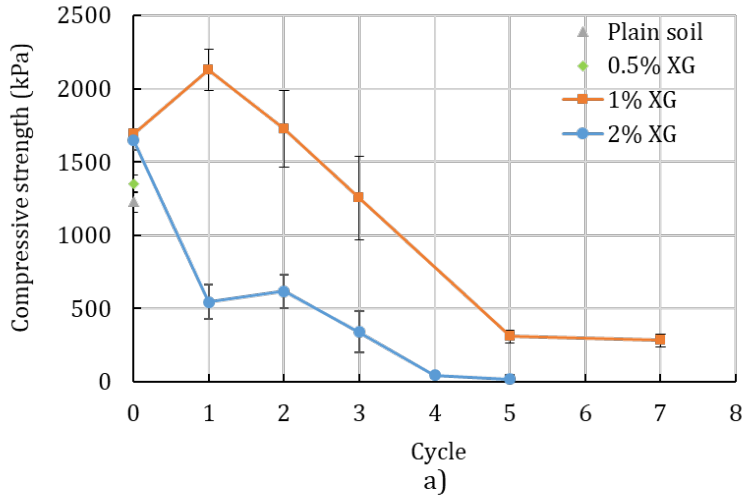

a)

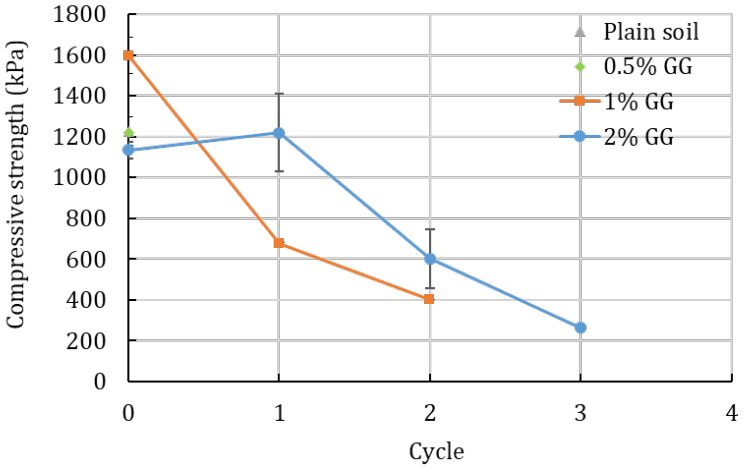

b)

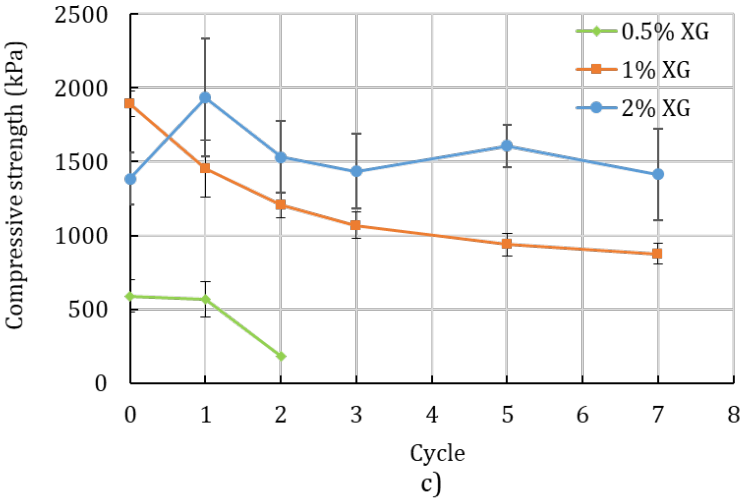

c)

Figure 4-5: Change in compressive strength for a) Silty sand with XG; b) Silty sand with GG; c) Sand with XG; (with standard deviation)

The change in the compressive strength of biopolymer-treated soil with wetting-drying cycles strongly depends on the biopolymer concentration, biopolymer type, and water content. Lower biopolymer concentration in soil results in a reduced number of biopolymer links and subsequent biopolymer-particle bonding. In other words, soils with the lower biopolymer concentration will have smaller compressive strength. On the other hand, a higher percentage of biopolymer causes greater water absorption. The decrease in the water content and degree of saturation increases the surface tension forces between soil particles, which subsequently increases the soil strength (Figure 4-6). It is noticeable that the biopolymer bond started to weaken after the first wetting and drying cycle because of constant water absorption and the thining of the biopolymer links. For the silty sand samples with 2% XG, the increased biopolymer concentration resulted in higher water absorption than samples with 1% XG. The higher presence of the trapped water caused a more rapid decrease in the compressive strength because of reduced tension forces and loosened biopolymer links.

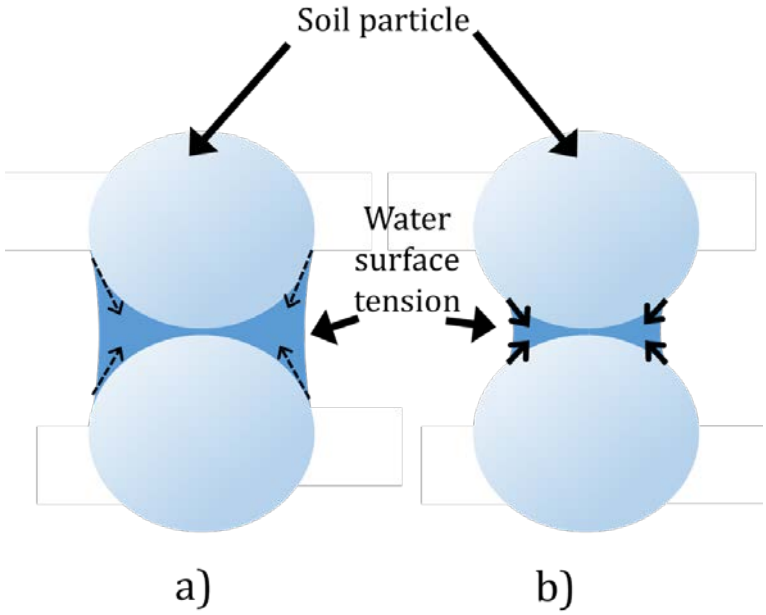

Figure 4-6: Interaction of water and soil particles: a) higher degree of saturation - lower surface tension forces, b) lower degree of saturation - higher surface tension forces

Figure 4-5b shows the decrease in the compressive strength for GG-treated silty sand with wetting-drying cycles. The vast majority of the 1% GG-treated cubicles were severely damaged and unusable for the UC test. Therefore, undiscarded specimens went under two cycles of wetting and drying where the change of their compressive strength was investigated. It is noticeable that after two cycles of wetting and drying, the compressive strength of 1% GG-treated cubicles decreased by 75%. In the case of 1% XG-treated silty sand, the decrease of the compressive strength by 75% would be estimated to happen after the fourth cycle of wetting and drying. The specimens with 2% GG showed better resistivity to water and higher strength through the cyclic wetting and drying. The first points, at cycle zero, which represent the specimens after five days of air drying indicates lower strength for the specimens with 2% GG. This trend was already observed with the samples treated with XG. The reason behind that is that higher concentrations of biopolymer need more air-drying time to completely harden and achieve the maximum strength. The same phenomena happened for the treated sand as well (Figure 4-5c).

Figure 4-5c represents the change of the compressive strength of XG-treated sand with wetting-drying cycles. During seven cycles of wetting and drying, sand with 1% XG kept 46% of the initial strength while the sand with 2% XG kept 75% of the initial strength. However, the biopolymer-treated sand samples did not sustain their shape and strength at the lowest biopolymer concentration. At the concentration of 0.5% XG, they lost 70% of the initial strength after the second cycle and completely degraded during the third cycle.

4.4.3 SAND HEALING

Xanthan gum is one of the partially reversible bond-based biopolymers (Prameela et al. 2018). That means that it can be brought to the previous state by reapplying the processes that initially induced the change of that state. That reversible nature of XG was examined in

biopolymer-treated sand samples that were tested under the UC test. After the third wetting-drying cycle, that was used to investigate the change in the compressive strength, the broken specimens were used to investigate the healing properties of XG. The broken specimens were submerged for 20 minutes and dried in the oven for 48 h, as described previously. After that, the same specimens were tested again under the UC test. The same process was repeated one more time. The results of two XG-treated sand specimens are summarized in Figure 4-7. The repeated process of wetting-drying stiffened the soil-biopolymer bond and the XG-treated sand specimen regained some level of the initial strength which is presented in Figure 4-7. Higher magnitudes of the compressive strength and the level of the regained strength were achieved for the higher concentration of XG. That is not surprising since a higher concentration of XG causes faster and broader linking with of XG molecules with each other and with the surrounding sand particles.

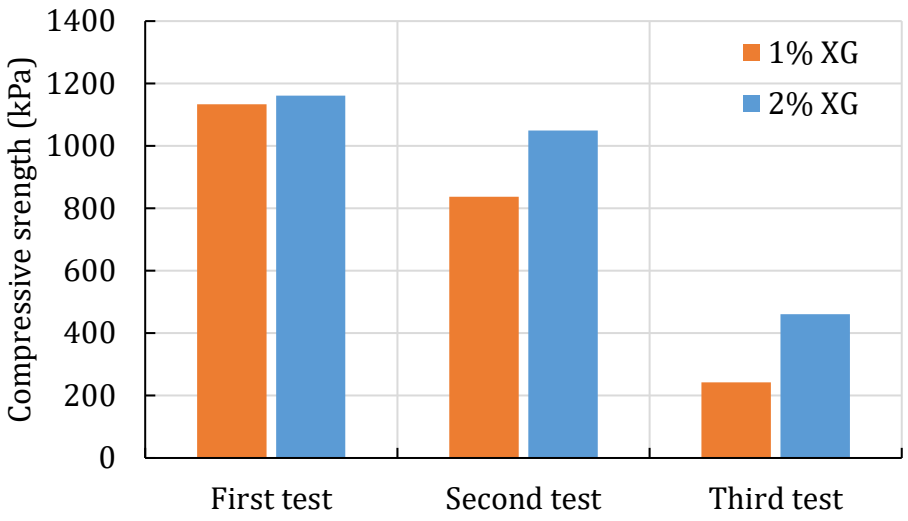

Figure 4-7: Compressive strength of regenerated sand XG-treated specimens

That reversible nature of XG is schematically represented in Figure 4-8. The sand particles bonded by XG-links (Figure 4-8a) brakes during the UC test (Figure 4-8b). After the broken specimens of XG-treated sand were put back together and submerged in water, the XG

linkages loosen their structure which allowed them to interact with the nearby sand particles again (Figure 4-8c) and mend the broken bonds (Figure 4-8 d).

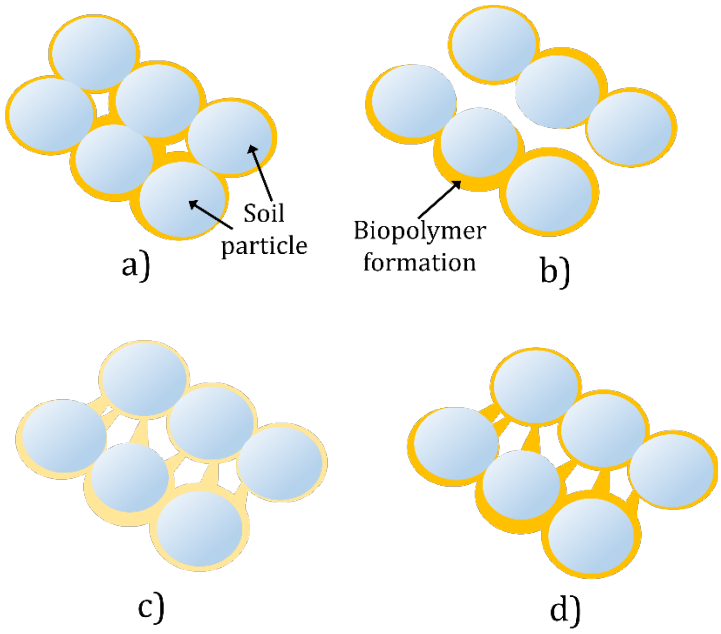

Figure 4-8: Healing cycle of biopolymer-treated sand

4.5 CONCLUSIONS

Recently, biopolymers XG and GG showed to be the promising environmentally friendly soil stabilization additives. However, they are prone to environmental influence, especially moisture changes. To best to the authors' knowledge, the previous research studies have not comprehensively investigated the effect of wetting-drying cycles on the strength and mass loss of the different biopolymer-treated soils. Therefore, the main aim of this study is to investigate the effect of wetting-drying cycles on the strength and mass loss of the biopolymer-stabilization. The types of soil were used in this study: silty sand and pure sand. In addition, two types of biopolymers (xanthan gum, and guar gum) and three biopolymer concentrations (0.5, 1, 2%) were used as testing variables in this research.

The first experimental study was focused on observing the change of the mass of the plain and biopolymer-treated soil during cyclic wetting and drying. It was shown that XG reduces

the loss of mass for both tested soil types, while GG was only effective when mixed with silty sand. For the silty sand, the most effective concentration of XG to reduce the mass loss during the cyclic wetting and drying process was found to be 1%. The highest used concentration of XG (2%) caused higher entrapment of water, which ultimately led to faster loss of mass. On the other hand, the lowest concentration of XG (0.5%) resulted in too weak biopolymer-soil bonds, which degraded faster. That points to an optimum concentration of XG that works the best with a certain type of soil. For the GG-treated silty sand, the loss of mass was more prominent for lower concentrations. For the XG- treated sand, the loss of mass was relatively low for concentrations of 1% and 2%, which can be explained by higher porosity of sand, which makes water evaporation easier in comparison to the silty sand. A low concentration of 0.5% XG caused weak bonding amount soil particles that rapidly degraded.

The second experiment investigated the change of the compressive strength of biopolymer-treated soil with wetting-drying cycles. XG proved to reduce the loss of compressive strength in silty sand and sand, while GG was only mildly effective in silty sand. However, the increase in the GG concentration reduced the strength loss. The concentration of 1% XG was more effective than 2% in reducing the strength loss in the silty sand due to higher water absorption for higher concentrations of XG. The XG-treated sand showed extremely good resistivity to the loss of the compressive strength through cyclic wetting and drying. The higher concentrations of XG resulted in higher compressive strength of sand. The concentration of 0.5% XG and GG showed to be mildly or non-effective for the proposed type of testing.

The broken XG-treated sand specimens were re-submerged, dried and subsequently tested in the UC test to study the healing properties of XG-treated sand. It was shown that rewetting and drying can restore some level of the compressive strength of XG- treated sand. The reason behind it is the regenerative nature of XG, which loosens its structure in water and re-attaches to the nearby soil particles. The healed soil-biopolymer bond stiffens while

the sample is subsequently dried and mends the cracks in sandy specimens. Sand samples with higher concentrations of XG showed to regain more of their lost strength. This research study showed that, even though biopolymers tend to be susceptible to water, certain biopolymer types and concentrations can significantly increase the durability of soil to water. It was also shown that the presence of water can activate the regenerative properties of XG, which shows its potential for soil stabilization. However, this field of research still requires a significant amount of investigation.

5. EFFECT OF BIOPOLYMERS ON THE STRAIN LOCALIZATION OF TREATED SOIL

This chapter is based on a paper in preparation by Antonio Soldo, Victor Aguilar, and Marta Miletić:

Soldo, A., Aguilar V., Miletić, M. (2020). Effect of biopolymers on the strain localization of treated soils. Geotechnique (Elsevier) (Impact Factor: 3.559, 5-Year Impact Factor: 4.09).

My primary contributions to the paper included: (i) understanding the inception of strain localization of biopolymer-treated soil, (ii) gathering and reviewing literature, (iii) development and design of methodology, (iv) collecting, processing, analyzing, and interpretation of the experimental and numerical data, (v) most of the writing.

5.1 ABSTRACT

The demand for bioinspired and eco-friendly soil improvement alternatives is continuously increasing. Biopolymers have been shown as one of the most promising eco-friendly options, and have demonstrated to have a high potential for accomplishing significant gains in future green geotechnical engineering. However, they have not yet found their way into engineering practice. One of the reasons for this may be the absence of computational models that would allow engineers to incorporate biopolymer-treated soil into their designs. Interest in biopolymer-treated soil is evident from the upsurge of related research activities in the last five years, most of which have been of experimental nature. Significant research in the development of analytical models and numerical tools, as well as design procedures, is needed for an accelerated uptake in the engineering practice. Therefore, the main goal of this study is to numerically capture a stress-strain response and predict the onset of strain localization in elastic-plastic biopolymer-treated soil. The biopolymer-treated soil is

described by a non-associated Drucker-Prager hardening plasticity model. Diagnostic strain localization analyses were conducted, thus providing strain and stress levels at the onset of strain localization, along with the corresponding orientations of the deformation band. Several unconfined compression and unconsolidated undrained triaxial tests on the plain, as well as on the biopolymer-treated soils, were modeled. Results showed that the presence of biopolymers significantly improved the mechanical behavior of the soil. Furthermore, the results indicated that biopolymers tend to postpone the onset of the strain localization for the unconfined compression, but advance the onset in the triaxial state of stress. The numerical results are confirmed by the image analysis of the unconfined compression tests. Digital image processing successfully captured high strain concentrations, which tend to occur close to the peak stress. In summary, biopolymers showed plenty of potential for future eco-friendly geotechnical engineering.

5.2 INTRODUCTION

The fast development of civilization results in a constant spread of urbanization. The urbanization growth often urges the need for construction work to be performed in a hostile environment. Building on a low-strength soil would affect the safety and workability of the structure. Therefore, the engineering properties of the low-strength soil have to be improved. Soil can be stabilized by different mechanical, biological, thermal, chemical, and combined methods (Holtz et al. 1981; Hinchee and Smith 1992; Umar et al. 2016; Ashraf et al. 2017).

Chemical soil stabilization is the modification of soil properties to improve its engineering performance. One of the most commonly used chemical stabilization methods is cement stabilization. Even though it is effective and cost-efficient, cement has several adverse effects on the environment. For instance, it can initiate the formation of the heat islands, contaminate underground water, and eradicate vegetation. However, the most

severe environmental impact is the production of carbon dioxide (CO2) during the production of cement. The estimations are that the cement production industry contributes to more than six percent of the world's CO_2 emission in recent years (Andrew 2018). Therefore, the need to replace environmentally-harmful solutions, such as cement, is in high demand.

One of the eco-friendly solutions is microbial induced carbonate precipitation (MICP). MICP is a biological approach that requires the presence of a large microbial community in the coarse-grained soil. The reactions between microorganisms and soil particles create a cementitious bond that improves soil properties. MICP proved to be effective in increasing the strength and load-bearing capacity of the soil (DeJong et al. 2010; Chang et al. 2016; Choi et al. 2016; Umar et al. 2016; Li et al. 2018). However, this approach comes with certain drawbacks. It can result in the generation of effluent ammonia, and it can only be implemented in coarse-grained soil. The reason for the latter is that the pores of the fine-grained soil are very small and hence not suitable for the habitation of microbes (Ashraf et al. 2017).

Another eco-friendly approach for soil stabilization is the utilization of biopolymers. Biopolymers are naturally made polymers extracted from plants, shells, fungi, and yeast. They have been used in the food industry, the cosmetic industry, medicine, and agriculture (Katzbauer 1998; Lee and Mooney 2012; Gombotz and Wee 2012; Thombare et al. 2016). Since many of them are known as harmless and edible, they can be considered as eco-friendly agents for soil treatment (Chang et al. 2016). Their advantage over the MICP treatment is that they can be used in both fine- and coarse-grained soils, and they do not generate the effluent ammonia (Chang et al. 2015; Aguilar et al. 2016). Up to date, several research studies have shown the positive biopolymer effect on the soil strength improvement, permeability reduction, and soil collapsibility decrease (Chang et al. 2015; Ayeldeen et al. 2017;

Wiszniewski et al. 2017; Cabalar et al. 2017; Soldo and Miletić 2019; Toufigh and Kianfar 2019).

The vast majority of the research on biopolymer-treated soil was experimental. One of the reasons why biopolymer treatment of soil has not found its way into civil engineering practice could be the absence of computational models that would allow engineers to incorporate biopolymer-treated soil into their designs. Some of the research that conducted numerical modeling is by Ayeldeen et al. (2017). They created a finite element model to investigate the behavior of the treated collapsible soil after and before water immersing. The treated and untreated soils were simulated by Mohr-Coulumb's criterion with an associated flow rule. The commercially available finite element software Plaxis 2D was used. The results of the numerical analysis showed the treating soil with a biopolymer would increase the soil bearing capacity and reduce soil settlement during and after saturation. The results of the numerical analysis on untreated soils were in close agreement with the results of the in situ plate load tests.

Another example of numerical modeling of the biopolymer treated soil was presented by Chen et al. (2016). In their experimental and numerical research, surface strength of biopolymer-treated mine tailings, made of finely ground rock, was investigated. They conducted experimental research on the biopolymer effect on the penetration force of a cylindrical penetrometer. In the numerical part of their study, they used the discrete element method to simulate the penetration test on the mine tailings stabilized with biopolymer solutions. Their numerical analysis, which was conducted in PFC3D v4.0 using the parallel bond model, showed coinciding results with their experimental analysis. The numerical simulations showed an increase in the tensile and shear strengths with higher biopolymer concentration, indicating that the higher concentration of biopolymer causes larger inter-particle bonding. Up to date, those are some of the first numerical analyses of the biopolymer-treated soil.

To the best knowledge of authors, no previous attempts have been made towards conducting a diagnostic strain localization analysis in biopolymer-treated soil. Thus, the main goal of this study was to numerically capture a stress-strain response and predict the onset of strain localization in elastic-plastic biopolymer-treated soil. Strain localization is a characteristic of elastic-plastic materials that indicates the inception of deformation bands. It is characterized by a jump in strain rate, which often indicates an imminent failure of the material. This study focused on soil treated with three types of biopolymers that were modeled by the linear Drucker-Prager model. A combined numerical-analytical algorithm that can capture a stress-strain response and inception of strain localization in biopolymer-treated soil was implemented. Actual unconfined compression and unconsolidated undrained tests, which were performed on plain and biopolymer-treated soil, were modeled.

The use of image-based methods in materials science has been increasing exponentially in the last decades. The image processing techniques are often used to detect and measure the displacements of a vast number of points on the specimen surface during the laboratory testing on different types of materials. The image analysis consists of the digital image acquisition of the sample during the experimental testing, which is followed by processing and analyzing the acquired series of images. The changes in the position of the pixels can then be quantified and presented as displacements and strains (Liu et al. 2013; Shit et al. 2015; Izzo and Miletić 2019).

Wattrisse et al. (2001) used a digital image correlation to analyze strain localization during the tensile test. In their study, a thin metal sheet with 5 cm length and 1.4 cm width was artificially spackled with white paint. The images with a speckled pattern are easier to analyze computationally. The metal sheet was placed in a tension-compressions, servomechanical testing machine. The camera was placed 1 m away from the sample during the tension test. The experimental approach gave a series of variables such as displacements, strain, and strain rate. The recorded images were computationally analyzed in order to find

the inception of the localization phenomena. The data comparison gave them a good overlap of the measured and computationally obtained results.

Tagliaferri et al. (2011) used x-ray image analysis to observe strain localization of bio-cemented sand. In their research, plain Ottawa and bio-treated Ottawa sand were tested in a triaxial stress state. At certain loading stages, the triaxial test was paused for the x-ray scan. The x-ray image observation showed the changes in the porosity and cementation density during the loading. Furthermore, observing multiple x-ray images, macroscopic behavior of the plain and bio-treated sand could be determined. It was shown that the strain localization occurred at earlier stages for the bio-treated sand and that the bifurcation angle was not significantly affected.

The previous research showed a good application of the image analysis for the study of the strain localization. Therefore, one aspect of this study utilized image processing software in order to observe the strain distribution during mechanical testing. The results of the image processing analysis were compared with the experimental and numerical data of the unconfined compression. A detailed explanation of the method and mechanical testing is explained in Section 5.5.

5.3 EXPERIMENTAL RESEARCH

5.3.1 SOIL

5.3.1.1 Silty sand

The main soil for this study was silty sand. It was classified following ASTM D6913-17 and ASTM D4318-17. The soil had 39% fine particles with the liquid limit, plastic limit, and the index of plasticity being 49, 29, and 20, respectively. Therefore, according to the Unified Soil Classification System, fine particles were classified as silt with low plasticity, and the overall classification of this soil was SM (silty sand).

5.3.1.2 Sand

Another type of soil that was used in this study was pure sand. It was obtained from a site close to Destin, Okaloosa County, Florida, USA. It was mostly made of quartz and was highly uniform. Fine particle content was almost non-existent. It was classified in accordance with ASTM D6913-17. The coefficient of uniformity and the coefficient of curvature that were calculated from the grain distribution curve were 1.46 and 0.93, respectively. Since the presence of gravel and fine particles was practically non-existent, USCS classifies this sand as SP (poorly graded sand). This type of sand was investigated only for the image processing segment of this research (section 5.5).

5.3.2 BIOPOLYMERS

4.3.2.1 Xanthan gum

Xanthan gum (XG) is a biopolymer created by the fermentation of a carbohydrate-source medium such as glucose. Xanthan gum was named after the bacterium that induces the process of fermentation, *Xanthomonas campestris*. Xanthan gum is easily dissolved in hot and cold water. Solutions containing Xanthan gum are non-Newtownians with high pseudoplasticity. At the low shearing rate, the xanthan gum chains are in the state of rest and bound by hydrogen bonds. Increasing the shear rate, the bonds are reduced, which leads to lower viscosity. Due to its fast interaction with water, rapid agitation and mixing are needed to dissolve xanthan gum in water efficiently. The chains of xanthan gum remain stable over wide ranges of pH values. Therefore, it can be successfully implemented in cleaning products as well as acidic food additives (Katzbauer 1998). Other than that, it can be found in the cosmetic industry, agriculture, and oil drilling industry (Katzbauer 1998).

4.3.2.2 Guar gum

Guar gum (GG) is a biopolymer extracted from *Cyamopsis tetragonoloba* that is commonly known as guar. Unlike the majority of plant-based gums, guar gum does not have any uronic acid in its molecular structure. Also, it has a high molecular weight when compared with other naturally occurring water-soluble polysaccharides. It is worth mentioning that guar gum formations are stable over a broad range of pH. Therefore, it can be dissolved in water. Even small concentrations of guar can significantly increase the viscosity of the solution it is mixed in. Some of its applications can be found in the cosmetic industry, food industry, agriculture, and oil drilling (Thombare et al. 2016).

4.3.2.3 Beta-glucan

Beta-glucan (BG) is a biopolymer that consists of glucose molecules. It is extracted from the cells of yeast, fungi, some types of bacteria, and certain types of cereals. The molecular structure of beta-glucans depends on the source they were extracted from. Beta-glucans molecules can vary on the kind of linkages, branching, molecular weight, solubility, and polymer charge (Volman et al. 2008). Beta-glucan used in this study was Beta 1.3/1.6 glucan. The extraction process of beta-glucan depends on the parent source and the molecular bonds of the polymer. Therefore, an appropriate solving agent has to be selected. Molecular structures of beta-glucan that are held loosely outside the cells can be extracted with hot water. Beta-glucan molecules that are held tightly to the cell walls can be released by hot alkali. Beta-glucan, in its powder form, can be dissolved in hot and cold water, which results in forming a gelatinous solution (Bacic et al. 2009). Beta-glucans are heavily investigated in medicine for health improvement (Volman et al. 2008; Bacic et al. 2009).

5.3.3 SPECIMEN PREPARATION

(The preparation of the specimens for image processing is included in Section 5.5. Therefore, it is omitted in this section).

All specimens were prepared by dry mixing of biopolymer and silty sand. The biopolymer concentrations that were used were 0, 1, 2, 4% with respect to the mass of the soil, where 0% represents the plain soil with no additives. After the biopolymer was uniformly mixed with soil, water was sprayed up to 16.5% of the soil mass. After the water was homogeneously added to the biopolymer-soil mixture, the biopolymer-soil was compacted in the molds that were intended for the unconfined compression, splitting tensile, and triaxial tests. The mold for the specimens which were tested for unconfined compression had a diameter of 3.3 cm and a height of 7.1 cm. Specimens for the triaxial test had a mold with a diameter of 7 cm and a height of 14 cm. Additionally, specimens for the splitting tensile strength test were made with attention to use them for calibration of the numerical model. The mold that was used to make the specimens for the splitting tensile strength test had a diameter and height of 3.5 and 1.8 cm, respectively. After preparation, specimens were extruded from the molds and left to cure for five days (specimens for the unconfined compression and splitting tensile test) of time and seven days (specimens for the triaxial test). The reason for different curing time is the fact that the triaxial specimens were larger and required more curing time to achieve their full strength.

5.3.4 MECHANICAL TESTING

For determination of strength in the unconfined compression test, the axial load was applied with a strain rate of 1.5% /min, as per ASTM D2166. The compressive strength of the specimen was computed by dividing the maximum load attained during the test by the corresponding cross-sectional area of the specimen.

The unconsolidated undrained test was performed in accordance with ASTM D2850-15. The specimens were placed in a plexiglass chamber under the confining pressure of 100 kPa. During the shearing stage of the test, the axial strain was applied under the rate of 0.7 %/min.

Splitting tensile tests were performed following general procedures described in the ASTM D3967-16 but with a modified apparatus to accommodate small specimen sizes and relatively low loads. The load was applied at the constant strain rate of 1.5 %/min. It must be noted that the splitting tensile test does not give direct soil tensile properties. Thus, the tensile strength was back-calculated from the maximum compressive load and the dimension of the specimens using the following formula (Akin and Likos 2017):

$$\sigma_T = \frac{2P}{\pi LD} \tag{2.1}$$

where σ_T is tensile strength; P is a compressive force at failure; D is the diameter of the specimen; L is specimen thickness.

5.4 NUMERICAL MODELING

5.4.1 STRESS-STRAIN RELATIONSHIP

The biopolymer-treated soil was assumed to be an elastic-plastic material experiencing an infinitesimal strain and obeying a general non-associative flow rule. Normal components of stress and strain tensors are positive in tension herein. The macroscopic stress-strain relationship for plastic loading is given by (Miletić and Perić 2018):

$$\dot{\sigma}_{ij} = D^e_{ijkl}(\dot{\varepsilon}_{kl} - \dot{\varepsilon}^p_{kl}) \tag{5.1}$$

where subscript notation represents the order of the tensor, superscripts indicate elastic (e), plastic (p) or elastic-plastic (ep) component, "·" over a symbol represents "rate" (time derivative). Therefore, $\dot{\sigma}_{ij}$, $\dot{\varepsilon}_{ij}$, and $\dot{\varepsilon}^p_{ij}$ are the rates of a second-order Cauchy stress tensor,

infinitesimal strain tensor, and infinitesimal plastic strain tensor, respectively. D^e_{ijkl} is the corresponding elastic stiffness moduli tensor of the biopolymer-treated soil, and is given by (Miletić and Perić 2018):

$$D^e_{ijkl} = \mu(\delta_{ik}\delta_{jl} + \delta_{jk}\delta_{il}) + \lambda\delta_{ij}\delta_{kl} \tag{5.2}$$

and δ_{ij} is Kronecker delta, and μ, λ are Lamé's constants of the composite.

The two-invariant yield function (F) was used to describe the plastic behavior of a pressure-sensitive cementitious biopolymer-treated soil. It is defined as:

$$F = F(\sigma_{ij}, \kappa) \tag{5.3}$$

where κ is a plastic hardening variable.

The plastic flow rule and hardening law are respectively given by:

$$\dot{\varepsilon}^p_{ij} = \dot{\lambda}\frac{\partial G}{\partial \sigma_{ij}} \tag{5.4}$$

and

$$\dot{\kappa} = h\left(\dot{\varepsilon}^p_{ij}\right) = \dot{\lambda}h\left(\frac{\partial G}{\partial \sigma_{ij}}\right) \tag{5.5}$$

where $\dot{\lambda} \geq 0$ is a plastic multiplier, $h(\dot{\varepsilon}^p_{ij})$ is the first order homogeneous generally nonlinear function, and G is a plastic potential function. The non-associated flow rule was used to more realistically model the behavior of treated pressure-sensitive materials such as biopolymer-soils (Hirai et al. 1989; Rahimi et al. 2015).

The plastic multiplier $\dot{\lambda}$ is obtained from the consistency condition in plastic loading, as:

$$\dot{\lambda} = \frac{f_{ij}D^e_{ijkl}\dot{\varepsilon}_{kl}}{H + f_{ij}D^e_{ijkl}g_{kl}} \tag{5.6}$$

where gradients of a yield function and plastic potential are denoted by f_{ij} and g_{ij}, respectively. The actual hardening modulus H is given by:

$$H = -\frac{\partial F}{\partial \kappa} h(g_{ij}) \tag{5.7}$$

It is positive, negative, or zero for hardening, softening, or perfect plasticity, respectively.

By combining Eqs. (5.1), (5.4), and (5.6), a tangent elastic-plastic stiffness moduli tensor D^{ep}_{ijkl} is obtained as:

$$D^{ep}_{ijkl} = D^{e}_{ijkl} - \frac{D^{e}_{ijmn} g_{mn} f_{pr} D^{e}_{prkl}}{H + f_{mn} D^{e}_{mnpr} g_{pr}} \quad . \tag{5.8}$$

The yield function, *F,* and rate of the plastic multiplier satisfy Kuhn-Tucker conditions as follows:

$$\dot{\lambda} \geq 0 \,,\; F(\sigma, \kappa) \leq 0 \,,\; \dot{\lambda} F(\sigma, \kappa) = 0. \tag{5.9}$$

5.4.2 ONSET OF STRAIN LOCALIZATION

The diagnostic strain localization analysis was performed on the constitutive level. The inception of strain localization may be considered as a bifurcation problem that signifies a loss of stability of the constitutive relation governing a uniform deformation.

It is assumed that the jump in a displacement rate along the singular surface Γ is constant, which is expressed as (Miletić and Perić 2018):

$$\left[\dot{u}_i\right]\Big|_{\Gamma} = \left(\dot{u}_i^{+} - \dot{u}_i^{-}\right)\Big|_{\Gamma} = \text{constant} \tag{5.10}$$

where $\dot{u}_i^{+}$ denotes the displacement rate on one side of the Γ and $\dot{u}_i^{-}$ the other side.

Equation (5.10) generally describes the kinematics of a strong discontinuity. The special case obtained by equalizing the right-hand side of Equation (5.10) to zero represents a weak discontinuity. At this point, no assumptions are made about the homogeneity and variation of $\left[\dot{u}_i\right]$ in the neighborhood of the singular surface Γ. Combining Eq. (5.10) with the kinematical definition of infinitesimal strain rate gives the following expression for a jump in strain rate across the singular surface Γ:

$$\left[\dot{\varepsilon}_{ij}\right]\Big|_{\Gamma} = \frac{1}{2}\left(z_i n_j + z_j n_i\right) \tag{5.11}$$

where z_i is the eigenvector corresponding to the relevant eigenvalue problem, as discussed below, n_i is the unit vector that is normal to the surface Γ.

Furthermore, the equilibrium along the singular surface imposes the following condition on the traction rate ($\dot{t}$):

$$\left[\dot{t}_i\right]\Big|_{\Gamma} = \left(\dot{t}_i^{+} - \dot{t}_i^{-}\right)\Big|_{\Gamma} = 0. \tag{5.12}$$

Combining Equations (5.1), (5.11), and (5.12) leads to the classical bifurcation criterion (Rudnicki and Rice 1975) which is, given by:

$$Q_{ik} z_k = n_i D^{ep}_{ijkl} n_l z_k = 0 \tag{5.13}$$

where Q_{ik} is an acoustic tensor, also known as a characteristic tangent stiffness tensor. Equation (5.13) is based on the assumption that a so-called plastic/plastic bifurcation precedes an elastic/plastic bifurcation. In the former case, the primary and bifurcated incremental fields both correspond to plastic loading, while in the latter, only one of the incremental fields corresponds to plastic loading. It was shown (Ottosen and Runesson 1991) that the plastic/plastic bifurcation always precedes elastic/plastic bifurcation.

In order to solve for the critical amount of hardening necessary for the onset of strain localization, the following eigenvalue problem was considered:

$$Q_{ik} z_k^{(j)} = \lambda^{(j)} Q^e_{ik} z_k^{(j)}, \; j = 1,2,3 \tag{5.14}$$

where *(j)* indicates the direction of principal stresses.

Nontrivial solutions of the eigenvalue problem are possible only when the acoustic tensor Q_{ik} is singular. The first two eigenvalues are elastic and equal to one while the third eigenvalue is plastic, and it was given by Runesson et al. (1991) as:

$$\lambda^{(3)} = 1 - \frac{b_i P^e_{ik} a_k}{H + f_{mn} D^e_{mnpr} g_{pr}} \tag{5.15}$$

where P_{ik}^{e} is the inverse of the elastic acoustic tensor and the vectors a_i and b_j are defined as

$$a_i = f_{mn} D_{mnij}^{e} n_j, \; b_j = n_i D_{ijmn}^{e} g_{mn} \tag{5.16}$$

The corresponding eigenvector is given by the following expression:

$$z_i^{(3)} = k P_{ij}^{e} b_j \tag{5.17}$$

where k is an arbitrary scalar.

By setting $\lambda^{(3)}$ from Equation (5.15) equal to zero, a hardening modulus H (n_i) was obtained. Finally, the critical amount of hardening necessary for the onset of strain localization was obtained by solving the following constrained optimization problem:

$$H_{cr} = \max_{n_i} H(n_i) \qquad \text{where } n_i n_i = 1 \tag{5.18}$$

where the right side of the equation above represents the maximization of the function.

The corresponding bifurcation angle θ represents the angle between the minor stress axis and the normal vector (n_1,0,n_3). It can be determined from the expression:

$$\tan^2 \theta = \frac{n_1^2}{n_3^2} \tag{5.19}$$

Analytical solutions for H_{cr} and corresponding critical bifurcation angles were given by (Ottosen and Runesson 1991).

5.4.3 APPLICATION TO DRUCKER-PRAGER MODEL

The analysis, in this study, was based on the linear Drucker-Prager model and the parameters of the total stress. Yield and plastic potential function were presented as follows:

$$F = \left(\frac{1}{3} \tan \beta \right) I_1 + \sqrt{J_2} - \kappa \tag{5.20}$$

$$G = \left(\frac{1}{3} \tan\psi \right) I_1 + \sqrt{J_2} \tag{5.21}$$

Gradients of linear Drucker-Prager yield and plastic potential functions are given by

$$f_{ij} = \frac{1}{3} \tan\beta \cdot \delta_{ij} + \frac{\sqrt{3}}{2\sqrt{J_2}} s_{ij} \tag{5.22}$$

$$g_{ij} = \frac{1}{3} \tan\psi \cdot \delta_{ij} + \frac{\sqrt{3}}{2\sqrt{J_2}} s_{ij} \tag{5.23}$$

where s_{ij} is stress deviator tensor; β is internal friction angle; ψ is dilatancy angle; I_1 and J_2 are first and second deviatoric stress invariants, respectively.

After the critical hardening has been obtained, the onset of strain localization can be determined. The onset can be determined by comparing the values of the critical hardening modulus with the actual hardening modulus. The actual hardening modulus (H_{act}) is calculated from the response representing the actual stress and plastic strain.

5.4.4 NUMERICAL SIMULATION

The actual stress-strain response was obtained by simulating the samples by a single eight-node element modeled with 3D integration. The unconfined compression tests were conducted by applying a constant vertical strain rate and keeping the principal stresses in the horizontal directions at zero. The unconsolidated undrained tests were performed under a constant vertical strain rate and applying the horizontal pressures following the experimental tests. The inception of the strain localization will occur at the moment when the actual hardening modulus equalizes with the critical hardening modulus.

5.4.5 CALIBRATION OF CONSTITUTIVE MODEL

The Drucker-Prager model was calibrated against the unconfined compression, splitting tensile strenght test, and the unconsolidated undrained tests that were performed on plain

and biopolymer-treated silty sand. The calibration example is presented in Figure 5-1. Additional calibration figures are represented in the Appendix (Figure 8-2).

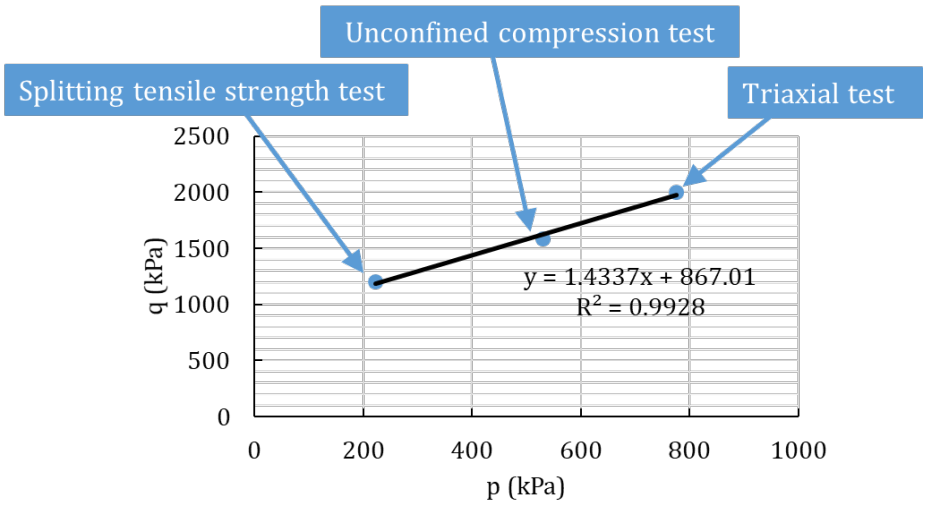

Figure 5-1: The example of the calibration procedure for the silty sand with 4% BG

The experimental data were available for the plain soil and the soil treated with three biopolymer concentrations (1, 2, and 4%). However, only the data for the soil treated with 0, 1, and 4% was used for the calibration. The data for the soil treated with 2% biopolymers was used for the validation of the proposed model. The elastic and plastic parameters were predicted from linear interpolation of the results for the soil with 0, 1, and 4% biopolymers. To achieve the best values of the input parameters, the least-squares fit was used. The least-squares fit minimizes the relative error, and it was based on the experimental data.

Young's modulus was obtained for the plain and treated soil from the unconfined compression tests. The Young's modulus was calculated as the slope of the elastic portion of the stress-strain response. The calculated values of Young's modulus for the plain and treated soil were in the range of previously reported values (Truty and Obrzud 2011; Chang et al. 2015). Poisson's ratio (ν) was kept constant for all biopolymer-treated soil and was selected from the recommended values for different types of materials (Das 2019).

For the linear Drucker-Prager criterion used in this study, the internal friction angle (β) and cohesion (d) were taken from the linear yield surface in the p-q stress plane (Figure 5-1). The cohesion for the samples with 2% of biopolymers was calculated from the predicted friction angle and the initial stress level of the predicted hardening. The plasticity models for the nonassociated flow require a value for the dilatation angle (ψ) that was kept constant for all biopolymer-treated soil and was assumed based on suggested values (Strömblad 2014). Table 5 1 summarizes the material properties used for the proposed model.

Table 5-1: Selected properties of the biopolymer-treated soil for the proposed model

Material	**E (MPa)**	**β(°)**	**d (MPa)**	***ψ* (°)**	**v**
Plain soil	88	34	0.7	0	0.3
GG (1%)	234	63	0.72	0	0.3
GG (2%)	217	64	0.48	0	0.3
GG (4%)	184	65	0.79	0	0.3
BG (1%)	114	42	0.1	0	0.3
BG (2%)	130	46	0.85	0	0.3
BG (4%)	162	55	0.87	0	0.3
XG (1%)	249	54	1	0	0.3
XG (2%)	243	51	1	0	0.3
XG (4%)	233	46	1.9	0	0.3

The isotropic non-linear hardening was used in all test simulations and was implemented into the model in a tabular form. The hardening was obtained from the averaged values of the experimental tests (unconfined compression). The plastic strains were calculated by subtracting the elastic strain components from the amount of total strains. Prior to that, the elastic strain components were calculated by dividing the axial

stress response with the modulus of elasticity. The example of actual and predicted hardening response for the unconfined compression is presented in Figure 5-2. The remaining hardening response for the unconfined compression can be found in the Appendix (Figure 8-3 and Figure 8-4). The hardening curve for the silty sand with 2% BG was interpolated from the parameters of the equations fitting the experimental data.

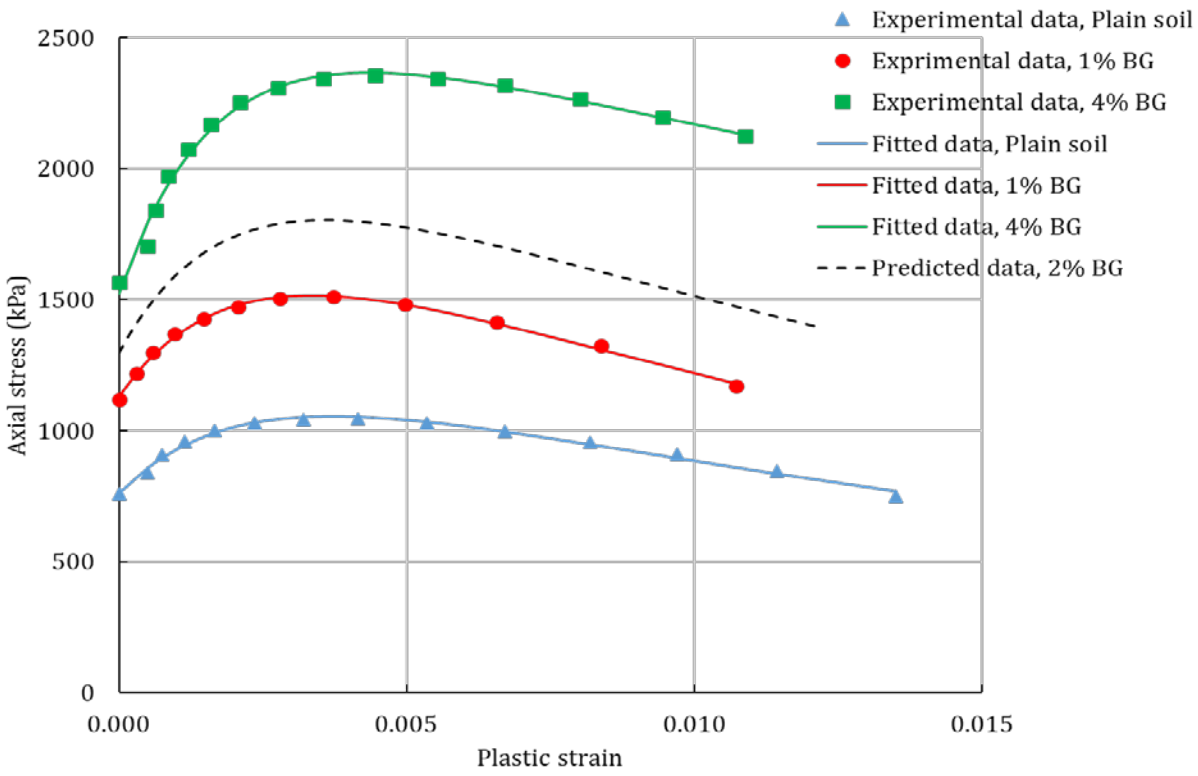

Figure 5-2: Hardening response for the unconfined compression test for silty sand treated with BG

5.4.6 RESULTS OF THE NUMERICAL MODELING

5.4.6.1 Unconfined compression test

The linear Drucker-Prager model was used to simulate the 3D stress state of the unconfined compression tests. A comparison between the numerically predicted responses and experimentally observed response for the unconfined compression test are presented in

Figure 5-3 - Figure 5-5. The stress-strain responses of specimens with 0, 1, and 4% were used for calibration of the model, while the specimens with 2% were used for validation.

Figure 5-3 shows the numerical response (solid line) and experimental data (scatter data) of the unconfined compression test of the BG-treated silty sand. For comparison, the same results of the plain silty sand are shown Figure 5-3a). From Figure 5-3 it can be seen that the onset of strain localization (OSL) of the silty sand increased with the addition of BG. Furthermore, it can be seen that the peak stress also increased with the biopolymer addition. Figure 5-3a, b, and d show a relatively better match between the experimental data and the numerical response when compared with Figure 5-3c. That is because of the numerical response in Figure 5-3a, b, and d was based on the calibrated material properties, whereas the numerical response in Figure 5-3c was obtained from the predicted material properties. The predicted model could not detect the OSL for the silty sand treated with 4% BG because the actual critical hardening never equalized with the calculated critical hardening.

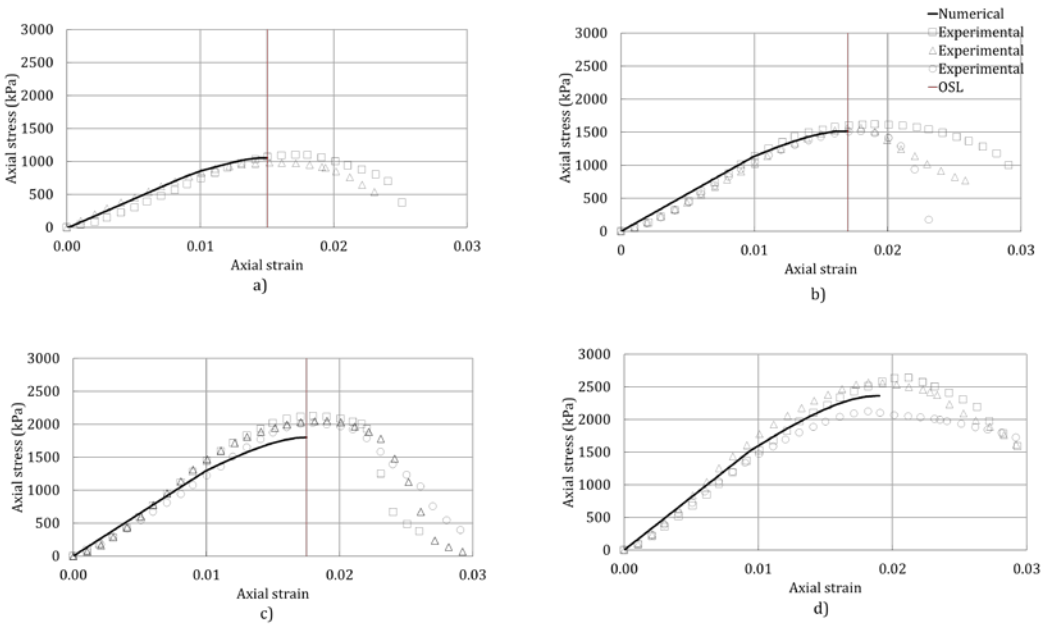

Figure 5-3: Unconfined compression test results of the silty sand with a)0% additives; b) 1% BG; c) 2% BG; d) 4% BG

In Figure 5-4, the numerical response and experimental data of the unconfined compression test of the GG-treated silty sand can be seen. Additionally, the experimental and numerical results of the treated silty sand were compared with the results of the plain silty sand (Figure 5-4a). It can be seen that the peak stress increased with the increase of the GG concentration. Figure 5-4 shows that the OSL of the silty sand increased with the addition of GG. The exception is the concentration of 1% GG (Figure 5-4b). Even though the peak stress of the silty sand increased with the addition of 1% GG, the OSL occurred at the lower strain level for 1% GG. The reason behind that is that the onset of strain localization depended on the yield stress and the peak stress, but it was primarily governed by the hardening response. Furthermore, the numerical response of the silty sand with 2% GG shows a relatively good match with the experimental data (Figure 5-4c).

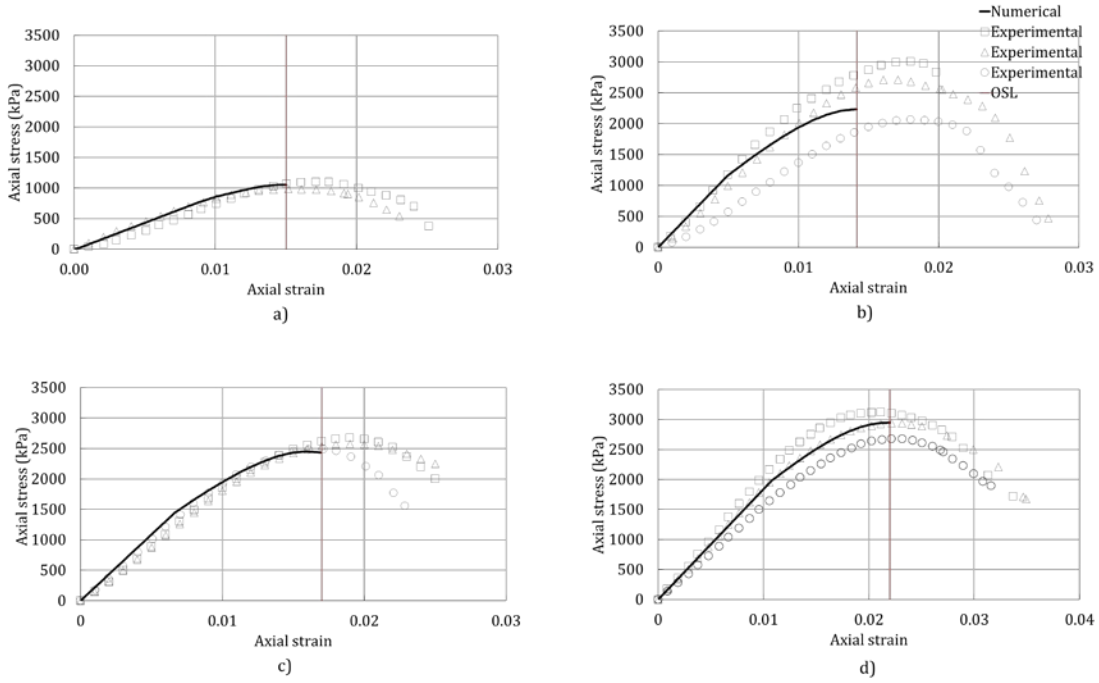

Figure 5-4: Unconfined compression test results of the silty sand with a) 0% additives; b) 1% GG; c) 2% GG; d) 4% GG

Figure 5-5 shows the experimental data and the numerical response of the unconfined compression test of the XG-treated silty sand. The same results of the silty sand are shown in Figure 5-5a. Figure 5-5 shows that the OSL of the silty sand was postponed with the addition of XG. Additionally, it can be seen that the peak stress also increases with the increase of XG. The numerical response of the silty sand treated with 2% XG showed a relatively good correspondence with the experimental data even though it was based on the predicted material properties. The predicted model could not detect the OSL for the silty sand treated with 4% XG because the actual critical hardening did not raise to the level of the calculated critical hardening.

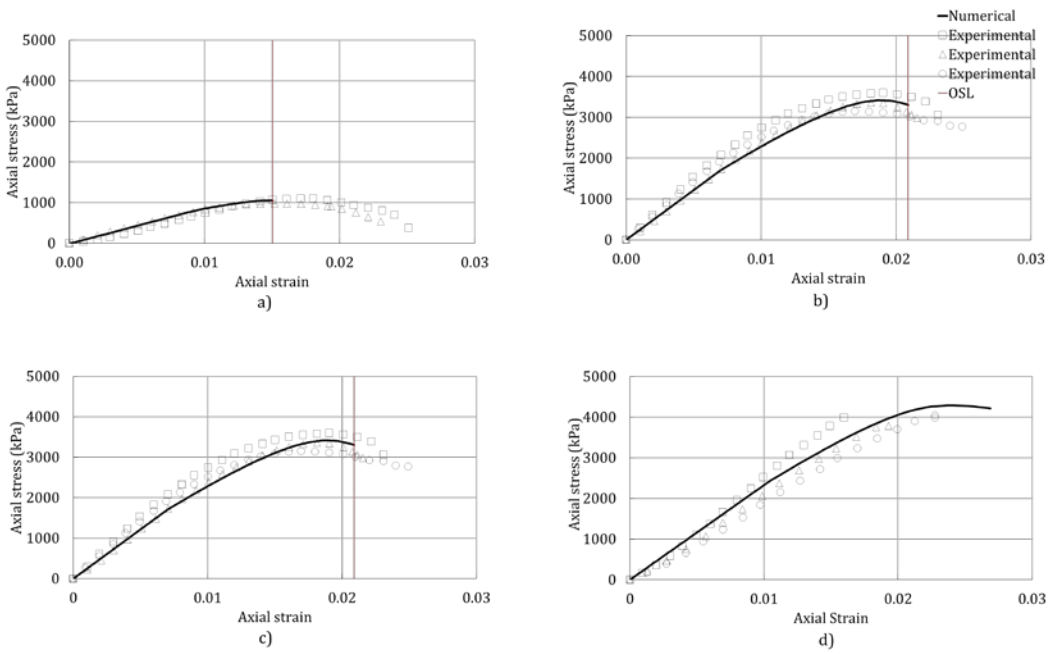

Figure 5-5: Unconfined compression test results of the silty sand with a)0% additives; b) 1% XG; c) 2% XG; d) 4% XG

Figure 5-6 summarizes the level of the total axial strain (Figure 5-6a) and the axial stress at the OSL (Figure 5-6b). It is evident that the stress at OSL increased with the increase

of biopolymer concentration, and that the level of total strain increased for most of the biopolymer concentrations.

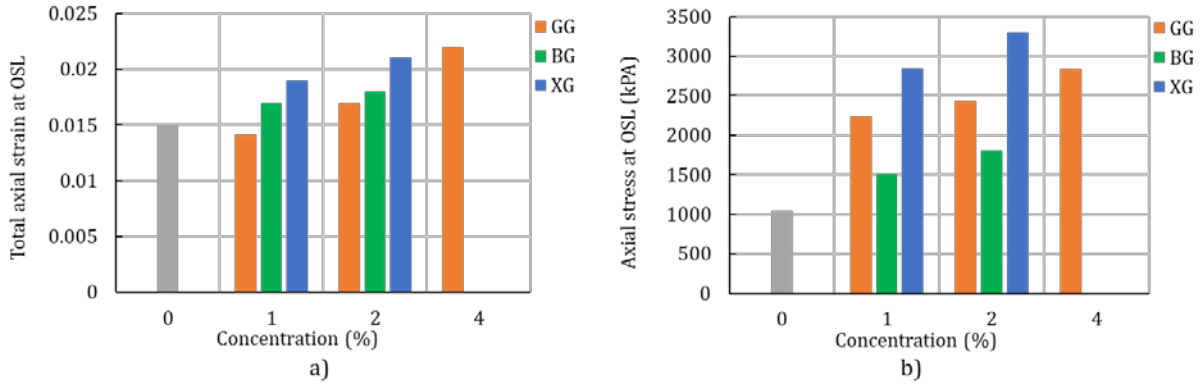

Figure 5-6: Unconfined compression test results: a) axial strain at OSL and b) axial stress at OSL for the unconfined compression test of silty sand

The bifurcation angle is represented by the angle between the minor stress axis (x_3) and the unit vector (n) that lays in the x_1, x_3 plane (Ottosen and Runesson 1991).

From Figure 5-7, it can be seen that the addition of the biopolymers altered the bifurcation angle. In particular, the results show that the bifurcation angle kept increasing with the increase of the GG and BG concentrations. For the XG-treated soil, the highest bifurcation angle was achieved for the concentration of 1%, and it kept decreasing with the increase of XG concentration. That phenomenon can be related to the increase in the ductility of the material with the increase of the XG concentration. However, in all cases of the treated soil, the bifurcation angle was higher than the bifurcation angle of the plain soil. In general,

the increase of the bifurcation angle results in a steeper deformation bend that changes the failure behavior.

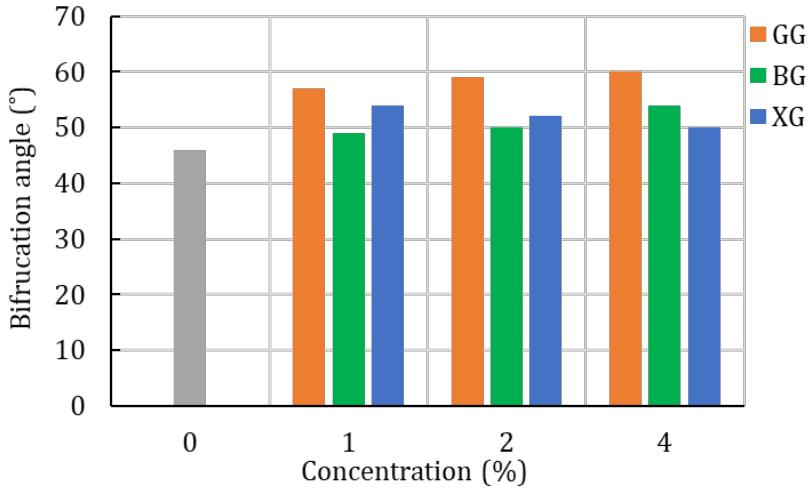

Figure 5-7: Bifurcation angle for the plain and biopolymer-treated silty sand (unconfined compression test)

5.4.6.2 Unconsolidated-undrained triaxial test

The linear Drucker-Prager model was also used to simulate the 3D stress state of the unconsolidated-undrained triaxial test. The experimental stress-strain response was compared with the numerical response. The onset of strain localization was considered when the actual hardening equalized with the critical hardening. The results were summarized in Figure 5-8. The level of the stress at OSL increased with the increase of the biopolymer concentration (Figure 5-8a). However, Figure 5-8 shows a trend of the decreasing level of strain at OSL with the increase of biopolymer concentration. The reason for that behavior is the fact that the onset of strain localization depends on the yield stress and the hardening response. These results indicate that the biopolymer-treated soil had a more brittle behavior than the plain soil at the higher confining pressures.

The change in the bifurcation angle of triaxial specimens (Figure 5-8c) showed a similar response, as seen in the unconfined compression test. For all biopolymer types and

biopolymer concentrations, the treated soil had a higher bifurcation angle than the plain soil. Additionally, the bifurcation angle kept increasing with the concentration increase of GG and BG. For the XG-treated soil, the highest bifurcation angle was achieved for the concentration of 1%, and it kept decreasing for the higher concentrations of XG.

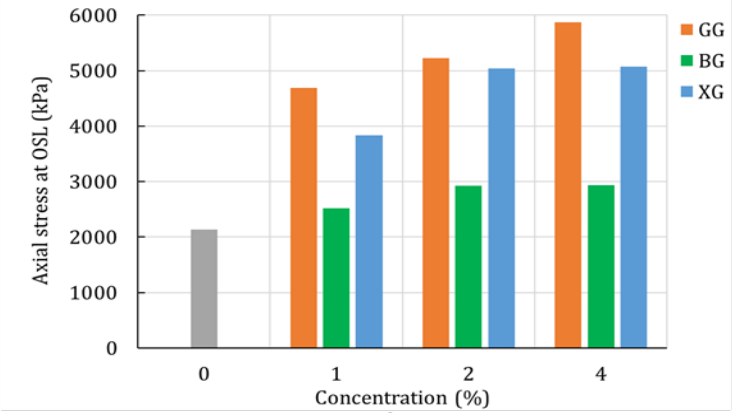

a)

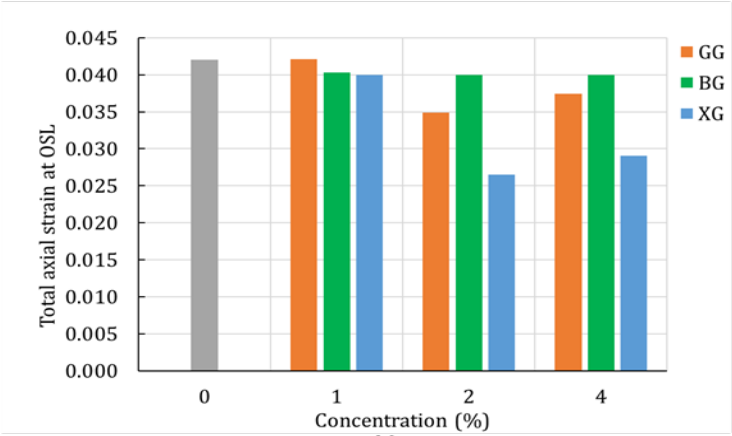

b)

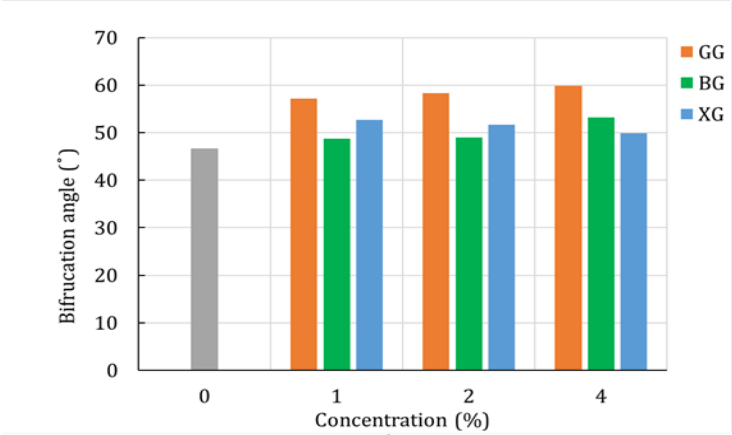

c)

Figure 5-8: Unconsolidated undrained triaxial test results a) axial stress at OSL; b) axial strain at OSL; c) bifurcation angle

Figure 5-9 compares the stress-strain responses of the unconfined compression tests and the triaxial tests of the silty sand. As described previously, the onset of strain localization occurs close to the peak of stress-strain curves. Comparing the peaks of the unconfined compression and triaxial test curves, it can be observed that the peaks occur at a higher stress-strain level for the triaxial tests. The reason for that is the applied confinement pressure in the triaxial test. Schnaid et al. (2001) demonstrated that the increase in confinement pressure increases the level of the peak stress in the cemented sand and it postpones the level of strain at which it occurs. Furthermore, the peak stress tends to increase with the increase of biopolymer concentration. Observing only the results of the unconfined compression tests, represented with scattered data, it can be seen that biopolymers tend to increase the level of the peak stress and the level of strain at the peak (represented by the arrow in Figure 5-9). The triaxial test results, represented by solid lines, also show that the level of the peak stress increases with the addition of biopolymers. However, the peak occurs at the lower strain level for the treated silty sand than for the plain silty sand. Furthermore, the level of strain tends to decrease with the increase of biopolymer concentration (represented by the arrow in Figure 5-9). Similar results were demonstrated in previous research of the stabilized soil (Schnaid et al. 2001; Kutanaei and Choobbasti 2016). That phenomenon is likely related to the ductility of the specimens. The plain soil in the triaxial test demonstrates a more ductile behavior than the treated specimens. Cemented soil can have an abrupt post-peak failure in the triaxial test (Tagliaferri et al. 2011) that indicates the brittleness of the treated soil. It is also more prominent in the sand with no or a small amount of fine particles.

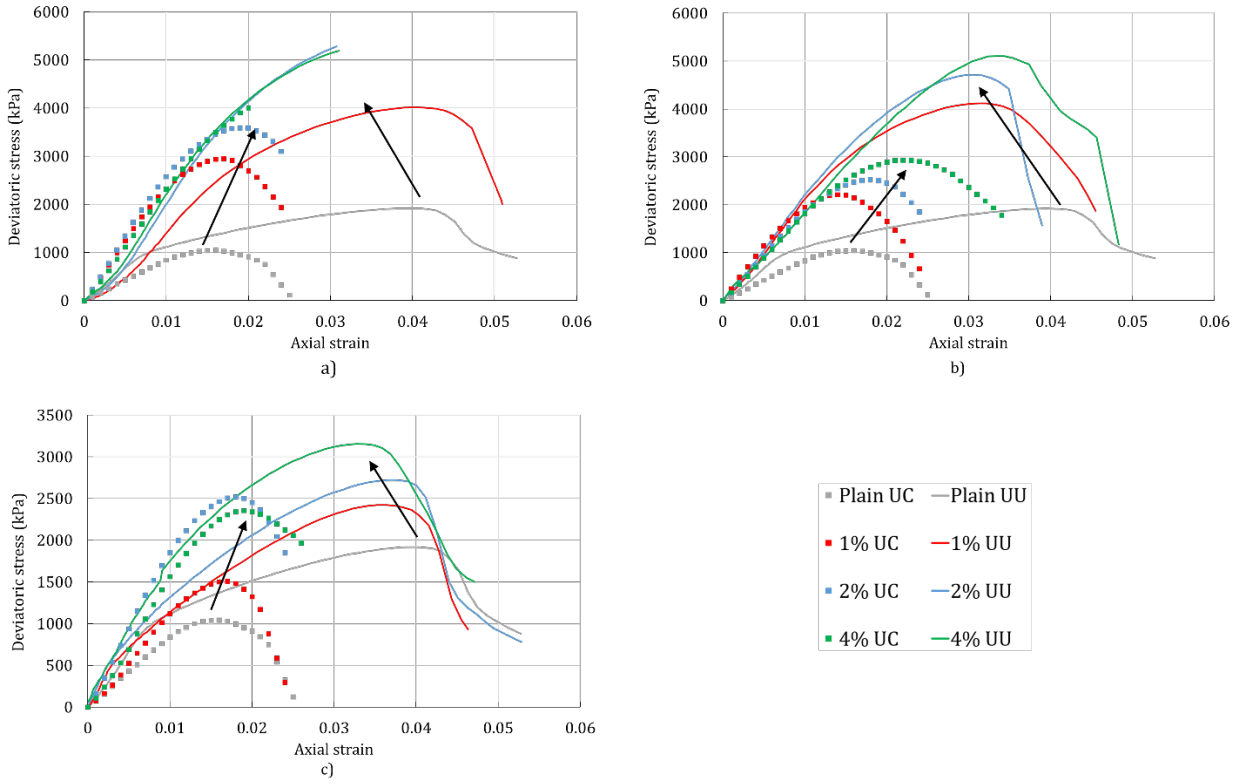

Figure 5-9: Comparing unconfined compression test (UC) with the triaxial test (UU) for the plain silty sand and silty sand treated with a) XG; b) GG; c) BG

5.5 IMAGE PROCESSING OF THE UNCOFINED COMPRESSION TEST

Several cube specimens made of plain and treated soil were tested for the unconfined compression. In addition, the digital image processing technique was used to monitor the development of the strain component and detect the inception of strain localization. The cube specimens were chosen because of the flat surface of the sides of the cube. The flat surface of the cube specimens was appropriate for the image processing software (GOM Correlate) that can record the strain development in pressure-sensitive materials.

Two types of soil were used in the image processing portion of the study, clean sand and silty sand. Clean sand was treated with 0.5% and 1% XG, while silty sand was treated with 0.5% XG and 1% GG. The biopolymer-treated soil was mixed and wetted in the same

manner, as described in Section 5.2. The biopolymer-treated soil was compacted in cube molds with dimensions of 5x5x5 cm and left to be air-dried for five days.

Since the quality and accuracy of the image processing rely on a high-contrast random pattern, a distinctive speckle pattern was applied to the surface of the specimen with a colored marker. The digital images of the soil samples were continuously recorded at a constant position (20 cm from the center of the specimen) for image consistency and uniformity. The resolution of the camera was 12 MP, and it was able to capture 30 frames per second.

The image processing software splits the recording as a series of images. The applied pattern is recognized by the software and isolated as a surface of observation. That surface is transformed into a group of pixels. In this study, the surface of interest (45×45 mm) was transformed into approximately 570×570 pixels. The position of each pixel and the distance from the surrounding pixels are tracked through the software. Each picture is compared to the previous one, therefore the software can detect the change of the pixel position. Following that technique, the software can detect and quantify displacement and strains that occur in the initial recording. Furthermore, the unconfined compression apparatus stores timestamps through the test, while the image processing software takes the time steps from the video recording. Therefore, the correlation between the experimental results and the image processing software could be drawn.

.

5.5.1 RESULTS OF IMAGE PROCESSING

Figure 5-10 and Figure 5-11 combine experimental response, numerical response, and image processing results for clean sand, and silty sand, respectively. The experimental responses of the unconfined compression tests were presented by markers in Figure 5-10and Figure

5-11. The solid dark and red lines represent the numerically obtained stress-strain curve, and OSL, respectively.

The heat maps in Figure 5-10 and Figure 5-11 are presented as overlays on the soil surface and show the strain concentration and strain propagation on cube samples. Three heat maps represent three different timestamps when the heat map was generated. The first image represents the early stage of the unconfined compression with no visible strain localization. The second image corresponds to the OSL from the analytical-numerical algorithm. The third image represents the post-peak strain propagation. The arrows in the figures represent the stress-strain level at which the heat map was captured.

Figure 5-10a represents the sand treated with 0.5% XG, whereas Figure 5-10b represents the sand treated with 1% XG. Comparing the onset of strain localization in the sands with different XG concentrations, it can be seen that OSL occurs for almost the same strain level, in fact, moderately lower for the sand with 1% XG. However, the peak stress reached was higher for the specimen treated with 1% XG. Shortly after reaching the peak stress, the stress drops more abruptly for the specimen with 1% XG because of the increased brittleness.

The heat maps in Figure 5-10a and Figure 5-10b show the process of strain concentration for the sand specimen. In both figures, in the early stages of the test, the strain distribution is uniform along the whole surface. While approaching the red line (OSL), the strains start to concentrate in one deformation plane. The third heat map image shows the propagation of the deformation plane with the increase in strain after the OSL has been reached. Additionally, the heat map shows the created bifurcation angle as the result of the strain localization. The bifurcation angle of sand with 0.5% XG was calculated as 65˚, while the bifurcation angle of sand with 1% XG was 75˚. It can be concluded that the increase of biopolymer concentration can increase the bifurcation angle of sand. A similar trend was

previously reported for the biopolymer-treated silty sand in Section 5.4.6 where the bifurcation angle was found through the analytical-numerical algorithm.

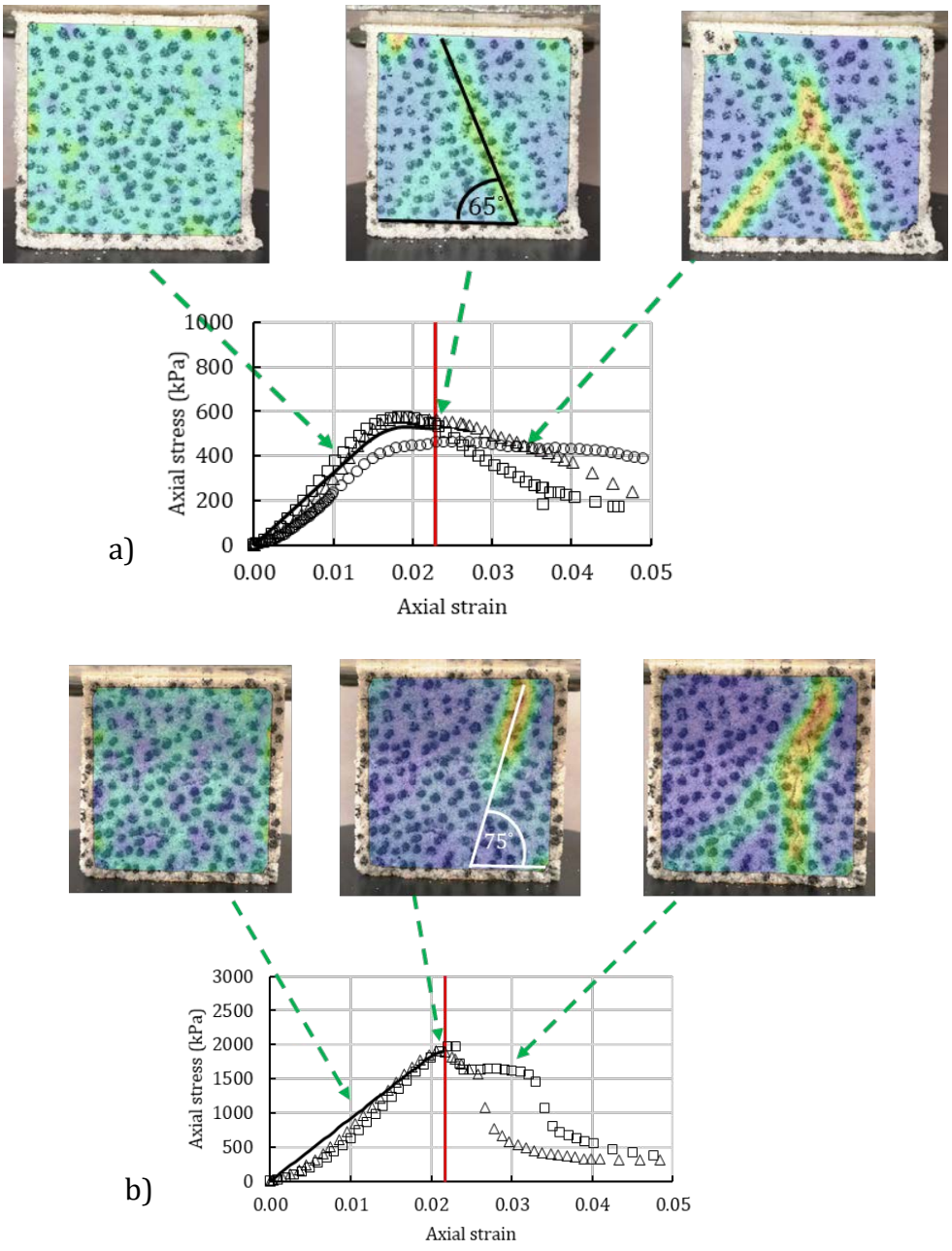

Figure 5-10: Image processing of strain localization for sand with a) 0.5% XG and b)1% XG under unconfined compression test compared with the numerically obtained OSL and experimental data

Observing Figure 5-11, a combined experimental response, numerical response and image processing results for silty sand can be seen. Figure 5-11a represents the plain silty sand, Figure 5-11b represents the silty sand treated with 0.5% XG, and Figure 5-11c shows the silty sand with 1% GG. Even though the peak stress increased with the addition of biopolymers, the strain level for the OSL did not significantly change. This indicates that higher concentrations of XG and GG are required to postpone the OSL of the silty sand.

The heat maps in Figure 5-11a, Figure 5-11b, and Figure 5-11c show the process of strain concentration for the biopolymer-treated silty sand. In all three figures, in the early stages of the test, the strain distribution is uniform along the specimens' surfaces. While approaching the OSL, the strains start to concentrate on one deformation plane. The second image shows the high strain concentration at the moment of the OSL which was determined from the analytical-numerical algorithm. The third heat map image shows the strain propagation that occurs after the OSL. Additionally, the heat maps show the created bifurcation angle due to the strain concentration. The bifurcation angle of the biopolymer treated soil shows higher values for the biopolymer-treated silty sand. The plain silty sand (Figure 5-11a) had the bifurcation angle of 55˚. The silty sand with 0.5% XG Figure 5-11b) had the bifurcation angle of 60˚, while the concentration of 1% GG (Figure 5-11b) resulted in the bifurcation angle of 70 ˚. As reported previously in this study, the bifurcation angle of the silty sand increased with the addition of biopolymers. The difference between the second heat map image (at the OSL), and the third image (after the OSL) was more prominent in the sand than in the silty sand. The reason for that is the difference in the nature of the base material. The treated sand had a more brittle response than the treated sand wilt. Furthermore, the break of the treated sand was cleaner, whereas the failure of the silty sand resulted in the partial crumbling of the material. Therefore, the nature of the treated sand was more suitable to observe under the image processing software.

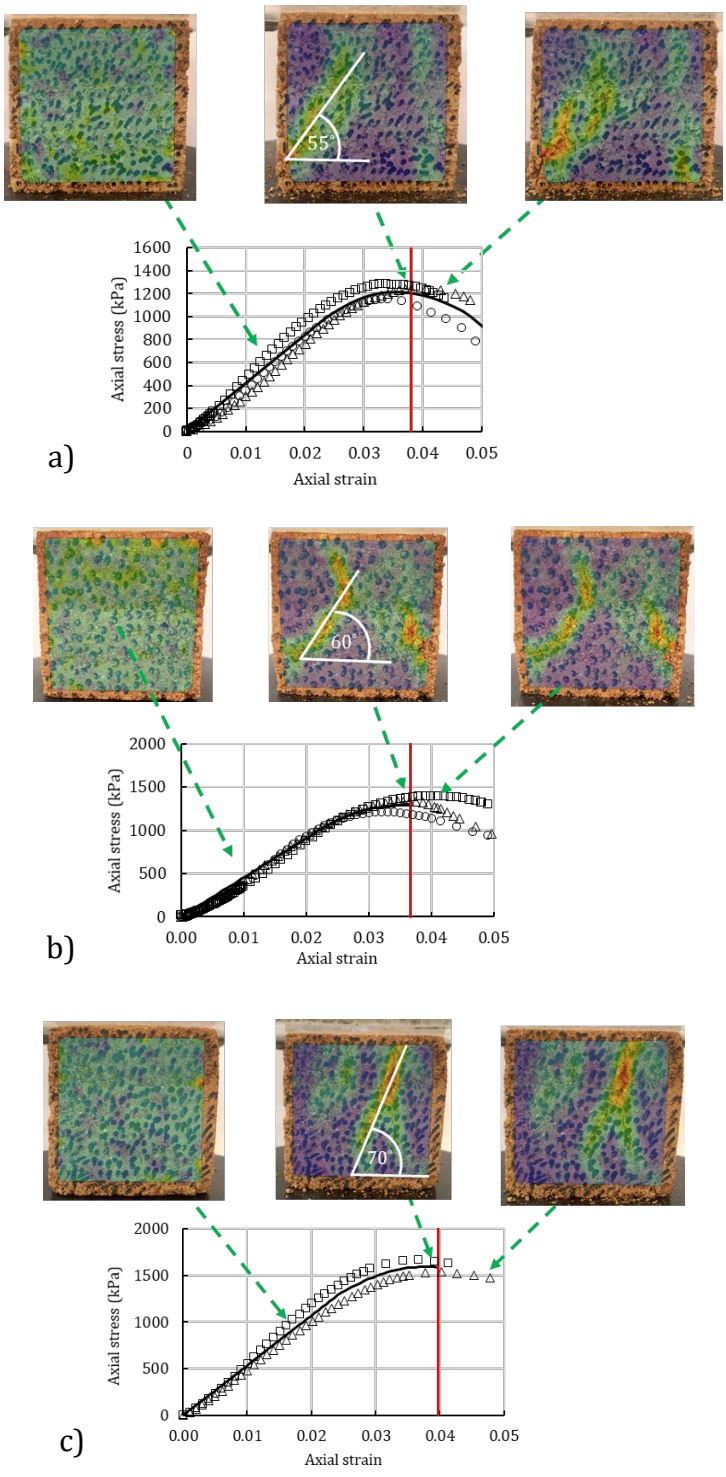

Figure 5-11: Image processing of strain localization for the silty sand with a) no additives; b)0.5% XG; c)1% GG under unconfined compression test compared with the numerically obtained OSL and experimental data

Observing the unconfined compression test under an image processing software showed high strain concentrations at the moment of the OSL. However, there are some drawbacks that should be considered. The image acquisition with a single camera and subsequent processing gave a 2D output only on one side of the specimen. However, during the actual 3D test, it is unknown on which specimen side will the deformation band occur. Therefore, the digitally obtained deformation planes for the tested specimens might not be the most critical ones. To solve these issues, multiple cameras facing each specimen side should be used.

5.6 CONCLUSIONS

The main objective of this research was to perform a diagnostic strain localization analysis in biopolymer-treated soil. Two types of soil (silty sand and clean sand) were investigated together with the three types of biopolymers (xanthan gum, guar gum, and beta-glucan). A numerical-analytical algorithm was implemented to capture the stress-strain response and the inception of the strain localization. The experimental data were collected for the plain silty sand and silty sand with 1, 2, and 4% biopolymer concentrations. Three tests used for the calibration purposes were unconfined compression, unconsolidated undrained triaxial, and splitting tensile strength tests. However, the experimental data of the silty sand with 2% biopolymers was not used for the calibration, but only for validation purposes.

The stress-strain response of the specimens subjected to uniaxial compression and triaxial stress states were simulated. In addition, the inception of the strain localization was calculated for each specimen and each stress state. For the unconfined compression test, it was found that the OSL was postponed for most concentrations of biopolymers. The peak stress in each test increased with the increase of biopolymer concentration, and OSL always occurred close to the level of the peak stress. The level of the bifurcation angle of the silty sand increased for all biopolymer concentrations. It was noticed that the increase of GG and

BG concentration increases the bifurcation angle. However, for XG, the highest bifurcation angle was noticed for 1% XG, and it kept decreasing for higher concentrations.

The unconsolidated undrained triaxial test showed an increase in the peak stress of the silty sand for all biopolymer concentrations. Also, the increase in the bifurcation angle was noticed for all biopolymer concentrations. The same trend as in the unconfined compression test was noticed. The increase of GG and BG concentrations lead to an increase in the of the bifurcation angle. The highest achieved bifurcation angle for XG treated silty sand was achieved at 1% XG. For higher concentrations, the bifurcation angle started decreasing. However, it was noticed that for the triaxial state of stress, OSL occurred close to the peak stress, and it was advanced for every tested biopolymer concentration.

Several cube specimens, made of silty sand and pure sand, were prepared and tested for the unconfined compression accompanied by image processing. The surface of the cube specimens was marked in a recognizable pattern before the testing. The testing process was recorded and observed in an image processing software GOM Correlate. The strain development was tracked and compared with calculated OSL. OSL appeared close to the peak stress, at which moment the image processing software reported the initiation of the high strain concentrations. To capture more precise strain distribution and bifurcation angles with the image processing software, a 3D image acquisition and analysis should be performed. That approach requires more equipment and will be utilized in future research.

In conclusion, the diagnostic strain analysis shows that the presence of biopolymers in the soil can influence the onset of strain localization. Depending on the stress state, soil type, biopolymer type, and concentration, the strain localization can be postponed or advanced. Analyzing the complex mechanics of biopolymer-treated soil helps to understand the strength limitations of biopolymer treated soil. Understanding how biopolymers affect the strain localization and failure of soil materials can lead to their utilization in engineering practice.

6. SUMMARY, CONCLUSIONS, AND FUTURE RESEARCH

6.1 SUMMARY AND CONCLUSIONS

The biggest motivation for this research was the current and future state of our environment. The constant urbanization and overpopulation are causing constant damage to the limited space that we are inhabiting. Therefore, every industry should turn to eco-friendly solutions that don't create irreparable damage to the environment.

The research presented in this study investigated several types of biopolymers as one of the potential eco-friendly solutions for soil stabilization. From this dissertation, several conclusions can be made.

- The main objective of Chapter 2 was to experimentally investigate the effect of five types of biopolymers on the mechanical properties of silty sand. The biopolymers that were used were xanthan gum, guar gum, beta 1.3/1.6 glucan, chitosan, and alginate. The research was conducted with four mechanical strength tests (unconfined compression test, splitting tensile strength test, direct shear test, and unconsolidated undrained test). Water content was kept the same, as well as the soil type. The strength tests were observed under different concentrations of biopolymers and different curing times. Chitosan and alginate did not show a significant positive influence on the soil strength, therefore, most of the focus was pointed towards xanthan gum, guar gum, and beta 1.3/1.6 glucan. The increase in soil strength was seen with the increase of biopolymer concentration and curing time. The unconfined compressive strength and the splitting tensile test showed that most of the strength was can be achieved during the first five days of curring. The triaxial test showed that for the bigger specimens, longer curing time is required to achieve the total strength. The direct shear test showed that cohesion of the silty sand with the presence of xanthan gum, guar gum or beta 1.3/1.6 glucan. The same test also showed that the same biopolymers decrease the friction angle with time. Furthermore, it was found that each biopolymer has

an optimum concentration that depends on the water level and soil type. That means that unreasonable high concentrations of biopolymers do not guarantee high strength. The first chapter showed that certain biopolymers have great potential for the improvement of soil strength but, that xanthan gum had the most dominant effect.

- While in Chapter 2 the soil type was a constant, and biopolymer type and biopolymer concentrations were changing variables, in Chapter 3 the soil type was a changing variable, and biopolymer type and concentrations were constant. In this part of the research, three types of soil were investigated, clay, silty sand and pure sand. They were treated by 1% XG. The strength of soil was investigated by three mechanical tests: unconfined compression test, unconsolidated undrained triaxial test, and direct shear test. Plain type of soil and treated soil was tested. They were tested five days after the preparation. The unconfined compression test and the unconsolidated undrained triaxial test showed the increase in strength for all types of soil. The direct shear test showed that the presence of XG can increase the shear strength of the sand and silty sand, but the effect on clay was marginal. Furthermore, the direct shear test revealed that XG significantly increases the cohesion in cohesionless soils such as pure sand, but that it does not have a significant effect on the friction angle of that type of soil. On the other hand, the direct shear test showed that the XG affects cohesion in the soils that initially have some level of cohesion and that it more affects the friction angle. The SEM images showed xanthan gum interacts differently with different types of soil. Xanthan gum coats coarse-grained particles, while fine particles in soil have an electrostatic bond with xanthan gum.

- Chapter 4 investigates the effect of cyclic wetting and drying on the biopolymer-treated soil. This aspect is out of utter importance in the goal to implement biopolymers in civil engineering practice because the soil in the field is likely to come into contact with water. Two types of soil (silty sand and pure sand) and two types of types of biopolymers (xanthan gum and guar gum) were investigated under two types of tests. The

first test observed the loss of mass during cyclic wetting and drying, and the second test observed the loss of strength during cyclic wetting and drying. The plain soil showed very low or non-existing resistivity to the influence of water. The research also showed that, unlike xanthan gum, guar gum does not correspond well with the pure wett sand. The research revealed the presence of an optimum biopolymer concentration under which the soil is most resistant to water. Higher concentrations of biopolymer in soil results in higher water absorption. Ultimately, higher water saturation reduces the apparent cohesion which results in a higher loss of mass and strength. Another interesting feature that biopolymer revealed is their healing properties. The broken xanthan gum-treated specimens showed to regain some level of the lost strength if they undergo the additional cycles of wetting and drying. The water reactivates the bonding abilities of xanthan gum that bind the soil particles together. This feature reveals that a high water saturation dissolves xanthan gum links in treated soil, but an optimum saturation can restore some level of the treated soil.

- Chapter 5 discusses a diagnostic strain localization analysis in biopolymer treated soil. Two types of soil and three types of biopolymers were investigated. A numerical-analytical algorithm was created to capture the stress-strain response and the beginning of the strain localization. The experimental data were collected for the silty sand with 0, 1, 2, 4 % biopolymers. The concentrations of 0, 1, 2, 4% were used for the calibration of the model, while the concentration of 2% was used for validation purposes. Three tests were used for the calibration: unconfined compression test, unconsolidated undrained triaxial test, and splitting tensile test. ABAQUS was used to replicate the unconfined compression test and unconsolidated undrained triaxial tests. For the unconfined compression test, it was found that the OSL was postponed for most concentrations of biopolymers. The level of the bifurcation angle and the peak stress of the silty sand increased for all biopolymer concentrations. The unconsolidated undrained triaxial test showed an increase in the peak stress and the bifurcation angles for all biopolymer concentrations. However, the onset of

strain localization was advanced. Several specimens were marked in a recognizable pattern before the testing. The testing process was recorded and observed in the image processing software. The software was able to track the pattern on the specimens and recognize deformations and strains. The onset of strain localization occurred close to the peak stress at which moment the image processing software reported high strain concentrations in the observed specimens. The diagnostic strain analysis shows that the presence of biopolymers in the soil can influence the onset of strain localization

In conclusion, it was shown that different biopolymers have a different interaction with the same soil and affect the soil strength in different magnitudes. Additionally, different biopolymer concentrations have a different effect on the soil. By investigating one type of biopolymer under one concentration, but with different soil types, it was noticed that certain soil types have a stronger response than others. Even though most biopolymers are degradable in water, investigating the influence of wetting and drying showed that biopolymers prevent soil degradation and the loss of strength. It was also shown that the presence of water can reactivate the bonding properties of biopolymers in biopolymer treated soil. The numerical research showed that the onset of strain localization in the soil can be influenced by the presence of biopolymers. This study showed that the onset of strain localization depends on biopolymer type, soil type, biopolymer concentration and the state of stress.

In general, it can be stated that biopolymers showed great potential for the future of clean soil stabilization and that additional research will lead to their utilization in geotechnical engineering.

6.2 FUTURE RESEARCH

Future research should further investigate the limits and drawbacks of biopolymer-treated soil. The main aim of future research should be to develop guidelines and recommendations for the utilization of biopolymers for soil stabilization.

Furthermore, suction and biopolymer bonding can increase soil strength. Future research should separate the effect of suction from the effect of particle bonding due to the biopolymer presence.

The investigation of the durability of soil under different environmental influences should be heavily researched. For example the influence of freezing and thawing, the influence of high temperatures, the resistivity of biopolymer-treated soil to microbes and acidic solutions.

Until now, the majority of the research on biopolymer treated soil consisted of experimental laboratory investigations. In situ investigations will be crucial to prove their effectiveness and lead to their utilization in practice. Therefore, in situ bearing-capacity of biopolymer treated soil will have to be investigated. Additionally, the proper mixing technique has to be adopted depending on the nature of the soil, biopolymer type and environment in which the mixing is conducted. For the purposes of this study, which was conducted in a laboratory-controlled environment, a dry mixing method was conducted for the majority of the specimens. However, in the field conditions, this process might be more efficiently conducted with different approaches. For deep subsurface mixing, the soil-biopolymer bond would be best achieved by mixing biopolymer slurry with soil through rotary machines. In the case of surface pavement stabilization, the dry mixing would be the most efficient approach. This would be similar to the dry mixing that was performed in this study, but it would be conducted on a larger scale. Therefore, heavy machinery would have to be utilized. After the dry machine-mixing, spraying water into the dry mix would activate the bonding properties of biopolymers.

Increasing experimental research (in the lab and the field) on this topic will increase confidence in their effectiveness which ultimately leads to their utilization in practice.

Additionally, the significant lack of numerical modeling of biopolymer-treated soil may be one of the reasons why biopolymers have not found their way in the engineering practice. Therefore, creating constitutive models that correspond to the behavior of biopolymer-treated soil should be a concern for future research.

7. REFERENCES

7.1 REFERENCES (CHAPTER 1)

Alsanad, A., 2011. Novel Biopolymer Treatment for Wind Induced Soil Erosion (Ph.D.). Arizona State University, United States -- Arizona.

Ashraf, M.S., Azahar, S.B., Yusof, N.Z., 2017. Soil Improvement Using MICP and Biopolymers: A Review. IOP Conf. Ser.: Mater. Sci. Eng. 226, 012058. https://doi.org/10.1088/1757-899X/226/1/012058

Ayeldeen, M., Negm, A., El-Sawwaf, M., Kitazume, M., 2017. Enhancing mechanical behaviors of collapsible soil using two biopolymers. Journal of Rock Mechanics and Geotechnical Engineering 9, 329–339. https://doi.org/10.1016/j.jrmge.2016.11.007

Ayeldeen, M.K., Negm, A.M., El Sawwaf, M.A., 2016. Evaluating the physical characteristics of biopolymer/soil mixtures. Arab J Geosci 9, 371. https://doi.org/10.1007/s12517-016-2366-1

Bacic, A., Fincher, G.B., Stone, B.A., 2009. Chemistry, Biochemistry, and Biology of 1-3 Beta Glucans and Related Polysaccharides. Academic Press.

Cabalar, A.F., Wiszniewski, M., Skutnik, Z., 2017. Effects of Xanthan Gum Biopolymer on the Permeability, Odometer, Unconfined Compressive and Triaxial Shear Behavior of a Sand. Soil Mech Found Eng 54, 356–361. https://doi.org/10.1007/s11204-017-9481-1

Chang, I., Cho, G.-C., 2012. Strengthening of Korean residual soil with β-1,3/1,6-glucan biopolymer. Construction and Building Materials 30, 30–35. https://doi.org/10.1016/j.conbuildmat.2011.11.030

Chang, I., Cho, G.-C., 2014. Geotechnical behavior of a beta-1,3/1,6-glucan biopolymer-treated residual soil. Geomechanics and Engineering 7, 633–647. https://doi.org/10.12989/GAE.2014.7.6.633

Chang, I., Im, J., Lee, S.-W., Cho, G.-C., 2017. Strength durability of gellan gum biopolymer-treated Korean sand with cyclic wetting and drying. Construction and Building Materials 143, 210–221. https://doi.org/10.1016/j.conbuildmat.2017.02.061

Chang, I., Im, J., Prasidhi, A.K., Cho, G.-C., 2015a. Effects of Xanthan gum biopolymer on soil strengthening. Construction and Building Materials 74, 65–72. https://doi.org/10.1016/j.conbuildmat.2014.10.026

Chang, I., Prasidhi, A.K., Im, J., Cho, G.-C., 2015b. Soil strengthening using thermo-gelation biopolymers. Construction and Building Materials 77, 430–438. https://doi.org/10.1016/j.conbuildmat.2014.12.116

Chen, C., Wu, L., Perdjon, M., Huang, X., Peng, Y., 2019. The drying effect on xanthan gum biopolymer treated sandy soil shear strength. Construction and Building Materials 197, 271–279. https://doi.org/10.1016/j.conbuildmat.2018.11.120

Chen, R., Ding, X., Ramey, D., Lee, I., Zhang, L., 2016. Experimental and numerical investigation into surface strength of mine tailings after biopolymer stabilization. Acta Geotech. 11, 1075–1085. https://doi.org/10.1007/s11440-015-0420-x

Chen, R., Lee, I., Zhang, L., 2015. Biopolymer Stabilization of Mine Tailings for Dust Control. J. Geotech. Geoenviron. Eng. 141, 04014100. https://doi.org/10.1061/(ASCE)GT.1943-5606.0001240

Chen, R., Zhang, L., Budhu, M., 2013. Biopolymer Stabilization of Mine Tailings. J. Geotech. Geoenviron. Eng. 139, 1802–1807. https://doi.org/10.1061/(ASCE)GT.1943-5606.0000902

Dehghan, H., Tabarsa, A., Latifi, N., Bagheri, Y., 2018. Use of xanthan and guar gums in soil strengthening. Clean Technologies and Environmental Policy 21, 155–165. https://doi.org/10.1007/s10098-018-1625-0

DeJong, J.T., Fritzges, M.B., Nüsslein, K., 2006. Microbially Induced Cementation to Control Sand Response to Undrained Shear. J. Geotech. Geoenviron. Eng. 132, 1381–1392. https://doi.org/10.1061/(ASCE)1090-0241(2006)132:11(1381)

Fatehi, H., Bahmani, M., Noorzad, A., 2019. Strengthening of Dune Sand with Sodium Alginate Biopolymer, in: Geo-Congress 2019. Presented at the Eighth International Conference on Case Histories in Geotechnical Engineering, American Society of Civil Engineers, Philadelphia, Pennsylvania, pp. 157–166. https://doi.org/10.1061/9780784482117.015

Galán-Marín, C., Rivera-Gómez, C., Petric, J., 2010. Clay-based composite stabilized with natural polymer and fibre. Construction and Building Materials 24, 1462–1468. https://doi.org/10.1016/j.conbuildmat.2010.01.008

Gombotz, W.R., Wee, S.F., 2012. Protein release from alginate matrices. Advanced Drug Delivery Reviews 64, 194–205. https://doi.org/10.1016/j.addr.2012.09.007

Guo, L., 2014. Investigation of soil stabilization using biopolymers 112.

Gupta, S.C., Hooda, K.S., Mathur, N.K., Gupta, S., 2009. Tailoring of Guar gum for desert sand stabilization. Indian j. Chem. Technol. 6.

Hataf, N., Ghadir, P., Ranjbar, N., 2018. Investigation of soil stabilization using chitosan biopolymer. Journal of Cleaner Production 170, 1493–1500. https://doi.org/10.1016/j.jclepro.2017.09.256

Kalia, S., Avérous, L. (Eds.), 2011. Biopolymers: biomedical and environmental applications. Wiley, Hoboken, N.J.

Karimi, S., 1998. A study of geotechnical applications of biopolymer treated soils with an emphasis on silt.

Katzbauer, B., 1998. Properties and applications of xanthan gum. Polymer degradation and Stability 59, 81–84.

Kavazanjian Jr, E., Iglesias, E., Karatas, I., 2009. Biopolymer soil stabilization for wind erosion control, in: Proc. 17th Int. Conf. Soil Mech. Geotech. Engng, Alexandria. pp. 881–884.

Khachatoorian, R., Petrisor, I.G., Kwan, C.-C., Yen, T.F., 2003. Biopolymer plugging effect: laboratory-pressurized pumping flow studies. Journal of Petroleum Science and Engineering 38, 13–21. https://doi.org/10.1016/S0920-4105(03)00019-6

Holtz, R.D., Kovacs, W.D. and Sheahan, T.C., 1981. An introduction to geotechnical engineering (Vol. 733). Englewood Cliffs, NJ: Prentice-Hall.

Lee, K.Y., Mooney, D.J., 2012. Alginate: Properties and biomedical applications. Progress in Polymer Science 37, 106–126. https://doi.org/10.1016/j.progpolymsci.2011.06.003

Qureshi, M.U., Chang, I., Al-Sadarani, K., 2016. Strength and Durability Characteristics of Bio-Improved Sand of Al- Sharqia Desert, Oman. Proceedings of the 2016 World Congress on Advances in Civil, Environmental, & Materials Research (ACEM16)

Smidsrod, O., Skjakbrk, G., 1990. Alginate as immobilization matrix for cells. Trends in Biotechnology 8, 71–78. https://doi.org/10.1016/0167-7799(90)90139-O

Thombare, N., Jha, U., Mishra, S., Siddiqui, M.Z., 2016. Guar gum as a promising starting material for diverse applications: A review. International Journal of Biological Macromolecules 88, 361–372. https://doi.org/10.1016/j.ijbiomac.2016.04.001

Toufigh, V., Kianfar, E., 2019. The effects of stabilizers on the thermal and the mechanical properties of rammed earth at various humidities and their environmental impacts. Construction and Building Materials 200, 616–629. https://doi.org/10.1016/j.conbuildmat.2018.12.050

Umar, M., Kassim, K.A., Ping Chiet, K.T., 2016. Biological process of soil improvement in civil engineering: A review. Journal of Rock Mechanics and Geotechnical Engineering 8, 767–774. https://doi.org/10.1016/j.jrmge.2016.02.004

Volman, J.J., Ramakers, J.D., Plat, J., 2008. Dietary modulation of immune function by β-glucans. Physiology & Behavior 94, 276–284. https://doi.org/10.1016/j.physbeh.2007.11.045

Wiszniewski, M., Skutnik, Z., Cabalar, A.F., 2013. Laboratory assessment of permeability of sand and biopolymer mixtures. Annals of Warsaw University of Life Sciences - SGGW. Land Reclamation 45, 217–226. https://doi.org/10.2478/sggw-2013-0018

ASTM C150/C150M-19a, Standard Specification for Portland Cement. 1–10 (2019).

ASTM C618-19a, Standard Specification for Coal Fly Ash and Raw or Calcined Natural Pozzolan for Usein Concrete. 1-5 (2019)

7.2 REFERENCES (CHAPTER 2)

Aguilar, R., Nakamatsu, J., Ramírez, E., Elgegren, M., Ayarza, J., Kim, S., Pando, M.A., Ortega-San-Martin, L., 2016. The potential use of chitosan as a biopolymer additive for enhanced mechanical properties and water resistance of earthen construction. Construction and Building Materials 114, 625–637. https://doi.org/10.1016/j.conbuildmat.2016.03.218

Ahlafi, H., Moussout, H., Boukhlifi, F., Echetna, M., Bennani, M.N., My Slimane, S., 2013. Kinetics of N-Deacetylation of Chitin Extracted from Shrimp Shells Collected from Coastal Area of Morocco. Mediterr.J.Chem 2, 503–513. https://doi.org/10.13171/mjc.2.3.2013.22.01.20

Alsanad, A., 2011. Novel Biopolymer Treatment for Wind Induced Soil Erosion (Ph.D.). Arizona State University, United States -- Arizona.

Andrew, R.M., 2018. Global CO2 emissions from cement production 23.

Ayeldeen, M., Negm, A., El-Sawwaf, M., Kitazume, M., 2017. Enhancing mechanical behaviors of collapsible soil using two biopolymers. Journal of Rock Mechanics and Geotechnical Engineering 9, 329–339. https://doi.org/10.1016/j.jrmge.2016.11.007

Ayeldeen, M.K., Negm, A.M., El Sawwaf, M.A., 2016. Evaluating the physical characteristics of biopolymer/soil mixtures. Arab J Geosci 9, 371. https://doi.org/10.1007/s12517-016-2366-1

Bacic, A., Fincher, G.B., Stone, B.A., 2009. Chemistry, Biochemistry, and Biology of 1-3 Beta Glucans and Related Polysaccharides. Academic Press.

Baldassano, S., Accardi, G., Vasto, S., 2017. Beta-glucans and cancer: The influence of inflammation and gut peptide. European Journal of Medicinal Chemistry 142, 486–492. https://doi.org/10.1016/j.ejmech.2017.09.013

Bourriot, S., Garnier, C., Doublier, J.-L., 1999. Phase separation, rheology and microstructure of micellar casein–guar gum mixtures. Food Hydrocolloids 13, 43–49. https://doi.org/10.1016/S0268-005X(98)00068-X

Cabalar, A.F., Wiszniewski, M., Skutnik, Z., 2017. Effects of Xanthan Gum Biopolymer on the Permeability, Odometer, Unconfined Compressive and Triaxial Shear Behavior of a Sand. Soil Mech Found Eng 54, 356–361. https://doi.org/10.1007/s11204-017-9481-1

Chang, I., Cho, G.-C., 2012. Strengthening of Korean residual soil with β-1,3/1,6-glucan biopolymer. Construction and Building Materials 30, 30–35. https://doi.org/10.1016/j.conbuildmat.2011.11.030

Chang, I., Cho, G.-C., 2014. Geotechnical behavior of a beta-1,3/1,6-glucan biopolymer-treated residual soil. Geomechanics and Engineering 7, 633–647. https://doi.org/10.12989/GAE.2014.7.6.633

Chang, I., Im, J., Cho, G.-C., 2016. Introduction of Microbial Biopolymers in Soil Treatment for Future Environmentally-Friendly and Sustainable Geotechnical Engineering. Sustainability 8, 251. https://doi.org/10.3390/su8030251

Chang, I., Im, J., Lee, S.-W., Cho, G.-C., 2017. Strength durability of gellan gum biopolymer-treated Korean sand with cyclic wetting and drying. Construction and Building Materials 143, 210–221. https://doi.org/10.1016/j.conbuildmat.2017.02.061

Chang, I., Im, J., Prasidhi, A.K., Cho, G.-C., 2015a. Effects of Xanthan gum biopolymer on soil strengthening. Construction and Building Materials 74, 65–72. https://doi.org/10.1016/j.conbuildmat.2014.10.026

Chang, I., Prasidhi, A.K., Im, J., Cho, G.-C., 2015b. Soil strengthening using thermo-gelation biopolymers. Construction and Building Materials 77, 430–438. https://doi.org/10.1016/j.conbuildmat.2014.12.116

Chang, I., Prasidhi, A.K., Im, J., Shin, H.-D., Cho, G.-C., 2015c. Soil treatment using microbial biopolymers for anti-desertification purposes. Geoderma 253–254, 39–47. https://doi.org/10.1016/j.geoderma.2015.04.006

Chen, C., Wu, L., Perdjon, M., Huang, X., Peng, Y., 2019. The drying effect on xanthan gum biopolymer treated sandy soil shear strength. Construction and Building Materials 197, 271–279. https://doi.org/10.1016/j.conbuildmat.2018.11.120

Chen, R., Ding, X., Ramey, D., Lee, I., Zhang, L., 2016. Experimental and numerical investigation into surface strength of mine tailings after biopolymer stabilization. Acta Geotech. 11, 1075–1085. https://doi.org/10.1007/s11440-015-0420-x

Chen, R., Lee, I., Zhang, L., 2015. Biopolymer Stabilization of Mine Tailings for Dust Control. J. Geotech. Geoenviron. Eng. 141, 04014100. https://doi.org/10.1061/(ASCE)GT.1943-5606.0001240

Chen, R., Zhang, L., Budhu, M., 2013. Biopolymer Stabilization of Mine Tailings. J. Geotech. Geoenviron. Eng. 139, 1802–1807. https://doi.org/10.1061/(ASCE)GT.1943-5606.0000902

Cho, G.-C., Chang, I., 2018. Cementless Soil Stabilizer–Biopolymer. Proceedings of the 2018 World Congress on Advances in Civil, Environmental, & Materials Research (ACEM18)

Choi, S.-G., Wang, K., Chu, J., 2016. Properties of biocemented, fiber reinforced sand. Construction and Building Materials 120, 623–629. https://doi.org/10.1016/j.conbuildmat.2016.05.124

Das, S.K., Mahamaya, M., Panda, I., Swain, K., 2015. Stabilization of Pond Ash using Biopolymer. Procedia Earth and Planetary Science 11, 254–259. https://doi.org/10.1016/j.proeps.2015.06.033

Day, S., 1999. Geotechnical techniques for the construction of reactive barriers. Journal of Hazardous Materials 67, 285–297. https://doi.org/10.1016/S0304-3894(99)00044-8

Dehghan, H., Tabarsa, A., Latifi, N., Bagheri, Y., 2018. Use of xanthan and guar gums in soil strengthening. Clean Technologies and Environmental Policy 21, 155–165. https://doi.org/10.1007/s10098-018-1625-0

DeJong, J.T., Fritzges, M.B., Nüsslein, K., 2006. Microbially Induced Cementation to Control Sand Response to Undrained Shear. J. Geotech. Geoenviron. Eng. 132, 1381–1392. https://doi.org/10.1061/(ASCE)1090-0241(2006)132:11(1381)

DeJong, J.T., Mortensen, B.M., Martinez, B.C., Nelson, D.C., 2010. Bio-mediated soil improvement. Ecological Engineering 36, 197–210. https://doi.org/10.1016/j.ecoleng.2008.12.029

Deniz Akin, I., Likos, W.J., 2017. Brazilian Tensile Strength Testing of Compacted Clay. Geotech. Test. J. 40, 20160180. https://doi.org/10.1520/GTJ20160180

Endres, H.-J., Siebert-Raths, A., 2011. Engineering biopolymers. Eng. Biopolym 71148.

Gombotz, W.R., Wee, S.F., 2012. Protein release from alginate matrices. Advanced Drug Delivery Reviews 64, 194–205. https://doi.org/10.1016/j.addr.2012.09.007

Gupta, S.C., Hooda, K.S., Mathur, N.K., Gupta, S., 2009. Tailoring of Guar gum for desert sand stabilization. Indian j. Chem. Technol. 6.

Hataf, N., Ghadir, P., Ranjbar, N., 2018. Investigation of soil stabilization using chitosan biopolymer. Journal of Cleaner Production 170, 1493–1500. https://doi.org/10.1016/j.jclepro.2017.09.256

Karimi, S., n.d. A study of geotechnical applications of biopolymer treated soils with an emphasis on silt.

Katzbauer, B., 1998. Properties and applications of xanthan gum. Polymer degradation and Stability 59, 81–84.

Kavazanjian Jr, E., Iglesias, E., Karatas, I., 2009. Biopolymer soil stabilization for wind erosion control, in: Proc. 17th Int. Conf. Soil Mech. Geotech. Engng, Alexandria. pp. 881–884.

Khatami Hamid Reza, O'Kelly Brendan C., 2013. Improving Mechanical Properties of Sand Using Biopolymers. J Geotech Geoenviron 139, 1402–1406. https://doi.org/10.1061/(ASCE)GT.1943-5606.0000861

Latifi, N., Horpibulsuk, S., Meehan, C.L., Abd Majid, M.Z., Tahir, M.M., Mohamad, E.T., 2017. Improvement of Problematic Soils with Biopolymer—An Environmentally Friendly Soil Stabilizer. J. Mater. Civ. Eng. 29, 04016204. https://doi.org/10.1061/(ASCE)MT.1943-5533.0001706

Lee, K.Y., Mooney, D.J., 2012. Alginate: Properties and biomedical applications. Progress in Polymer Science 37, 106–126. https://doi.org/10.1016/j.progpolymsci.2011.06.003

Li, M., Fang, C., Kawasaki, S., Achal, V., 2018. Fly ash incorporated with biocement to improve strength of expansive soil. Scientific Reports 8, 2565. https://doi.org/10.1038/s41598-018-20921-0

Ma, H., Ma, Q., 2019. Experimental Studies on the Mechanical Properties of Loess Stabilized with Sodium Carboxymethyl Cellulose [WWW Document]. Advances in Materials Science and Engineering. https://doi.org/10.1155/2019/9375685

Metz, B., Davidson, O., De Coninck, H., Loos, M., Meyer, L., 2005. IPCC special report on carbon dioxide capture and storage. Intergovernmental Panel on Climate Change, Geneva (Switzerland).

Muguda, S., Booth, S.J., Hughes, P.N., Augarde, C.E., Perlot, C., Bruno, A.W., Gallipoli, D., 2017. Mechanical properties of biopolymer-stabilised soil-based construction materials. Géotechnique Letters 7, 309–314. https://doi.org/10.1680/jgele.17.00081

Rosalam, S., England, R., 2006. Review of xanthan gum production from unmodified starches by Xanthomonas comprestris sp. Enzyme and Microbial Technology 39, 197–207. https://doi.org/10.1016/j.enzmictec.2005.10.019

Shahidi, F., Synowiecki, J., 1991. Isolation and characterization of nutrients and value-added products from snow crab (Chionoecetes opilio) and shrimp (Pandalus borealis) processing discards. Journal of agricultural and food chemistry 39, 1527–1532.

Smidsrod, O., Skjakbrk, G., 1990. Alginate as immobilization matrix for cells. Trends in Biotechnology 8, 71–78. https://doi.org/10.1016/0167-7799(90)90139-O

Swain, K., Mahamaya, M., Alam, S., Das, S.K., 2018. Stabilization of Dispersive Soil Using Biopolymer, in: Singh, D.N., Galaa, A. (Eds.), Contemporary Issues in Geoenvironmental Engineering. Springer International Publishing, Cham, pp. 132–147.

Thombare, N., Jha, U., Mishra, S., Siddiqui, M.Z., 2016. Guar gum as a promising starting material for diverse applications: A review. International Journal of Biological Macromolecules 88, 361–372. https://doi.org/10.1016/j.ijbiomac.2016.04.001

Toufigh, V., Kianfar, E., 2019. The effects of stabilizers on the thermal and the mechanical properties of rammed earth at various humidities and their environmental impacts. Construction and Building Materials 200, 616–629. https://doi.org/10.1016/j.conbuildmat.2018.12.050

Umar, M., Kassim, K.A., Ping Chiet, K.T., 2016. Biological process of soil improvement in civil engineering: A review. Journal of Rock Mechanics and Geotechnical Engineering 8, 767–774. https://doi.org/10.1016/j.jrmge.2016.02.004

Volman, J.J., Ramakers, J.D., Plat, J., 2008. Dietary modulation of immune function by β-glucans. Physiology & Behavior 94, 276–284. https://doi.org/10.1016/j.physbeh.2007.11.045

Wiszniewski, M., Skutnik, Z., Biliniak, M., Çabalar, A.F., 2017. Some geomechanical properties of a biopolymer treated medium sand. Annals of Warsaw University of Life Sciences – SGGW. Land Reclamation 49, 201–212. https://doi.org/10.1515/sggw-2017-0016

ASTM D2166/D2166M-13, Standard Test Method for Unconfined Compressive Strength of Cohesive Soil. 1–7 (2016).

ASTM D3967-16, Standard Test Method for Splitting Tensile strength of Intact Rock Core Specimens. 1–5 (2016).

ASTM D2850-15, Standard Test Method for Unconsolidated-Undrained Triaxial Compression Test on Cohesive Soils. 1–7 (2015).

ASTM D3080-11, Test Method for Direct Shear Test of Soils Under Consolidated Drained Conditions. 1–9 (2012).

ASTM D6913-17, Standard Test Methods for Particle-Size Distribution (Gradation) of Soils Using Sieve Analysis. 1–34 (2017).

ASTM D4318-17, Standard Test Methods for Liquid Limit, Plastic Limit, and Plasticity Index of Soils.. 1–20 (2017).

7.3 REFERENCES (CHAPTER 3)

Ashraf, M.S., Azahar, S.B., Yusof, N.Z., 2017. Soil Improvement Using MICP and Biopolymers: A Review. IOP Conf. Ser.: Mater. Sci. Eng. 226, 012058. https://doi.org/10.1088/1757-899X/226/1/012058

Ayeldeen, M., Negm, A., El-Sawwaf, M., Kitazume, M., 2017. Enhancing mechanical behaviors of collapsible soil using two biopolymers. Journal of Rock Mechanics and Geotechnical Engineering 9, 329–339. https://doi.org/10.1016/j.jrmge.2016.11.007

Ayeldeen, M.K., Negm, A.M., El Sawwaf, M.A., 2016. Evaluating the physical characteristics of biopolymer/soil mixtures. Arab J Geosci 9, 371. https://doi.org/10.1007/s12517-016-2366-1

Bourriot, S., Garnier, C., Doublier, J.-L., 1999. Phase separation, rheology and microstructure of micellar casein–guar gum mixtures. Food Hydrocolloids 13, 43–49. https://doi.org/10.1016/S0268-005X(98)00068-X

Cabalar, A.F., Wiszniewski, M., Skutnik, Z., 2017. Effects of Xanthan Gum Biopolymer on the Permeability, Odometer, Unconfined Compressive and Triaxial Shear Behavior of a Sand. Soil Mech Found Eng 54, 356–361. https://doi.org/10.1007/s11204-017-9481-1

Chang, I., Im, J., Cho, G.-C., 2016. Introduction of Microbial Biopolymers in Soil Treatment for Future Environmentally-Friendly and Sustainable Geotechnical Engineering. Sustainability 8, 251. https://doi.org/10.3390/su8030251

Chang, I., Im, J., Prasidhi, A.K., Cho, G.-C., 2015a. Effects of Xanthan gum biopolymer on soil strengthening. Construction and Building Materials 74, 65–72. https://doi.org/10.1016/j.conbuildmat.2014.10.026

Chang, I., Prasidhi, A.K., Im, J., Cho, G.-C., 2015b. Soil strengthening using thermo-gelation biopolymers. Construction and Building Materials 77, 430–438. https://doi.org/10.1016/j.conbuildmat.2014.12.116

Chang, I., Prasidhi, A.K., Im, J., Shin, H.-D., Cho, G.-C., 2015c. Soil treatment using microbial biopolymers for anti-desertification purposes. Geoderma 253–254, 39–47. https://doi.org/10.1016/j.geoderma.2015.04.006

Chen, R., Zhang, L., Budhu, M., 2013. Biopolymer Stabilization of Mine Tailings. J. Geotech. Geoenviron. Eng. 139, 1802–1807. https://doi.org/10.1061/(ASCE)GT.1943-5606.0000902

Cho, G.-C., Chang, I., n.d. Cementless Soil Stabilizer–Biopolymer. Proceedings of the 2018 World Congress on Advances in Civil, Environmental, & Materials Research (ACEM18) (2012)

DeJong, J.T., Fritzges, M.B., Nüsslein, K., 2006. Microbially Induced Cementation to Control Sand Response to Undrained Shear. J. Geotech. Geoenviron. Eng. 132, 1381–1392. https://doi.org/10.1061/(ASCE)1090-0241(2006)132:11(1381)

DeJong, J.T., Mortensen, B.M., Martinez, B.C., Nelson, D.C., 2010. Bio-mediated soil improvement. Ecological Engineering 36, 197–210. https://doi.org/10.1016/j.ecoleng.2008.12.029

Hataf, N., Ghadir, P., Ranjbar, N., 2018. Investigation of soil stabilization using chitosan biopolymer. Journal of Cleaner Production 170, 1493–1500. https://doi.org/10.1016/j.jclepro.2017.09.256

Hou, C.T., Barnabe, N., Greaney, K., 1986. Biodegradation of xanthan by salt-tolerant aerobic microorganisms. Journal of Industrial Microbiology 1, 31–37.

Katzbauer, B., 1998. Properties and applications of xanthan gum. Polymer degradation and Stability 59, 81–84.

Kavazanjian Jr, E., Iglesias, E., Karatas, I., 2009. Biopolymer soil stabilization for wind erosion control, in: Proc. 17th Int. Conf. Soil Mech. Geotech. Engng, Alexandria. pp. 881–884.

Latifi, N., Horpibulsuk, S., Meehan, C.L., Abd Majid, M.Z., Tahir, M.M., Mohamad, E.T., 2017. Improvement of Problematic Soils with Biopolymer—An Environmentally Friendly Soil Stabilizer. J. Mater. Civ. Eng. 29, 04016204. https://doi.org/10.1061/(ASCE)MT.1943-5533.0001706

Metz, B., Davidson, O., De Coninck, H., Loos, M., Meyer, L., 2005. IPCC special report on carbon dioxide capture and storage. Intergovernmental Panel on Climate Change, Geneva (Switzerland).

Orts, W.J., Sojka, R.E., Glenn, G.M., 2000. Biopolymer additives to reduce erosion-induced soil losses during irrigation. Industrial Crops and Products 11, 19–29. https://doi.org/10.1016/S0926-6690(99)00030-8

Rosalam, S., England, R., 2006. Review of xanthan gum production from unmodified starches by Xanthomonas comprestris sp. Enzyme and Microbial Technology 39, 197–207. https://doi.org/10.1016/j.enzmictec.2005.10.019

Shahidi, F., Synowiecki, J., 1991. Isolation and characterization of nutrients and value-added products from snow crab (Chionoecetes opilio) and shrimp (Pandalus borealis) processing discards. Journal of agricultural and food chemistry 39, 1527–1532.

Umar, M., Kassim, K.A., Ping Chiet, K.T., 2016. Biological process of soil improvement in civil engineering: A review. Journal of Rock Mechanics and Geotechnical Engineering 8, 767–774. https://doi.org/10.1016/j.jrmge.2016.02.004

Volman, J.J., Ramakers, J.D., Plat, J., 2008. Dietary modulation of immune function by β-glucans. Physiology & Behavior 94, 276–284. https://doi.org/10.1016/j.physbeh.2007.11.045

Wiszniewski, M., Skutnik, Z., Biliniak, M., Çabalar, A.F., 2017. Some geomechanical properties of a biopolymer treated medium sand. Annals of Warsaw University of Life Sciences – SGGW. Land Reclamation 49, 201–212. https://doi.org/10.1515/sggw-2017-0016

ASTM D2166/D2166M-13, Standard Test Method for Unconfined Compressive Strength of Cohesive Soil. 1–7 (2016).

ASTM D2216-10, Standard Test Methods for Laboratory Determination of Water (Moisture) Content of Soil and Rock by Mass. 1-7 (2010).

ASTM D2850-15, Standard Test Method for Unconsolidated-Undrained Triaxial Compression Test on Cohesive Soils. 1–7 (2015).

ASTM D3080-11, Test Method for Direct Shear Test of Soils Under Consolidated Drained Conditions. 1–9 (2012).

ASTM D6913-17, Standard Test Methods for Particle-Size Distribution (Gradation) of Soils Using Sieve Analysis. 1–34 (2017).

ASTM D4318-17, Standard Test Methods for Liquid Limit, Plastic Limit, and Plasticity Index of Soils.. 1–20 (2017).

7.4 REFERENCES (CHAPTER 4)

Ashraf, M.S., Azahar, S.B., Yusof, N.Z., 2017. Soil Improvement Using MICP and Biopolymers: A Review. IOP Conf. Ser.: Mater. Sci. Eng. 226, 012058. https://doi.org/10.1088/1757-899X/226/1/012058

Ayeldeen, M., Negm, A., El-Sawwaf, M., Kitazume, M., 2017. Enhancing mechanical behaviors of collapsible soil using two biopolymers. Journal of Rock Mechanics and Geotechnical Engineering 9, 329–339. https://doi.org/10.1016/j.jrmge.2016.11.007

Ayeldeen, M.K., Negm, A.M., El Sawwaf, M.A., 2016. Evaluating the physical characteristics of biopolymer/soil mixtures. Arab J Geosci 9, 371. https://doi.org/10.1007/s12517-016-2366-1

Bourriot, S., Garnier, C., Doublier, J.-L., 1999. Phase separation, rheology and microstructure of micellar casein–guar gum mixtures. Food Hydrocolloids 13, 43–49. https://doi.org/10.1016/S0268-005X(98)00068-X

Chang, I., Im, J., Cho, G.-C., 2016. Introduction of Microbial Biopolymers in Soil Treatment for Future Environmentally-Friendly and Sustainable Geotechnical Engineering. Sustainability 8, 251. https://doi.org/10.3390/su8030251

Chang, I., Im, J., Prasidhi, A.K., Cho, G.-C., 2015a. Effects of Xanthan gum biopolymer on soil strengthening. Construction and Building Materials 74, 65–72. https://doi.org/10.1016/j.conbuildmat.2014.10.026

Chang, I., Prasidhi, A.K., Im, J., Cho, G.-C., 2015b. Soil strengthening using thermo-gelation biopolymers. Construction and Building Materials 77, 430–438. https://doi.org/10.1016/j.conbuildmat.2014.12.116

Chang, I., Prasidhi, A.K., Im, J., Shin, H.-D., Cho, G.-C., 2015c. Soil treatment using microbial biopolymers for anti-desertification purposes. Geoderma 253–254, 39–47. https://doi.org/10.1016/j.geoderma.2015.04.006

Chen, R., Zhang, L., Budhu, M., 2013. Biopolymer Stabilization of Mine Tailings. J. Geotech. Geoenviron. Eng. 139, 1802–1807. https://doi.org/10.1061/(ASCE)GT.1943-5606.0000902

Cho, G.-C., Chang, I., n.d. Cementless Soil Stabilizer–Biopolymer. Proceedings of the 2018 World Congress on Advances in Civil, Environmental, & Materials Research (ACEM18) (2012)

Dehghan, H., Tabarsa, A., Latifi, N., Bagheri, Y., 2018. Use of xanthan and guar gums in soil strengthening. Clean Technologies and Environmental Policy 21, 155–165. https://doi.org/10.1007/s10098-018-1625-0

DeJong, J.T., Fritzges, M.B., Nüsslein, K., 2006. Microbially Induced Cementation to Control Sand Response to Undrained Shear. J. Geotech. Geoenviron. Eng. 132, 1381–1392. https://doi.org/10.1061/(ASCE)1090-0241(2006)132:11(1381)

DeJong, J.T., Mortensen, B.M., Martinez, B.C., Nelson, D.C., 2010. Bio-mediated soil improvement. Ecological Engineering 36, 197–210. https://doi.org/10.1016/j.ecoleng.2008.12.029

Hou, C.T., Barnabe, N., Greaney, K., 1986. Biodegradation of xanthan by salt-tolerant aerobic microorganisms. Journal of Industrial Microbiology 1, 31–37.

Hataf, N., Ghadir, P., Ranjbar, N., 2018. Investigation of soil stabilization using chitosan biopolymer. Journal of Cleaner Production 170, 1493–1500. https://doi.org/10.1016/j.jclepro.2017.09.256

Jindal, N., Singh Khattar, J., 2018. Chapter 4 - Microbial Polysaccharides in Food Industry, in: Grumezescu, A.M., Holban, A.M. (Eds.), Biopolymers for Food Design, Handbook of Food Bioengineering. Academic Press, pp. 95–123. https://doi.org/10.1016/B978-0-12-811449-0.00004-9

Katzbauer, B., 1998. Properties and applications of xanthan gum. Polymer degradation and Stability 59, 81–84.

Kavazanjian Jr, E., Iglesias, E., Karatas, I., 2009. Biopolymer soil stabilization for wind erosion control, in: Proc. 17th Int. Conf. Soil Mech. Geotech. Engng, Alexandria. pp. 881–884.

Latifi, N., Horpibulsuk, S., Meehan, C.L., Abd Majid, M.Z., Tahir, M.M., Mohamad, E.T., 2017. Improvement of Problematic Soils with Biopolymer—An Environmentally Friendly Soil Stabilizer. J. Mater. Civ. Eng. 29, 04016204. https://doi.org/10.1061/(ASCE)MT.1943-5533.0001706

Metz, B., Davidson, O., De Coninck, H., Loos, M., Meyer, L., 2005. IPCC special report on carbon dioxide capture and storage. Intergovernmental Panel on Climate Change, Geneva (Switzerland).

Orts, W.J., Sojka, R.E., Glenn, G.M., 2000. Biopolymer additives to reduce erosion-induced soil losses during irrigation. Industrial Crops and Products 11, 19–29. https://doi.org/10.1016/S0926-6690(99)00030-8

Prameela, K., Murali Mohan, C., Ramakrishna, C., 2018. Chapter 1 - Biopolymers for Food Design: Consumer-Friendly Natural Ingredients, in: Grumezescu, A.M., Holban, A.M. (Eds.), Biopolymers for Food Design, Handbook of Food Bioengineering. Academic Press, pp. 1–32. https://doi.org/10.1016/B978-0-12-811449-0.00001-3

Rayment, P., Ellis, P.R., 2003. GUMS | Nutritional Role of Guar Gum, in: Caballero, B. (Ed.), Encyclopedia of Food Sciences and Nutrition (Second Edition). Academic Press, Oxford, pp. 3012–3021. https://doi.org/10.1016/B0-12-227055-X/00576-9

Shahidi, F., Synowiecki, J., 1991. Isolation and characterization of nutrients and value-added products from snow crab (Chionoecetes opilio) and shrimp (Pandalus borealis) processing discards. Journal of agricultural and food chemistry 39, 1527–1532.

Soldo, A., Miletić, M. and Auad, M.L., 2020. Biopolymers as a sustainable solution for the enhancement of soil mechanical properties. Scientific Reports, 10(1), pp.1-13.

Thombare, N., Jha, U., Mishra, S., Siddiqui, M.Z., 2016. Guar gum as a promising starting material for diverse applications: A review. International Journal of Biological Macromolecules 88, 361–372. https://doi.org/10.1016/j.ijbiomac.2016.04.001

Toufigh, V., Kianfar, E., 2019. The effects of stabilizers on the thermal and the mechanical properties of rammed earth at various humidities and their environmental impacts. Construction and Building Materials 200, 616–629. https://doi.org/10.1016/j.conbuildmat.2018.12.050

Umar, M., Kassim, K.A., Ping Chiet, K.T., 2016. Biological process of soil improvement in civil engineering: A review. Journal of Rock Mechanics and Geotechnical Engineering 8, 767–774. https://doi.org/10.1016/j.jrmge.2016.02.004

Volman, J.J., Ramakers, J.D., Plat, J., 2008. Dietary modulation of immune function by β-glucans. Physiology & Behavior 94, 276–284. https://doi.org/10.1016/j.physbeh.2007.11.045

Wiszniewski, M., Skutnik, Z., Cabalar, A.F., 2013. Laboratory assessment of permeability of sand and biopolymer mixtures. Annals of Warsaw University of Life Sciences - SGGW. Land Reclamation 45, 217–226. https://doi.org/10.2478/sggw-2013-0018

Wiszniewski, M., Skutnik, Z., Biliniak, M., Çabalar, A.F., 2017. Some geomechanical properties of a biopolymer treated medium sand. Annals of Warsaw University of Life Sciences – SGGW. Land Reclamation 49, 201–212. https://doi.org/10.1515/sggw-2017-0016

ASTM D559 - 15, Standard Test Methods for Wetting and Drying Compacted Soil-Cement Mixtures. 1-6 (2015).

ASTM D6913-17, Standard Test Methods for Particle-Size Distribution (Gradation) of Soils Using Sieve Analysis. 1–34 (2017).

ASTM D4318-17, Standard Test Methods for Liquid Limit, Plastic Limit, and Plasticity Index of Soils.. 1–20 (2017).

7.5 REFERENCES (CHAPTER 5)

ABAQUS FEA, 2019, Dassault Systèmes Simulia Corporation, Providence, RI, USA.

Aguilar, R., Nakamatsu, J., Ramírez, E., Elgegren, M., Ayarza, J., Kim, S., Pando, M.A., Ortega-San-Martin, L., 2016. The potential use of chitosan as a biopolymer additive for enhanced mechanical properties and water resistance of earthen construction. Construction and Building Materials 114, 625–637. https://doi.org/10.1016/j.conbuildmat.2016.03.218

Andrew, R.M., 2018. Global CO2 emissions from cement production 23.

Ashraf, M.S., Azahar, S.B., Yusof, N.Z., 2017. Soil Improvement Using MICP and Biopolymers: A Review. IOP Conf. Ser.: Mater. Sci. Eng. 226, 012058 . https://doi.org/10.1088/1757-899X/226/1/012058

Ayeldeen, M., Negm, A., El-Sawwaf, M., Kitazume, M., 2017. Enhancing mechanical behaviors of collapsible soil using two biopolymers. Journal of Rock Mechanics and Geotechnical Engineering 9, 329–339. https://doi.org/10.1016/j.jrmge.2016.11.007

Bacic, A., Fincher, G.B., Stone, B.A., 2009. Chemistry, Biochemistry, and Biology of 1-3 Beta Glucans and Related Polysaccharides. Academic Press.

Cabalar, A.F., Wiszniewski, M., Skutnik, Z., 2017. Effects of Xanthan Gum Biopolymer on the Permeability, Odometer, Unconfined Compressive and Triaxial Shear Behavior of a Sand. Soil Mech Found Eng 54, 356–361. https://doi.org/10.1007/s11204-017-9481-1

Chang, I., Im, J., Cho, G.-C., 2016. Introduction of Microbial Biopolymers in Soil Treatment for Future Environmentally-Friendly and Sustainable Geotechnical Engineering. Sustainability 8, 251. https://doi.org/10.3390/su8030251

Chang, I., Im, J., Prasidhi, A.K., Cho, G.-C., 2015a. Effects of Xanthan gum biopolymer on soil strengthening. Construction and Building Materials 74, 65–72. https://doi.org/10.1016/j.conbuildmat.2014.10.026

Chang, I., Prasidhi, A.K., Im, J., Cho, G.-C., 2015b. Soil strengthening using thermo-gelation biopolymers. Construction and Building Materials 77, 430–438. https://doi.org/10.1016/j.conbuildmat.2014.12.116

Chen, R., Zhang, L., Budhu, M., 2013. Biopolymer Stabilization of Mine Tailings. J. Geotech. Geoenviron. Eng. 139, 1802–1807. https://doi.org/10.1061/(ASCE)GT.1943-5606.0000902

Choi, S.-G., Wang, K., Chu, J., 2016. Properties of biocemented, fiber reinforced sand. Construction and Building Materials 120, 623–629. https://doi.org/10.1016/j.conbuildmat.2016.05.124

Das, B.M., 2019. Advanced Soil Mechanics, Fifth Edition. CRC Press.

Deniz Akin, I., Likos, W.J., 2017. Brazilian Tensile Strength Testing of Compacted Clay. Geotech. Test. J. 40, 20160180. https://doi.org/10.1520/GTJ20160180

DeJong, J.T., Mortensen, B.M., Martinez, B.C., Nelson, D.C., 2010. Bio-mediated soil improvement. Ecological Engineering 36, 197–210. https://doi.org/10.1016/j.ecoleng.2008.12.029

Gom Correlate, 2020, Knucklehead Productions, Trilion Quality Systems, King of Prussia, PA, USA

Gombotz, W.R., Wee, S.F., 2012. Protein release from alginate matrices. Advanced Drug Delivery Reviews 64, 194–205. https://doi.org/10.1016/j.addr.2012.09.007

Hirai, H., Takahashi, M. and Yamada, M., 1989. An elastic-plastic constitutive model for the behavior of improved sandy soils. *Soils and foundations*, *29*(2), pp.69-84.

Izzo, M.Z., Miletić, M., 2019. Sustainable Improvement of the Crack Resistance of Cohesive Soils. Sustainability 11, 5806. https://doi.org/10.3390/su11205806

Katzbauer, B., 1998. Properties and applications of xanthan gum. Polymer degradation and Stability 59, 81–84.

Kutanaei, S.S., Choobbasti, A.J., 2016. Triaxial behavior of fiber-reinforced cemented sand. Journal of Adhesion Science and Technology 30, 579–593. https://doi.org/10.1080/01694243.2015.1110073

Lee, K.Y., Mooney, D.J., 2012. Alginate: Properties and biomedical applications. Progress in Polymer Science 37, 106–126. https://doi.org/10.1016/j.progpolymsci.2011.06.003

Li, L., Cetin, B., Yang, X., 2018. Proceedings of GeoShanghai 2018 International Conference: Ground Improvement and Geosynthetics. Springer.

Liu, C., Tang, C.-S., Shi, B., Suo, W.-B., 2013. Automatic quantification of crack patterns by image processing. Computers & Geosciences 57, 77–80. https://doi.org/10.1016/j.cageo.2013.04.008

Ottosen, N.S., Runesson, K., 1991. Properties of discontinuous bifurcation solutions in elasto-plasticity. International Journal of Solids and Structures 27, 401–421. https://doi.org/10.1016/0020-7683(91)90131-X

Rahimi, M., Chan, D. and Nouri, A., 2016. Bounding surface constitutive model for cemented sand under monotonic loading. International Journal of Geomechanics, 16(2), p.04015049.

Schnaid, F., Prietto, P.D.M., Consoli, N.C., 2001. Characterization of Cemented Sand in Triaxial Compression. J. Geotech. Geoenviron. Eng. 127, 857–868. https://doi.org/10.1061/(ASCE)1090-0241(2001)127:10(857)

Shit, P.K., Bhunia, G.S., Maiti, R., 2015. Soil crack morphology analysis using image processing techniques. Model. Earth Syst. Environ. 1, 35.

Soldo, A. and Miletić, M., 2019. Study on Shear Strength of Xanthan Gum-Amended Soil. Sustainability, 11(21), p.6142.

Strömblad, N., n.d. Modeling of Soil and Structure Interaction Subsea 70. 2014

Tagliaferri, F., Waller, J., Andò, E., Hall, S.A., Viggiani, G., Bésuelle, P., DeJong, J.T., 2011. Observing strain localisation processes in bio-cemented sand using x-ray imaging. Granular Matter 13, 247–250. https://doi.org/10.1007/s10035-011-0257-4

Thombare, N., Jha, U., Mishra, S., Siddiqui, M.Z., 2016. Guar gum as a promising starting material for diverse applications: A review. International Journal of Biological Macromolecules 88, 361–372. https://doi.org/10.1016/j.ijbiomac.2016.04.001

Toufigh, V., Kianfar, E., 2019. The effects of stabilizers on the thermal and the mechanical properties of rammed earth at various humidities and their environmental impacts. Construction and Building Materials 200, 616–629. https://doi.org/10.1016/j.conbuildmat.2018.12.050

Truty, A. and Obrzud, R., 2011. The Hardening soil model–a practical guidebook. Zace Services Ltd, Software engineering. Lausanne.

Umar, M., Kassim, K.A., Ping Chiet, K.T., 2016. Biological process of soil improvement in civil engineering: A review. Journal of Rock Mechanics and Geotechnical Engineering 8, 767–774. https://doi.org/10.1016/j.jrmge.2016.02.004

Volman, J.J., Ramakers, J.D., Plat, J., 2008. Dietary modulation of immune function by β-glucans. Physiology & Behavior 94, 276–284. https://doi.org/10.1016/j.physbeh.2007.11.045

Wattrisse, B., Chrysochoos, A., Muracciole, J.-M., Némoz-Gaillard, M., 2001. Analysis of strain localization during tensile tests by digital image correlation. Experimental Mechanics 41, 29–39. https://doi.org/10.1007/BF02323101

Wiszniewski, M., Skutnik, Z., Biliniak, M., Çabalar, A.F., 2017. Some geomechanical properties of a biopolymer treated medium sand. Annals of Warsaw University of Life Sciences – SGGW. Land Reclamation 49, 201–212. https://doi.org/10.1515/sggw-2017-0016

ASTM D2166/D2166M-13, Standard Test Method for Unconfined Compressive Strength of Cohesive Soil. 1–7 (2016).

ASTM D3967-16, Standard Test Method for Splitting Tensile strength of Intact Rock Core Specimens. 1–5 (2016).

ASTM D2850-15, Standard Test Method for Unconsolidated-Undrained Triaxial Compression Test on Cohesive Soils. 1–7 (2015).

ASTM D6913-17, Standard Test Methods for Particle-Size Distribution (Gradation) of Soils Using Sieve Analysis. 1–34 (2017).

ASTM D4318-17, Standard Test Methods for Liquid Limit, Plastic Limit, and Plasticity Index of Soils.. 1–20 (2017).

8. APPENDIX

8.1 CHAPTER 2

Table 8-1: Experimental data for the unconfined compression test of biopolymer-treated silty sand

	Compressive strength (kPa)										
	After 5 days						After 30 days				
	Test No						Test No				
	1	2	3	4	Standard deviation		1	2	3	4	Standard deviation
Plain	1163	1083	1208	1334	105		1193	1100	1213		60
1% CHI	1298	1222	1262		38						
1% ALG	1850	1870	1632		132		1933	1915	1989		38
1% BG	1616	1567	1693		63		1592	1625	1899		169
1% GG	2738	2713	3005		162		3336	2932	2564		386
1% XG	3299	3331	3415		60		3044	3325	3405		190
Plain	1355	1327	1366	1547	100		1193	1100	1213		60
2% CHI	1406	1368	1429		31						
2% ALG	1648	1725	1728	1613	57		1808	2142	2182		205
2% BG	2128	2015	2050		58		1899	1777	2080	2433	286
2% GG	2887	2979	2932		46		2882	3116	2999		117
2% XG	5910	5990	6066		78		5942	5952	5922		15
Plain	1163	1083	1208	1334	105		1193	1100	1213		60
4% CHI	1090	1106	1020	1019	46						
4% ALG											
4% BG	2389	2617	2638	2408	133		2317	2201	2882		364
4% GG	3270	3079	3179	2993	120		3480	3318	3034		226
4% XG	5987	6285	6282		171		7495	6677	7088		409

Table 8-2: Experimental data for the splitting tensile strength test of biopolymer-treated silty sand

	Tensile strength (kPa)										
	After 5 days						After 30 days				
	Test No						Test No				
	1	2	3	4	Standard deviation		1	2	3	4	Standard deviation
Plain	260	254	268	248	8		219	274	226		30
1% CHI	337	242	259	315	45						
1% ALG	272	221	278	260	26		346	319	268		39
1% BG	314	319	347		18		408	319	319	293	50
1% GG	469	440	374		48		485	458	395		46
1% XG	661	757	605		77		591	699	642		54
Plain	260	254	268	248	8		219	274	226		30
2% CHI	257	220	171		43						
2% ALG	244	221	255	236	14		290	371	317		41
2% BG	371	468	356		61		350	410	440		46
2% GG	377	319	340		29		409	462	392		37
2% XG	650	710	689		30		615	693	675		41
Plain	260	254	268	248	8		219	274	226		30
4% CHI	85	70	82	154	38						
4% ALG											
4% BG	355	351	274	355	40		390	436	443		29
4% GG	514	387	446	413	55		411	463	440		26
4% XG	815	704	624		96		1152	976	1021	1095	78

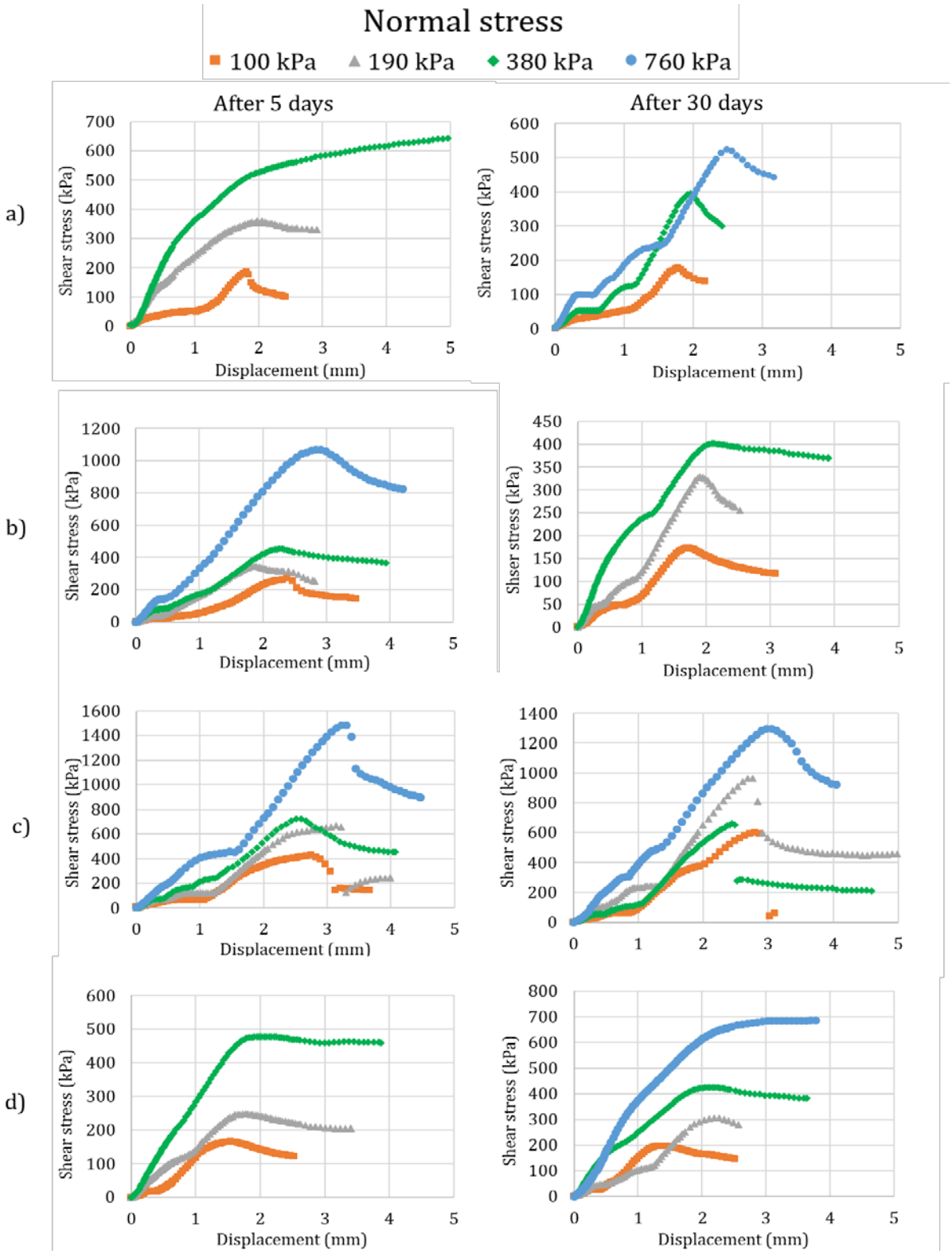

Figure 8-1: The results of the the direct shear tests for a) Plain silty sand; and Silty sand treated with b) 2% XG; c) 1% GG; d) 4% BG

8.2 CHAPTER 5

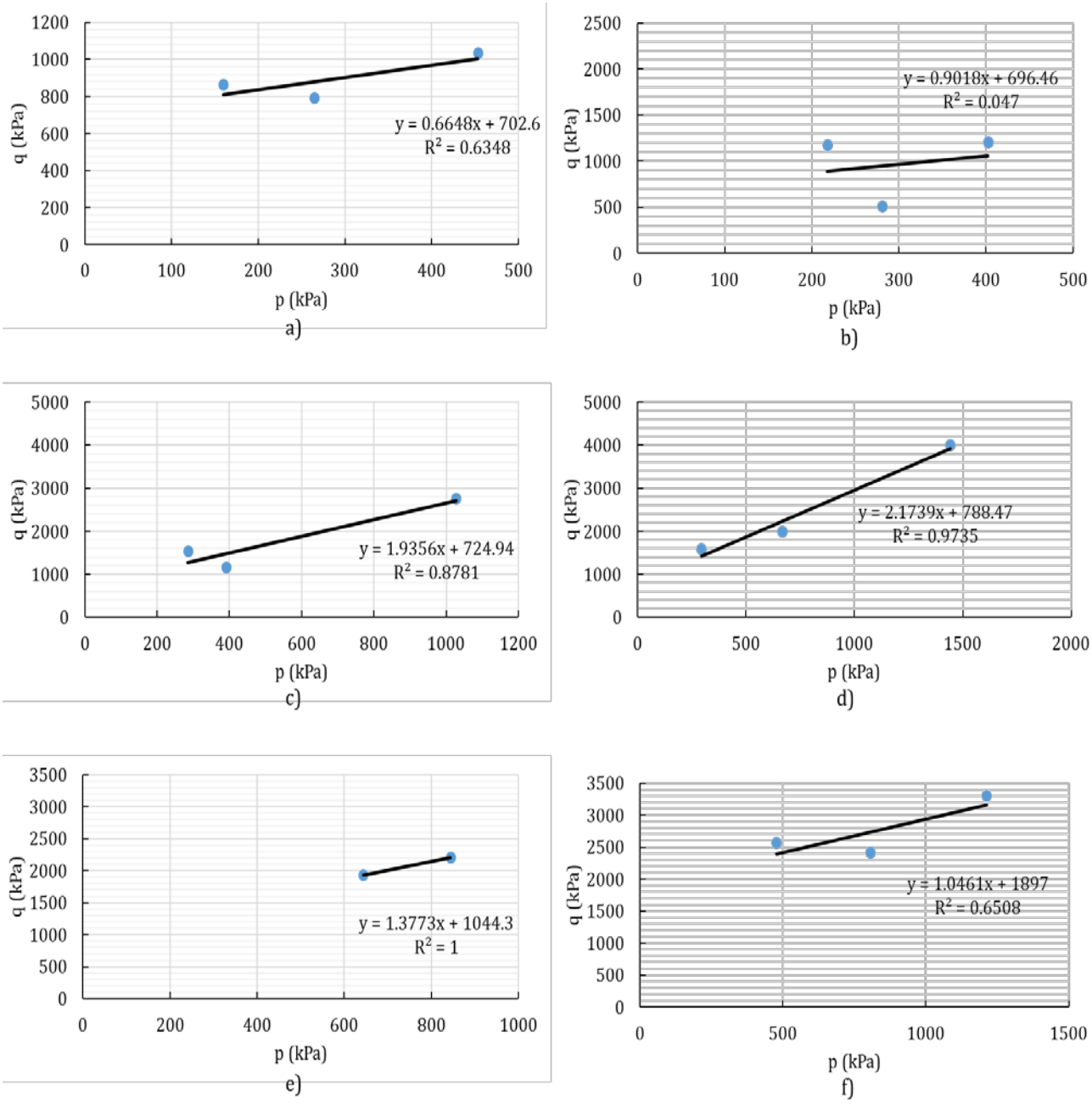

Figure 8-2: Calibration for numerical modeling for a) Plain silty sand; and silty sand with b) 1% BG; c) 1% GG; d) 4% GG; e) 1% XG; f) 4% XG

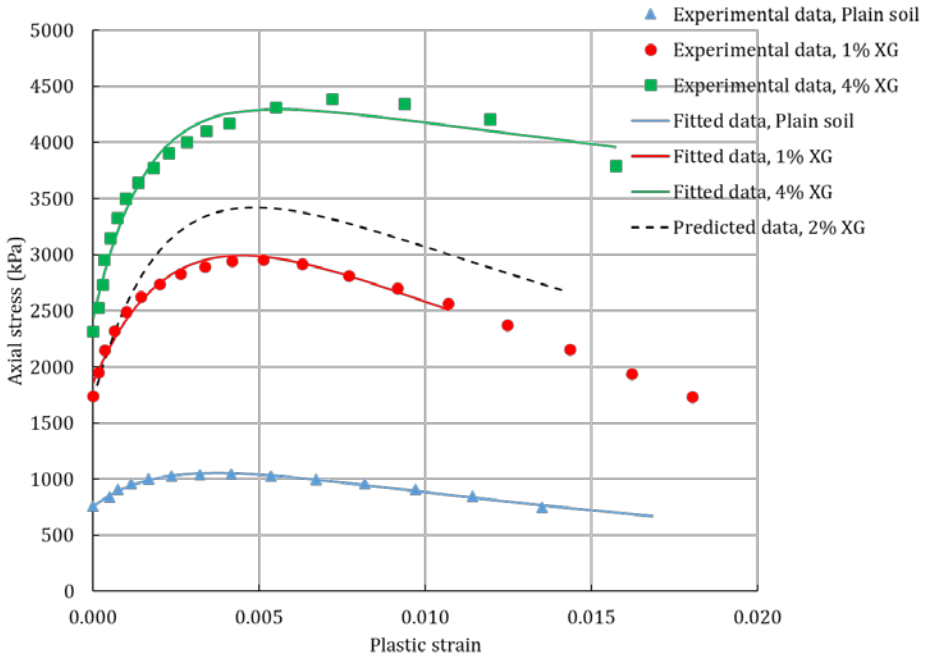

Figure 8-3: Hardening response of the silty sand treated with XG (unconfined compression test)

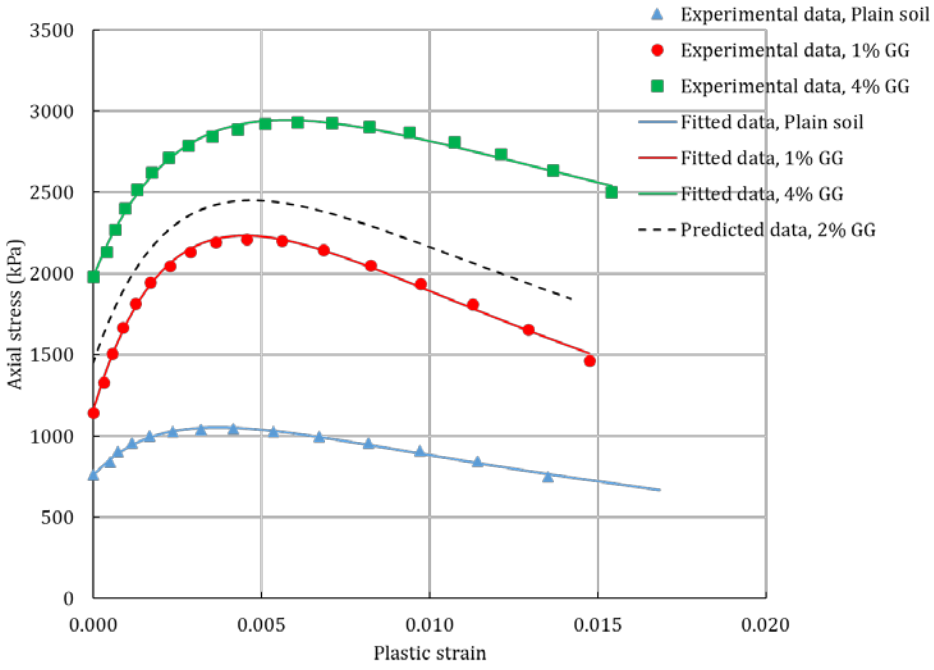

Figure 8-4: Hardening response of the silty sand treated with GG (unconfined compression test)